UNIVERSITÉ DE SHERBROOKE

Faculte de Genie

Département de génie electrique et de génie informatique

Titre En Français:

Biodétection de *Legionella pneumophila* par biocapteur à photocorrosion digitale à base de peptide antimicrobien

English Title:

Antimicrobial peptide biosensing of *Legionella pneumophila* with digital photocorrosion biosensor

A Thesis

Submitted in Partial Fulfilment of the Requirements for the Degree of

Doctor of Philosophy in Electrical Engineering

By

Mohammed Amirul Islam

Sherbrooke, Quebec, Canada February 2022

Doctoral Committee

Jan J. Dubowski (Co-directeur**)**
Professeur
Université de Sherbrooke

Azam F. Tayabali (Co-directeur)
Professeur agrégé de recherche
Université de Sherbrooke

Khalid Moumanis (Examinateur)
Professeur agrégé de recherche
Université de Sherbrooke

Michael Canva (Examinateur)
Directeur de recherche CNRS, LN2
Université de Sherbrooke

Paul G. Charette (Rapporteur)
Professeur, Université de Sherbrooke
Université de Sherbrooke

Résumé

La détection de bactéries pathogènes par culture microbienne est lente, nécessite un milieu de culture spécifique pour garantir la croissance de certaines souches bactériennes fastidieuses telle que *Legionella pneumophila* (*L. pneumophila*) et en plus pourrait ne pas déceler les bactéries viables mais non cultivables mais restant dangereuse en termes de pathogénicité. Par conséquent, l'usage de biocapteurs pour la détection de *L. pneumophila* serait, potentiellement, une approche attrayante permettant une détection précise et rapide. Cependant, la sensibilité et la spécificité des biocapteurs dépendent fortement des molécules de bioreconnaissance utilisées. Jusqu'à présent, différents ligands tels que les anticorps, les enzymes, les acides nucléiques fonctionnels (aptamères) et les bactériophages ont été utilisés comme éléments de bioreconnaissance. En raison de leur haute spécificité, Les anticorps de mammifères ont été largement employés pour le développement de divers biocapteurs. Cependant, les anticorps sont connus pour souffrir de la variabilité des lots produits et d'une stabilité limitée, ce qui réduit l'usage et la constance des performances des biocapteurs à base d'anticorps. Au cours des dernières années, les peptides antimicrobiens (PAM) ont été de plus en plus investigués pour des applications thérapeutiques en plus d'être considérés comme des ligands de bioreconnaissance prometteurs en raison de leur grande stabilité et leurs fortes réactivités aux bactéries. Dans le but d'améliorer les performances du biocapteur à DIP, notre hypothèse reposait sur l'usage de bioarchitectures à base de PAM à courte séquence pour une capture efficace des bactéries et une détection considérablement améliorée en raison du transfert de charge plus facilitée vers dans la biopuce à base de semiconducteur III-V. Dans la première phase du projet, nous avons évalué un biocapteur à DIP consistant en une puce d'arséniure de gallium/arséniure de gallium aluminium (GaAs/AlGaAs) fonctionnalisée par le warnericine RK pour la détection directe in situ de *L. pneumophila* dans l'eau. Nous avons démontré une détection linéaire de *L. pneumophila* pour des concentrations allant de 10^3 à 10^6 CFU/mL. De plus, le nombre relativement important d'interfaces constituant la bioarchitecture d'un tel biocapteur pourrait affecter sa reproductibilité et sa sensibilité. Dans ce cas, la couche de bioreconnaissance est plus mince (~ 2 nm) permettant une distance plus courte entre les bactéries et la surface du biocapteur, ce qui pourrait jouer un rôle important dans la promotion du transfert de charge entre les bactéries et la biopuce, et ainsi nous avons pu démontrer une

détection efficace de *L. pneumophila* à une concentration de 2 x 10^2 CFU/mL. Cette configuration a permis d'atteindre des LODs de 50 et 100 UFC/mL, respectivement pour de légionnelle dans du PBS et collectées d'échantillons d'eau de tour de refroidissement. Nous avons observé une détection sélective de *L. pneumophila* sérogroupe 1 (SG1) comparé au sérogroupe 5 (SG 5). Les biocapteurs à photocorrosion digitale (DIP) en configuration sandwich PAM et Ab pourraient être une approche prometteuse pour développer un biocapteur à faible coût, hautement sensible et spécifique pour la détection rapide de *L. pneumophila* dans l'eau.

Abstract

Culture based detection of pathogenic bacteria is time consuming, and needs specific culture medium to identify bacterial strains such as *Legionella pneumophila* (*L. pneumophila*) which does not flourish in typical growth medium. Culture based methods cannot detect viable but unculturable bacteria. Therefore, the detection of *L. pneumophila* with biosensors potentially could be an attractive approach enabling accurate and rapid detection. The sensitivity and specificity of biosensors depend critically on the biorecognition probes employed for the detection. Until now, different elements such as antibodies, enzymes, functional nucleic acids (aptamers) and bacteriophages have been utilized as biorecognition elements. Due to high specificity of antibodies, and the advanced technology of their production, mammalian antibodies have been widely investigated for the development of various biosensors. However, mammalian antibodies are known to suffer from batch-to-batch variation, as well as limited stability, which could reduce the consistent utility of the proposed biosensors. In recent years, antimicrobial peptides (AMPs) have been increasingly investigated for their therapeutic applications. At the same time, AMPs are considered as promising biorecognition ligands due to their high stability and multiple niches for capturing bacteria. The hypothesis was that AMP-based bioarchitectures allows for highly efficient capturing of bacteria, and the short length of the AMP would significantly enhance detection due to limited obstructive charge transfer in the charge sensing biosensor. In the first phase of the project, we investigated a warnericin RK AMP functionalized gallium arsenide/aluminum gallium arsenide (GaAs/AlGaAs) photonic biosensor for direct detection of *L. pneumophila* in water environments. This approach allowed for detecting a low to high concentration of *L. pneumophila* (10^3 to 10^6 CFU/mL) with a 10^3 CFU/mL limit of detection (LOD). In addition, a relatively large number of interfaces constituting the architecture of such biosensors could affect their reproducibility and sensitivity. A thinner biorecognition layer (~2 nm) resulted in a shorter distance between bacteria and the biosensor surface, which played important role in promoting charge transfer between bacteria and biochip. *L. pneumophila* was detected at concentrations as low of 2 x 10^2 CFU/mL. This configuration allowed the detection sensitivity of *L. pneumophila* as low as 50 CFU/mL and 100 CFU/mL in clean water and water originated from cooling tower, respectively, along with the selective detection of whole cell *L.*

pneumophila serogroup 1 (SG1) and serogroup 5 (SG5). The proposed AMP and Ab conjugated sandwich architecture with digital photocorrosion (DIP) biosensors is a promising approach for developing low cost, highly sensitive and specific biosensors for rapid detection of *L. pneumophila* in water environments.

Keywords: *Legionella pneumophila*, antimicrobial peptides, warnericin RK, polyclonal antibody, sandwich configuration, GaAs/AlGaAs biosensor, digital photocorrosion, photoluminescence

Dedicated to my kind parents
& beloved wife and kids!

Acknowledgment

The research presented in this thesis has been carried out at the Interdisciplinary Institute of Technological innovation (3IT) under the Faculty of Engineering, Université de Sherbrooke, Sherbrooke, Canada. The journey of my research would not be possible without help and support of a number of persons.

At first, I wish to express my humble gratefulness and sincere thanks to my honourable research director, Prof. Jan J. Dubowski for his numerous contributions including valuable support and guidance throughout the study. Indeed, it was great opportunity for me having him as my research supervisor. He has always been collaborative with his introspective thinking, ideas and insights. I would like to give special thanks to my co-supervisor, Prof. Azam F. Tayabali for his continuous support in editing and reviewing manuscripts and the thesis document.

I acknowledge the B2X scholarship from the Fonds de Recherche sur la Nature et les Technologies du Québec (FRQNT).

I would like to express my sincere gratitude to Dr. Walid M. Hassen for his unconditional support by providing materials and reviewing my thesis as well as research papers. I also thank Dr. Khalid Moumanis for his suggestions and technical assistance. Some special thanks also to Dr. Jonathan Vermette, Dr. Amanpreet Singh, Dr. Juliana Chawich, Dr. Mohammad Reza Aziziyan, Dr. Ahasanul Karim, Miss Ishika, Mr. René St-Onge, Mr. Lucas Paladines Alvarez and Mr. Topu Raihan for sharing their resources and materials in the lab.

Lastly, I also want to give heartfelt thanks to my parents and family particularly my wife for their continuous support, encouragements and inspirations. It would be really tough to finish my study without their support and devotions.

Table of contents

List of figures

List of tables

List of Acronyms

Ab	Antibody
AFM	Atomic force microscopy
AMP	Antimicrobial peptide
ATP	Adenosine triphosphate
BCFA	Branch Chain Fatty Acid
CFU/mL	Colony forming units per milliliter
EET	Extracellular electron transfer
EDC	1-ethyl-3-(-3-dimethylaminopropyl) carbodiimide
FTIR	Fourier-transform infrared spectroscopy
FESEM	Field emission scanning electron microscopy
g/L	Gram per liter
MHDA	16-Marcaptohexadecanoic acid
µg	Micro gram
mg/L	Milligram per litre
mM	Millimole
NHS	N-hydroxysuccinimide
mW	Mill watt
OCV	Open circuit voltage
OD	Optical density
PBS	Phosphate buffer saline
PCR	Polymerize chain reaction
PL	Photoluminescence
QW	Quantum well
QSPB	Quantum semiconductor photonic biosensing
rpm	Revolutions per minute
SAM	Self-assembled monolayer
SD	Standard deviation
SPR	Surface plasmon resonance
UV	Ultraviolet

Chapter 1. Introduction

1.1 Context and Issues

Rapid detection of pathogenic bacteria in water environments is of primary importance to health organizations responsible for providing effective protection against diseases among humans exposed to industrial and surface waters (Ashbolt, 2004; Rose et al., 2001). Presently, culture-based methods are considered as the gold standard for detecting pathogenic bacteria (Dwivedi and Jaykus, 2011; Foddai and Grant, 2020). However, these techniques are both labour and time intensive (Lazcka et al., 2007; Velusamy et al., 2010). For instance, in typical culture-based methods, detection of *Legionella pneumophila* (*L. pneumophila*) requires up to ~10 days, since test results are determined based on visible colonies (Behets et al., 2007). In contrast, some rapid tests such as polymerase chain reaction (PCR) and matrix-assisted laser desorption/ionization (MALDI-TOF) based rapid detection of bacteria have gained popularity as they provide accurate and fast detection (Quirino et al., 2014; Trevino et al., 2011). However, highly trained personnel and sophisticated lab requirements are the main constraints for these techniques (Dingle and Butler-Wu, 2013; Tran et al., 2021). Therefore, the biosensors of pathogenic bacteria have gained attention due to their potential to offer fast, portable, cost-effective and easy-to-handle detection (da Silva et al., 2017; Hoyos-Nogués et al., 2018).

L. pneumophila is a pathogenic bacterium, commonly found in water environments and responsible for Legionnaire's disease (Berjeaud et al., 2016; Marchand et al., 2011). Generally, *L. pneumophila* enters to the lungs and causes Legionnaire's disease (Verdon et al., 2008). The remarkable existence of *L. pneumophila* in man-made artificial water systems (*i. e.*, spas, and cooling water towers) has been documented in numerous research reports (Leoni et al., 2018; Mazzotta et al., 2021). It is important to note that among the 60 reported *Legionella* species, the *L. pneumophila* serogroup 1 (SG1) has been found mostly associated (85-90%) with the Legionnaire's disease (Gleason and Cohn, 2022; Verdon et al., 2008). In view of the continuously increasing outbreaks of Legionnaire's diseases, the detection of *L. pneumophila* in water environments is important to protect the users of man-made artificial

water systems. Thus, there is a significant interest in developing a rapid, accurate, sensitive, and inexpensive biosensor for *L. pneumophila*.

A variety of immunosensors have been investigated, such as those based on optical (Manera et al., 2013), piezoelectric (Lucarelli et al., 2008) and electrochemical effects (Arora et al., 2011; Hoyos-Nogués et al., 2018). However, many sensors are restricted to laboratory testing as they are highly sensitive to operational environments such as temperature and pH (Castle et al., 2021; Kim et al., 2019). Electrochemical impedance spectroscopy (EIS) biosensors have renewed attention due to highly sensitive detection approaching 1 CFU/mL (Castle et al., 2021; Jafari et al., 2019). However, it is hard to get reproducible results since the performance is highly influenced by the operational buffers conditions and chemistry (Castle et al., 2021; Vogiazi et al., 2019). Surface plasmon resonance (SPR) biosensors offer several advantages including high sensitivity, label-free detection, and real-time measurements (Lin et al., 2007; Šípová et al., 2010). SPR-based biosensors are highly influenced by temperature variations and require special temperature-stabilizing chambers (Huang et al., 2012; Šípová et al., 2010). Colorimetric paper-based biosensors have the ability to monitor the presence of bacteria by visually monitoring color changes without any complex and expensive transducers like other biosensors (Albalat et al., 2014; Nuthong et al., 2018). Nevertheless, this technique suffers from its low sensitivity and the high concentration of target needed to transform biochemical reactions into measurable color variations (Albalat et al., 2014).

Recently, the opto-electronic properties of GaAs/AlGaAs semiconductors have been investigated for the operation of innovative photocorroding transducers (Aziziyan et al., 2016; Nazemi et al., 2015). They provide a highly sensitive response to environmental changes occurring in the vicinity of their surfaces (Aziziyan et al., 2020; Nazemi et al., 2017) that could be easily monitored through the photoluminescence (PL) emission. Thus, the GaAs/AlGaAs nano-heterostructures could be an attractive option for the detection and monitoring biological activities of pathogenic bacteria with the PL signal (Aziziyan et al., 2020) that strongly depends on the presence of surface trapped electrically charged molecules (*i.e.* proteins, virus and bacteria) (Aziziyan et al., 2016; Nazemi et al., 2015). The formation of PL intensity maximum is observed with the transition from GaAs-electrolyte to AlGaAs-electrolyte (Aziziyan et al., 2016). Once the semiconductor sample is exposed to light

(photons with the energy exceeding the GaAs bandgap), the built-in electric potential separates photo-excited electrons (e^-) and holes (h^+) in the depletion region of the semiconductor (Aziziyan et al., 2016). The holes (h^+), driven by the electric surface potential, arrive at the electrolyte/semiconductor interface and induce the formation of surface oxides. Among those oxides, Ga_2O_3 is quite stable in water (Choi et al., 2002; Ruberto et al., 1991), but is easily dissolvable in ammonia environments (Aziziyan et al., 2016). Generally, the formation of Ga_2O_3 reduces the formation of surface states and thus decreases the electron-hole surface recombination velocity (Aziziyan et al., 2016). This leads to the enhanced intensity of the PL signal emitted by the semiconductor (Nazemi et al., 2015; Passlack et al., 1995). It is important to note that the rate of photocorrosion and the formation of PL maximum could be delayed or accelerated with the exposure to negatively charged molecules in the vicinity of GaAs/AlGaAs biochips (Aziziyan et al., 2016). We hypothesized that the length of bio-architecture or biorecognition ligands for trapping targeted analytes such as bacteria could also influence the sensitivity of such biosensors.

A few recent studies accomplished by our group have shown that this sensor offers highly sensitive and rapid detection of bacteria like *L. pneumophila* at 10^3 - 10^4 CFU/mL within an hour (Aziziyan et al., 2016; Aziziyan et al., 2020), which is a relatively short time and sensitive compared to most available biosensing techniques. Moreover, this sensor is associated with low cost and can easily be miniaturized (Nazemi et al., 2018) compared to other biosensors.

The selective bacterial capture efficiency of bio-recognition ligands and the charge transfer are crucial for obtaining a proper and accurate biosensing signal, especially in the case of charge sensitive biosensors (Elakkiya and Matheswaran, 2013; Ramanavičius et al., 2006). Several bio-recognition ligands such as antibody (Ab) (Skottrup et al., 2008), carbohydrate (Guo et al., 2012), aptamer (Yi-Xian et al., 2012), peptides (Etayash et al., 2014a) and combinations of these have been widely investigated in biosensing research. Among these, antibodies have been considered as an attractive option due to their highly specific reaction with the antigenic target sites (Pérez-López and Merkoçi, 2011; Skottrup et al., 2008). Some researchers have employed Ab-based biosensors for detection of *L. pneumophila* in the range of 10^3 to 10^4 CFU/mL (Aziziyan et al., 2016; Li et al., 2012). However, it has been known that

antibodies suffer from the lack of stability, especially while detecting pathogens under harsh environments (Iqbal et al., 2000; Templier et al., 2016). In some cases, additional binding agents (*i.e.*, biotin and neutravidin) could enhance the surface coverage with Abs, which would increase the probability for the efficient trapping of bacteria (Estevez et al., 2014; Schiller, 2019). Also, the distance between the biochip surface and bacteria captured by Ab-based bio-architecture is at least at ~15-18 nm, which could result a less sensitive response of biosensors due to the inefficient charge transfer between bacteria and sensor substrates.

Recently, some studies have shown that antimicrobial peptides (AMPs) could be employed as bio-recognition elements in biosensing platforms (de Miranda et al., 2017; Dong and Zhao, 2015; Etayash et al., 2013). AMPs contain multiple niches that act as recognition elements, which is advantageous for an enhanced binding of bacteria and fungi (de Miranda et al., 2017; Mannoor et al., 2010). The increased stability of AMPs in comparison to typical globular proteins is also considered attractive for biosensing applications (Hoyos-Nogués et al., 2018; Mannoor et al., 2010). It has also been reported that some cationic AMPs show attractive binding abilities even under extreme environmental conditions, such as autoclaving and boiling (Mannoor et al., 2010; Qiao et al., 2020a). Therefore, the AMPs based biosensing could be considered as a potential replacement of typical antibody-based biosensing techniques. Some AMPs, such as Magainin I (Kulagina et al., 2005), Clavanin A (Andrade et al., 2015) and polymyxin B (Kulagina et al., 2006), have been employed as bio-recognition probes in biosensing devices. In related studies, some AMPs have shown a semi-selective binding nature to the target cells. Hence, the sensors suffered from a lack of specificity (Mannoor et al., 2010). Other AMPs have shown high specificity to the target cells. For instance, Mannoor et al. (2010) reported that the gold electrode functionalized with Magainin I AMP showed differential binding affinity to the pathogenic bacterial strains of *E. coli* and *Salmonella* spp. In another study, Hossein-Nejad-Ariani et al. (2018) reported that the gold microelectrode functioned with Leucocin A (Leu A) showed high binding specificity/affinity to the *Listeria monocytogenes*. Recently, the warnericin RK (WRK) AMP has been reported to be selective against *L. pneumophila* (Berjeaud et al., 2016; Corre et al., 2018; Marchand et al., 2011; Verdon et al., 2008; Verdon et al., 2011). Thus, this peptide could be considered as a ligand for designing *L. pneumophila* sensors and alleviate limitations of traditional Ab based

immunosensors. However, the advantage of the specific interaction between WRK AMP and *L. pneumophila* has not been exploited in biosensing technology to date.

1.2 Problem statement

To date, results have indicated that the digital photocorrosion (DIP) biosensing technique allows direct detection of *L. pneumophila* down to 10^3 - 10^4 CFU/mL (Aziziyan et al., 2016; Aziziyan et al., 2020). As the sensitivity of DIP biosensors (and other biosensors) is associated with the efficiency of bacterial capture, identifying new immobilization architectures different than those based on mammalian antibodies (Ab) seems justifiable. This is particularly important in view that the mammalian antibodies are known to suffer from batch-to-batch inconsistencies, as well as having a limited stability that could reduce the consistency of biosensors (Byrne et al., 2009; Silva et al., 2020). Moreover, Ab based architectures maintain significantly longer distance (~10-12 nm) between biosensor substrate and target analytes which might not be advantageous for charge transfer in charge sensitive biosensors. Therefore, I propose to investigate the possibility of building short ligand biosensing architecture with minimized distance between the sensor substrate and a target analytes for enhancing the sensitivity of biosensors. In this context, AMPs are investigated for building an innovative GaAs/AlGaAs DIP biosensor for *L. pneumophila*.

In general, the biorecognition ligands including AMPs are immobilized on biosensor surfaces by utilizing a covalent interaction between an alkanethiol self-assembled monolayer (SAM) and ligands (de Miranda et al., 2017; Li et al., 2015; Mannoor et al., 2010). In this context, sulphur containing long carbon chain molecules such as 16 mercaptohexadecanoic acid (MHDA), 11- mercaptoundecanoic acid (MUDA) *etc.* thiols are covalently immobilized on gold and Ga based surfaces and followed by the conjugation of AMP with thiols (Aziziyan et al., 2016; Etayash et al., 2014a). However, the entire process requires more than 20 hours plus detection time for employing a biosensor. This procedure is associated with several steps that might not be effective to obtain reproducible performance of biosensors. Furthermore, in the case of charge-sensitive biosensors, the short distance between the biochip surface and target analytes could substantially improve the process of charge transfer. Therefore, the ligand with short linker could significantly enhance charge transfer efficiency and reduce the time and steps of the biosensors functionalization process.

Despite the known inferior ability of AMP to selectively capture bacteria compared to antibodies, the AMP based biosensors showed an attractive sensitivity to targeted bacteria. Some AMPs have shown higher binding affinity against certain bacterial species (D'Souza et al., 2018; Qiao et al., 2017b). For instance, the warnericin RK has been found to have higher biding affinity against *L. pneumophila* compared to other *Legionella* species. However, the relatively broad specificity spectrum of AMP towards bacteria raises the question of selective detection of *L. pneumophila*, especially serogroup 1 (SG1) that is responsible for over 85% of *L. pneumophila* related disease outbreaks (Berjeaud et al., 2016). To address this problem, I proposed a hybrid sandwich based biosensing architecture consisting of AMP for capturing *L. pneumophila* and subsequent decoration of bacteria with antibody produced after rabbit immunisation *L. pneumophila philadelphia* (SG1 strain) which could be advantageous for selective detection of *L. pneumophila* SG1.

1.3 Objectives and research hypothesis

The major objective of this project was to investigate the functionalization of DIP biosensors with warnericin AMP for selective detection of *L. pneumophila*. In view of the unknown response of the proposed biosensing architecture for capturing and detecting *L. pneumophila*, the objective was also to determine if the proposed warnericin AMP architecture would allow detecting *L. pneumophila* with sensitivity comparable to that of the other *L. pneumophila* biosensors. Depending on the results of the preliminary research, the proposal was to continue the research of warnericin AMP based DIP biosensors, or execute a plan B, *e.g.*, addressing the research of recombinant antibody-based DIP biosensors. In the frame of this project I also investigated the feasibility of an AMP DIP biosensor for selective detection of *L. pneumophila* at low concentration in samples originating from cooling tower water.

1.3.1 Investigation of a direct (label free) detection of *L. pneumophila* with AMP functionalized GaAs/AlGaAs DIP biosensors

Warnericin AMP can selectively interact with *L. pneumophila* through the phosphatidylcholines lipids present on the surface of bacteria. The hypothesis was that warnericin AMP based DIP biosensor would selectively capture *L. pneumophila* with a sensitivity at least comparable to that of a polyclonal Ab functionalized DIP biosensor. This

would justify undertaking follow-up research in view of the greater temperature and pH tolerance of AMPs compared to antibodies.

1.3.2 Investigate sensitivity of GaAs/AlGaAs DIP biosensors with cysteine-modified warnericin RK AMP for detecting *L. pneumophila*

The attachment of warnericin AMP to the surface of a DIP biochip requires the attachment procedure similar to that of antibody. This involves deposition of MHDA SAM on the biochip surface and the 1-ethyl-3-(-3-dimethylaminopropyl) carbodiimide/N-hydroxysuccinimide (EDC/NHS) chemistry producing amine-reactive NHS-ester. In contrast, the use of a cysteine modified AMP would allow its capture directly on the GaAs/AlGaAs surface and eliminate the need of MHDA SAM. Furthermore, the shorter length of a cysteine-based ligand would address the question concerning potentially more efficient interaction between bacteria and the biochip sensitive to charge transfer from/to bacteria. The hypothesis was that a short-ligand DIP biochip would deliver sensitivity comparable to that of a biochip comprising a MHDA SAM. The advantage of such a solution would be a much simpler biofunctionalization procedure completed in a significantly shorter time.

1.3.3 Investigate an antibody based sandwich method to provide a more specific (selective) detection of *L. pneumophila* with a warnericin AMP biosensor

The specificity of the proposed sensor is a concern and might not be attractive compared to other reported ligands. Thus, the integration of another ligand highly selective to the *L. pneumophila* could enhance the specificity and, potentially, sensitivity of DIP biosensors. If *L. pneumophila* can be captured through AMP functionalized biosensors, as this peptide exhibits higher capture ability, the subsequent decoration with another specific ligands such as antibodies would allow alleviating the problem of insufficient specificity of warnericin AMP towards *L. pneumophila*. To investigate this effect, the selective detection of *L. pneumophila* serogroup-1 (SG1) and serogroup-5 (SG5) was attempted in water from cooling tower.

1.4 Thesis layout

This thesis is designed with 6 chapters

Chapter 1 deals with the current contexts and issues of biosensors for the detection of pathogenic microbes. The limitations of currently practiced culture and biosensors-based detection of pathogenic bacteria especially *L. pneumophila* are discussed in this chapter. Moreover, the influence of biorecognition ligands for detecting *L. pneumophila* is described in this section. The prospects of short ligands in biosensing techniques are also discussed in this chapter. Finally, the objectives of current thesis including research questions and hypothesis are presented.

Chapter 2 reviews the different biosensing approaches for detecting pathogenic bacteria. The prospects and concerns, limit of detection (LOD), time of detection, and dynamic range of performances for these approaches are included in this chapter. Moreover, the structure and components of typical biosensors and common bioreceptors used to detect pathogens including their advantages and limitations are discussed in this section. The application of short ligand (*e.g.* AMP) in biosensing techniques is widely discussed in different aspects such as i) structure of AMP, ii) the interaction between AMPs and bacteria, iii) the tethering mechanism of AMP on biosensors surface, iv) the specificity of AMP towards bacteria and application of AMP as ligand of biosensors. The concept of a semiconductor optical biosensor and digital photocorrosion (DIP) biosensing is also discussed in the chapter.

Chapter 3 presents the detection of *L. pneumophila* using AMP functionalized GaAs/AlGaAs DIP biosensor. This chapter describes the limitation of mammalian antibodies related to batch-to-batch variation, as well as their limited stability while used as biorecognition ligands in biosensors. In this context, an AMP warnericin RK functionalized GaAs/AlGaAs biosensors was developed to detect *L. pneumophila*. The binding affinity and specificity of designed sensors were investigated by exposing some of non-targeted bacteria such as *E. coli*, *B. subtilis* and *P. fluorescens* (which may be found in natural and industrial water environments). The advantages and limitations of such AMP functionalized biosensors

in terms of detection time, specificity, and LOD are discussed in this chapter. This chapter has been published in *Biochemical Engineering Journal* (Elsevier).

Chapter 4 demonstrates the innovative concept of a short linker architecture (Cys-AMP) for designing a GaAs/AlGaAs biosensor to detect low concentrated *L. pneumophila* in water environment. The optimum concentration of peptide for capturing *L. pneumophila* was determined using several techniques, such as Fourier-transform infrared (FTIR) absorption spectroscopy, atomic force microscopy (AFM), X-ray photoelectron spectroscopy (XPS), and water contact angle measurements. The specificity of developed biosensor was investigated against a number of bacteria abundantly found in samples of the environmental water (*i. e., P. fluorescens*, *B. subtilis*, and *E. coli*). Some important consequences of the designed biosensors including functionalization time, reproducibility, applicability in real water environment, LOD, total time of detection are discussed in this chapter. This chapter is published in *ACS Omega* (American Chemical Society journal).

Chapter 5 focuses on selective detection of *L. pneumophila* SG1 and SG5 in water originated from cooling tower with a DIP sandwich strategy. The biochips were functionalized with Cys-WRK AMP for capturing bacteria and subsequently decorated with the anti-*L. pneumophila* polyclonal Ab (pAb). The influence of additional negatively charges molecules on response of charge sensitive DIP biosensors is investigated and discussed in this chapter. The specificity of the biosensor was rated against *P. fluorescens*, *B. subtilis*, and *E. coli*. The limitations of conventional biosensors particularly for selectively detecting *L. pneumophila* SG1 in harsh water environment (*i.e.,* water originated from cooling tower) has been discussed in this chapter. This chapter is published in *Biosensors* (Molecular Diversity Preservation International journal).

Chapter 6 summarizes and overviews the entire document. The perspectives and suggested future research are discussed in this chapter.

Chapter 2. State of the art

2.1 Detection of pathogenic bacteria

The detection of pathogenic bacteria is crucial for preventing crises related to human health, safety and security (Hameed et al., 2018; Rajapaksha et al., 2019). A number of conventional approaches such as microscopic visualization, culture-based identification, biochemical tests or molecular analysis have been employed to detect pathogenic bacteria as presented in Table 2.1. However, these techniques require either lengthy time, specialized laboratories, or expensive equipment (Burlage and Tillmann, 2017; Hameed et al., 2018). Although the microscopic analysis of bacteria is relatively quick and inexpensive, the identification of pathogenic bacteria is not accurate as it does not offer selective detection of bacteria (Beveridge et al., 2007). Moreover, the microbial staining for microscopic visualization of bacteria requires a proper bacterial smear that can be difficult to execute (Beveridge et al., 2007). Improper bacterial smearing could result in over-staining, break bacterial membrane or destroy cells, or even loss of morphological characteristics of the bacteria (Jayan et al., 2019). The culture-based detection of pathogens is a time-consuming process required for the bacterial cell to develop a visually observable colonies on selective media (colony-forming units on agar media or turbid liquid media) that may require even several days (Hameed et al., 2018; Roda et al., 2012) and not all bacteria can be grown in laboratory conditions using conventional culture media (Ahmed et al., 2014; Hameed et al., 2018). Immunological tests and biochemical assays such as enzyme-linked immunosorbent assay (ELISA) and matrix-assisted laser desorption/ionization-time of flight (MALDI-TOF) are attractive methods for detecting specific bacteria (De Bruyne et al., 2011; Hameed et al., 2018). However, they are costly and time-consuming, requiring advanced technical skills and expertise for data interpretation (Burlage and Tillmann, 2017). The molecular analysis allows the detection of specific bacteria using the genetic material of bacteria; however, it is an expensive and sophisticated procedure (Gilbride et al., 2006; Jayan et al., 2019). Although the real-time polymerase chain reaction (PCR) technique requires short analytical time (a few hours), it is associated with trained users along with specialized equipment (Oblath et al., 2013; Valones et al., 2009). In addition, sample enrichment and DNA purification are needed for reverse

Table 2.1 An overview of conventional pathogenic bacteria detection techniques.

Detection techniques	Representative bacteria detected	Sample pre-concentration time	Detection time	Limit of detection	References
Lateral flow immunoassay	*S. typhimurium*	12 h	-	4.6×10^7 CFU/mL	(Shukla et al., 2014)
	S.enterica serovar *typhi*	6 h	10 h	10^4–10^5 CFU/mL	(Kumar et al., 2008)
Conventional PCR	*E. coli* and *Shigella* spp.	8 h		1–2 Cells/100 mL	(Tsen et al., 1998)
Multiplex PCR	*S. enteritidis, Salmonella* spp.	24 h	-	10^5 CFU/mL	(Shi et al., 2010)
	Staphylococcus aureus, E. coli O157, Salmonella spp. *L. monocytogenes, Yersinia enterocolitica*	24-48 h	15 min	10^1-10^3 CFU/mL	(Guan et al., 2013)
Real-time PCR	*L. monocytogenes, Salmonella* spp.	24 h	1 h	5 CFU/25 g	(Shi et al., 2010)
	S. aureus, Salmonella, Shigella	-	-	9.6 CFU/g 2.0 CFU/g 6.8 CFU/g	(Ma et al., 2014)
	Conjugated E. coli DH5α	Overnight	<3 h	Low	(Nayak et al., 2013)
NABSA	*S. typhimurium* *S. enteritidis*	24 h	<90 min	10 CFU/mL	(Mollasalehi and Yazdanparast, 2013)
LAMP	*V. vulnificus*	6 h	8 h	5.4 CFU per reaction	(Han et al., 2011; Singhal et al., 2015)
	V. parahaemolyticus	Overnight	1 h	10 CFU/ reaction	(Wang et al., 2013)
	V. parahaemolyticus	12 h	1 h	7.2 copies/μL	(Xia et al., 2016)
MALDI-TOF	*Leuconostoc* spp., *Fructobacillus* spp., *Lactococcus* spp.	24 h	<1 h	-	(De Bruyne et al., 2011)

DGGE	*Bacillus pumilus, B. megaterium, B. thuringiensis, B. firmus*	48 h	-	10 CFU/mL	(Garbeva et al., 2003)
Metagenomics approach	*Borrelia* spp., *Rickettsia* spp., *Candidatus* spp., *Neoehrlichia* spp.	-	<48 h	-	(Carpi et al., 2011)
ELISA	*E. coli* O157	24 h	3 h	68 CFU/mL in PBS and 6.8×10^3 CFU/mL in food samples	(Shen et al., 2014)
DNA microarray (Coupled with qPCR)	*E. coli*	-	-	5 ng of *E. coli* DNA	(Deshmukh et al., 2016)
FISH	*P.aeruginosa*, *S. aureus, Streptococcus* spp., *Micrococcus* spp.	24-28 h	-	-	(Malic et al., 2009)

DGGE: denaturing gradient gel electrophoresis; PCR: polymerase chain reaction; qPCR: quantitive polymerase chain reaction; MALDI-TOF: matrix-assisted laser desorption ionization time-of-flight; NABSA: nucleic-acid sequence-based amplification; LAMP: loop-mediated isothermal amplification; FISH: fluorescence in situ hybridization.

transcriptase-polymerase chain reaction (RT-PCR) (Burlage and Tillmann, 2017; Oblath et al., 2013). Therefore, it is necessary to develop a fast, sensitive, easy to handle and cost-effective method, to detect pathogenic bacteria.

2.2 Biosensors for pathogens detection

The biosensor can be defined as an analytical device, capable of converting biological responses into an electrical signals (Habimana et al., 2018; Kumar et al., 2016). A biosensor conventionally comprises two major elements, a bio-recognition element and a transducer (as shown in Figure 2.1) together with signal amplification, processing system and software (Hoyos-Nogués et al., 2018; Riedel and Lisdat, 2017). Bio-recognition elements are also known as bio-receptors, *i.e.,* enzymes, antibodies, peptides, functional nucleic acids, bacteriophages and even whole cells that could specifically recognize as well as interact with ~~a~~ target analytes (Hoyos-Nogués et al., 2018; Pashazadeh et al., 2017). Generally, the

electrochemical, mechanical, and optical or combinations of them are considered as transducing elements (Hoyos-Nogués et al., 2018; Li et al., 2018).

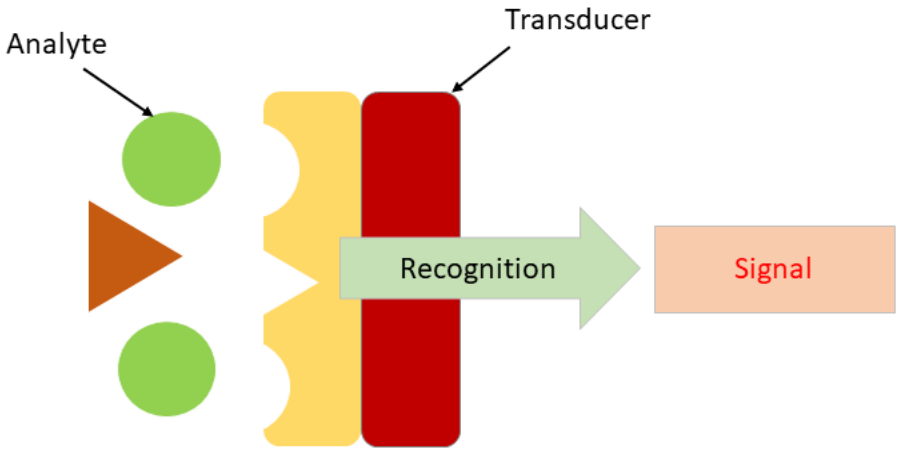

Figure 2.1 Schematic view of typical biosensor architecture.

Biosensor-based detection of pathogenic bacteria has gained attention as it is advantageous compared to conventional methods and requires minimal pre-enrichment of samples (Hoyos-Nogués et al., 2018; Roda et al., 2012). Moreover, this technique addresses rapid, robust, cost-effective, and portable detection that could be advantageous compared to conventional methods (D'Souza et al., 2018; Wisuthiphaet et al., 2019). It is worthy to note that some viable but non-culturable bacteria can be detected through the biosensor (Leonard et al., 2003; Pienaar et al., 2016). The biosensors based detection of pathogenic bacteria is summarized in Table 2.2. Recent studies (Ahmed et al., 2014; Li et al., 2012) have shown that biosensors can successfully detect low concentrations of pathogenic bacteria, which is attractive for field level application. However, most of the biosensing techniques suffer from several limitations such as sensitivity, specificity, and reproducibility that make them practically inapplicable.

Table 2.2 An overview of biosensor based detection of pathogenic bacteria.

Detection techniques	Types	Advantages	Limitations	Bacteria detected	Sample pre-concentration time	Detection time	Limit of detection	References
Optical biosensors	SPR/SERS	- Highly specific - Rapid - Real-time	- High cost -Surface modification is challenging	*L. pneumophila*	-	30 min	$1x10^3$ CFU/ mL	(Manera et al., 2013)
				E. coli O157	9-12 h	16 min	5 CFU/25g of food samples	(Mondani et al., 2016)
				S. enterica serovar Typhimurium	24 h	N. A	15 CFU/mL	(Duan et al., 2016)
				E. coli O157	Overnight	1 h	$1x10^2$ CFU/mL	(Najafi et al., 2014)
	Colorimetric	- Not require transducers - Low cost	-Not quantitative -Low sensitivity	*V. Parahaemolyti -cus*	18 h	45 min	2.4 CFU/mL	(Sadsri et al., 2020)
Electroche-mical biosensors	Amperometric	- Simple - Low cost	-Highly sensitive to the environment	*L. pneumophila*	5 days	3 h	10^4 CFU/mL	(Martín et al., 2015)
	Potentiometric	- Can analyze multiple samples	-Highly sensitive to the environment	*S. aureus*	48 h	N. A	$8x10^2$ CFU/mL	(Zelada-Guillén et al., 2012)

	Impedimetric	- Simple -Real-time detection	-Highly sensitive to the environment	*L. monocytogenes*	19 h	3 h	10^4-10^5 CFU/mL	(Kanayeva et al., 2012)
Mass-based biosensors	Cantilever	- Simple -Real-time detection	-Low reproducibility	*S. typhimurium*	-	N. A	$1x10^3$ CFU/mL	(Shi et al., 2017)
	QCM			*B. anthracis*	-	N. A	$1x10^3$ CFU/mL	(Hao et al., 2009)

SPR; SERS (Surface enhanced Raman spectroscopy), and QCM (quartz crystal microbalance) techniques.

2.3 Bioreceptors used for pathogenic bacteria detection

Bioreceptors play a crucial role in biosensing, as they recognize targeted analytes and also determine the efficiency of sensors through the specificity and sensitivity (Justino et al., 2015; Velusamy et al., 2010). Therefore, the performance of a sensor is associated with the selection of bioreceptors (Hoyos-Nogués et al., 2018; Qiao et al., 2020a). However, the stability of bioreceptors strongly influences the binding affinity and performance of biosensors (Templier et al., 2016; Vasilescu et al., 2016). Bioreceptors ranging from small molecules (*i.e.,* enzymes, short peptides, sugars, and nucleic acid) to large molecules (*i.e.,* proteins, viruses, and whole cells) are being widely used for detecting bacteria (Hoyos-Nogués et al., 2018; Qiao et al., 2020a). Several representative biomolecules used as bioreceptors are presented in Figure 2.2.

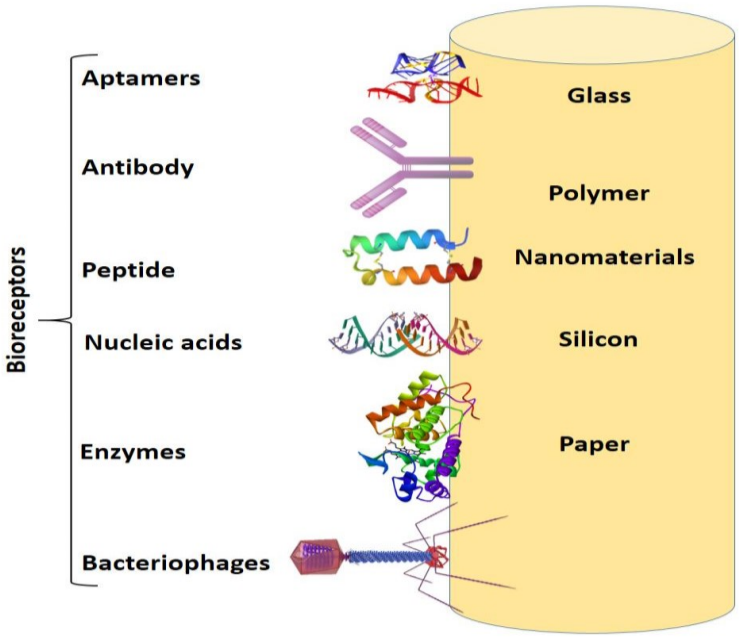

Figure 2.2 Graphical representations of different biorecognition elements for bacterial detection.

In general, large molecules, especially proteins and bacteriophages, have shown higher specificity compared to the smaller molecules (Justino et al., 2015; Templier et al., 2016). In contrast, synthetic and small molecules have found with higher stability and can easily be optimized (Cambray et al., 2018; Lazcka et al., 2007). However, none of them are considered

a perfect candidate to make the sensors practically applicable. The advantages and limitations of different biorecognition elements used in biosensing platforms are discussed in Table 2.3. In biosensing technology, antibodies are widely used for bacteria detection due to high specificity in pathogen seizing as well as recognition (Aziziyan et al., 2016; Habimana et al., 2018; Wu et al., 2014). The polyclonal, monoclonal, and recombinant antibodies can be distinguished based on their selective natures and their production methods as shown in Table 2.4. Among the three types of antibodies, monoclonal antibodies are more advantageous compared to others due to their high specificity (Mo and Drancourt, 2004). The antibody is preferred as a bio-receptor because it is simple and easy to handle during bio-functionalization of sensor substrates (Law et al., 2015). However, the differentiation between

Table 2.3 An overview of different bio-recognition elements used for bacteria detection.

Category	Advantages	Limitations	Reference
Antibody	• Allows to detect different kinds of cells and cell metabolites • Allows highly specific reaction between antigen-antibody conjugates • Allows direct recognition • Allows non-invasive interaction	• They are not capable of distinguishing between live and dead bacterial cells • Batch-to-batch consistency is found, especially in the case of polyclonal antibody • Longer times and higher costs are required to produce them • Cannot recognize after slight modification in the target analytes • Lower stability in low or high pH, ionic solutions, and high temperature	(Bazin et al., 2017; Liu et al., 2018)
Enzymes	• Detecting target analytes based on catalytic activity • They are highly stable even for a year • Strongly bind with the target analytes	• Require more than one assay steps • Show less stability under extreme environmental conditions (*e.g.,* temperature, pH) • In some cases,	(Habimana et al., 2018; Hwang et al., 2016)

		interfere with endogenously produced enzymes by target analytes • Catalytic efficiency predominantly depends on the sequence of the DNA	
Nucleic acids	• Determine target analytes based on complementary nucleic acid sequences, hence it allows highly specific detection • Nucleic acids could be promptly extracted and regenerated compared to typical antibody, enzymes, and proteins production	• Costly methods • They are less soluble in the water environment • Not stable in harsh environment (sensitive to pH and temperature) and difficult to make portable and automated sensors using them	(Habimana et al., 2018)
Aptamer	• Recognition of analytes based on shape but not sequences • They are highly stable and easy to modify • Enhances interaction due to possession of multiple functional groups • Rigid backbone • Capacity to confer a cellular phenotype	• False-positive results are seen while dealing with large molecules • Semi-selective binding	(Habimana et al., 2018; Mascini et al., 2012).
Antimicrobial peptides	• Highly stable and could be produced in a large quantity using synthetic methods • Multiple niches are advantageous to capture a significant number of target analytes	• In most of the cases, they are semi-selective or non-selective • They are not considered as efficient for a long time incubation since they are invasive to the target analytes	(Habimana et al., 2018)

Bacteriophages	• Wide-range libraries • Allows to genetically modify after selection • Allows selection against a toxic or low immunogenic target	• Unable to recognize gram-negative bacteria because of thick outer membrane • Targets are required to be immobilized for identifying the efficiency of pages • The immobilization of bacteriophage is considered challenging among biosensors substrate due to weak interactions.	(Harada et al., 2018; Schmelcher and Loessner, 2016)
Molecular imprinted polymers	• Detain original properties in an extreme thermal and chemical condition • Not easily degraded by enzyme • Can be handled both aqueous and organic solvents	• Highly skilled personnel are required to produce them • The production process is time-consuming	(Dinc et al., 2019)

live and dead cells cannot be achieved through the antibody based techniques. In addition, several limitations such as batch-to-batch inconsistency, production challenges, and high cost, restrict their application in biosensing technology (Etayash et al., 2013; Silva et al., 2020).

Table 2.4 Comparison of different types of antibodies.

	Polyclonal	**Monoclonal**	**Recombinant**
Production time	2-3 months	4-6 months	1 week
Reproducibility	Limited	High (in the same batch)	Very high
Specificity	Specific	Highly specific	Very high specificity
Binding mechanism	Multiple	Single	Single
Stability	Moderate	High	Moderate
Cost	Moderate	High	Very high

Nucleic acids (NA) allow quick and specific detection of pathogenic bacteria with low detection limit reaching a single bacterium (Bouguelia et al., 2013). The versatility of NA-based methods allows for designing a specific probe sequence typically in the length of 10-20 base pairs to target a selective gene of bacteria (Lui et al., 2009; Simmel et al., 2019). In NA-based biorecognition elements, DNA is considered as an attractive signal transducer as it contains a negative charge, therefore, producing promising results through the electrical measurements over other typical biosensing detections (*i.e.,* optical and mechanical measurements) (Lui et al., 2009; Riedel and Lisdat, 2017). NA-based detection techniques have shown higher sensitivity compared to others ligands(Bal et al., 2017; Simmel et al., 2019). The inhibitors present in the sample, and the deteriorated DNA could lead to false-negative/positive results (Maffert et al., 2017; Simmel et al., 2019).

Aptamers are short, single-stranded, highly specific and sensitive synthetic oligonucleotides that, can specifically bind to target analytes (*e.g.,* toxins, bacteria, proteins, and hormones) (Hong and Sooter, 2015; Kaur et al., 2018). Generally, aptamers are selected via systemic evolution of ligands by exponential enrichment (SELEX) technique; an efficient screening approach, where the desired aptamers could be successively determined from the oligo-nucleic acid library using repeated cycles of amplification (Habimana et al., 2018; Hong and Sooter, 2015). Aptamer functionalized aptasensors can detect pathogenic bacteria with several advantages, particularly due to the ease of modification and stability (Hoyos-Nogués et al., 2018; Majdinasab et al., 2018). However, aptasensors are not preferred to detect large molecules such as whole bacteria due to the capture inefficiency(Paniel et al., 2013; Saha et al., 2012).

Bacteriophages are considered an efficient bio-recognition element as they allow fast and highly selective detection of bacteria (Richter et al., 2018; Singh et al., 2012). In the biosensors, the natural affinity of bacteriophages towards the host bacterial cells can be utilized to design highly specific biosensor substrates (Gervais et al., 2007; Richter et al., 2018). In addition, bacteriophages can survive and retain their activity in high temperatures (up to 76 $^{\circ}$C) and inorganic solvents (Ertürk and Lood, 2018; Richter et al., 2018). Hence, they are considered as robust bioreceptors compared to others (Brigati and Petrenko, 2005; Ertürk and Lood, 2018). Unlike antibodies, a larger quantity of phages

could be easily and inexpensively produced. A significant number of phages can be generated by simply infecting a bacterium with a phage. Thus, the phages are considered as promising bio-recognition elements in biosensor-based detection of pathogens (Richter et al., 2018; Singh et al., 2012). Besides, the phage-based biosensors can distinguish live and dead cells as the phages can replicate solely within the viable bacteria (Richter et al., 2018; Singh et al., 2012). However, several limitations are involved with the use of phages in biosensing techniques, especially due to difficulty to immobilize on the sensor surface, and the lower stability (Aliakbar Ahovan et al., 2020; Hussain et al., 2021).

Molecularly imprinted polymers (MIPs) are another bioreceptor applied in the form of matrices of polymers that target specificity of an analyte in several ways, such as size exclusion or inclusion (Cieplak and Kutner, 2016; Hebert, 2016). The turbidity of MIPs is regulated by several factors such as functional monomers, target bio-analytes, cross linkers, and solvents (Hebert, 2016; Wackerlig and Schirhagl, 2016). Generally, MIPs can capture target analytes as they can form synthetic bio-recognition between the polymer matrix and bio-analyte (Hebert, 2016). Unlike typical bio-recognition elements, MIPs are synthetically fabricated for an individual target bio-analyte (Hoyos-Nogués et al., 2018). Hence, the main advantage of MIPs is the specific interaction between bio-analyte and bio-recognition element. However, the stability of polymer is a major concern in designing MIP-based biosensors for bacterial pathogen detection.

2.4 Antimicrobial peptides

AMPs are small peptide fragments commonly found in several living organisms in the range of prokaryotes to multi-cellular organisms (Marshall and Arenas, 2003; Qiao et al., 2020b). AMPs are a vital part of native immune systems that attack pathogens for protect the hosts (Gomez et al., 2013; Zhang et al., 2019). Moreover, AMPs have been considered as potential therapeutic agents to treat infections because of their substantial performance against pathogens (Cruz et al., 2014; Mahlapuu et al., 2020). It has been reported that the AMP contains 6–50 amino acids (AAs) residue, which generally possess a net positive charge (in the range of +2 to +11) (Hancock and Sahl, 2006; Lai et al., 2019). Typically, more than 50% of AMPs are hydrophobic in nature (Cruz et al., 2014; Qiao et al., 2020b). They are commonly

divided into three categories such as i) α-helix, ii) β-helix, or iii) peptides based on their secondary structures (Li et al., 2017; Mahlapuu et al., 2016). Most AMPs are usually unstructured in aquatic solutions, however, they can easily be adopted and converted into the amphipathic helical structure while getting in contact with negatively charged bacterial membranes, which is crucial to demonstrate their activity against bacteria (Li et al., 2017; Qiao et al., 2020b). To date, over 2500 AMPs have been reported in the literature (Geitani et al., 2020; Qiao et al., 2020b). A representative helical structure of a peptide is presented in Figure 2.3.

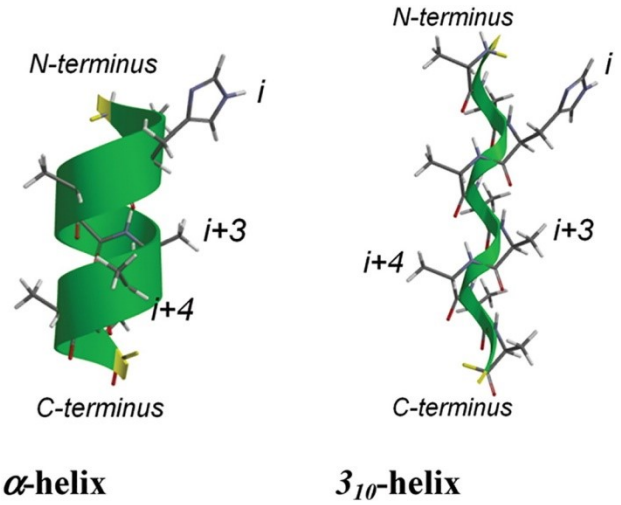

Figure 2.3 The helical conformation of peptides, α-helix (a), 3_{10} helical conformations based on a histidine/polyalanine 9-mer peptide displaying the positions of *i* residues (*i* + 3, and *i* + 4) (Puiu and Bala, 2018) (b).

AMPs are highly stable molecules that could be produced in large quantities using several synthetic methods (Giuliani et al., 2007; Zasloff, 2002). It is interesting to note that these molecules have also been used as biorecognition elements for selectively capturing target analytes, particularly bacteria (Hoyos-Nogués et al., 2018; Mannoor et al., 2010). The interaction between AMPs and the phosphate group of bacteria LPS has been exploited in biosensing technology addressing detection, quantification, and classification of bacteria (Etayash et al., 2013; Pavan and Berti, 2012). AMPs can be employed as spacers or chemo-selective anchors to selectively functionalize a diverse range of surfaces (Li et al., 2020; Qiao et al., 2020a). These chemo-selective anchoring groups allows them to efficiently immobilize target analytes on the surface of sensor substrates (Hoyos-Nogués et al., 2018; Zhang et al., 2019).

2.5 Interaction between AMP and bacteria

Several mechanisms of interaction between bacteria and AMPs have been reported to date, however, the exact mechanism is not well known (Qiao et al., 2020b; Yeaman and Yount, 2003). It has been suggested that the cationic AMPs at first bind with the surface of bacterial membrane through the hydrophobic and electrostatic interactions, and subsequently, alter the structure of cell membranes in several ways (*i.e.,* Carpet model, Barrel-staves" model, and Toroidal-pore model) (Qiao et al., 2020b) as shown in Figure 2.4. The cationic AMPs attach to the outer cell membrane through the phosphate group present in lipopolysaccharides or the

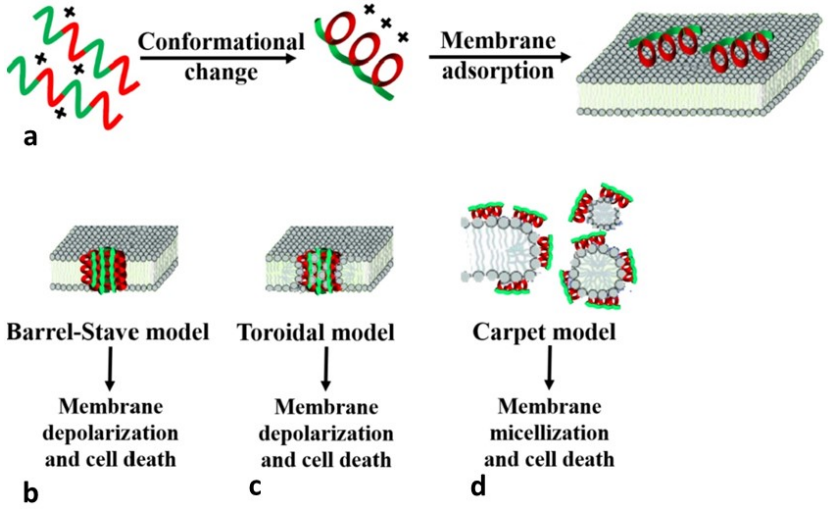

Figure 2.4 The interaction between AMPs and bacteria membrane (a); the schematic diagram of three predominant models such as Barrel-Stave (b), Torroidal (c), Carpet (d) model proposed for interaction between AMP and bacteria (Qiao et al., 2020b).

teichoic acids (Puiu and Bala, 2018). It has been reported that the AMPs interact with the bacterial surfaces as an "I state" or a "S state", where I is denoted for insertion and S is denoted for surface (Huang, 2000; Qiao et al., 2020b). Notably, the AMPs adsorb on the microbial surfaces by following the ratio of low peptide to lipid. While the peptide-to-lipid ratio reaches a threshold concentration, the AMP orientation becomes perpendicular (Dennison et al., 2007). During this process, the linear AMPs tended to fold due to the creation of a hydrophobic environment on the cell membrane (Manzo et al., 2015). Subsequently, the peptides start interacting with the cytoplasmic membrane of microorganisms (Geitani et al., 2020).

2.6 Specificity of AMP towards bacteria

The selectivity or specificity of AMP towards bacteria plays an important role for the detection accuracy of pathogenic microbes. It is well known that AMPs can selectively interact with Gram positive and Gram negative bacteria (Etayash et al., 2014a; Malanovic and Lohner, 2016). Bacteria are broadly classified as either Gram-positive or Gram-negative, based on their cell envelopes. Generally, Gram-positive bacteria contain a crosslinked peptidoglycan layer (PGL) surrounded by various negatively charged molecules (*i.e.,* teichoic acid, lipoteichoic acid) as illustrated in Figure 2.5 (Li et al., 2017). AMPs electrostatically interact with

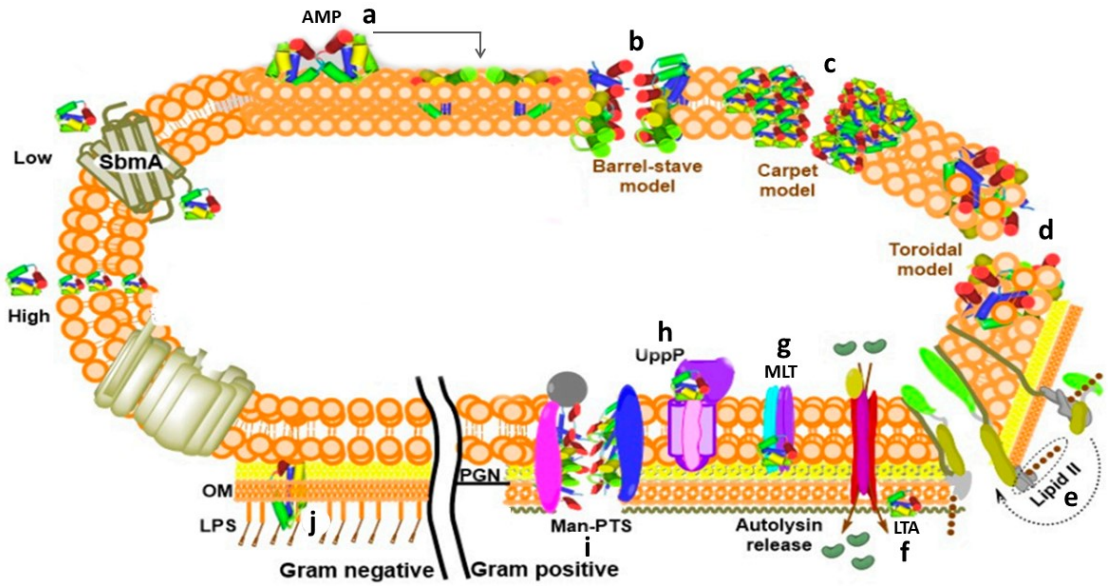

Figure 2.5 Several mechanisms of interaction between AMP and bacteria, the molecular interaction of an AMP and the phospholipid bilayer (a), different mechanisms of peptide attachment into the phospholipid bilayer (b-d), other non-invasive interactions of AMP with lipid II (e), lipoteichoic acid (LTA) (f), maltose transporter (MLT) (g), undecaprenyl pyrophosphate phosphatase (UppP) (h), phosphotransferase system (Man-PTS) (i), and lipopolysaccharides (LPS) (j). PGN: peptidoglycan; OM: outer membrane (Ongey et al., 2018).

these negatively charged molecules and subsequently diffuse through the nano-sized pores present in PGLs (Li et al., 2017; Malanovic and Lohner, 2016). The PGL is less cross-linked and thinner in the case of Gram-negative bacteria. However, Gram-negative bacteria contain an additional membrane known as lipopolysaccharide (LPS) located on the outer part of PGL

(Malanovic and Lohner, 2016). The LPS molecules are decorated with a significant amount of negatively charged phosphate groups, resulting in the interaction between AMP and bacterial envelopes (Li et al., 2017). The reactivity of AMPs with Gram-negative and Gram-positive bacteria varies due to different atomistic interactions (Malanovic and Lohner, 2016). Thus, AMPs such as Lucocin A, C15G2cys were reported to have high activity against Gram-positive bacteria, while negligible activity was observed against Gram-negative bacteria (Lillehoj et al., 2014).

Several factors such as i) length of AMP sequence, ii) immobilization or orientation of AMPs, iii) expression level of man-PTS receptors by bacteria, iv) conformation and site-specific orientation of peptides (as shown in Figure 2.5) can substantially influence the selectivity of AMPs (Bagheri et al., 2009; Hilpert et al., 2009). Among these factors, the length of the AMP sequence significantly influences the affinity towards bacteria in several ways. Soares et al. (2004) chemically immobilized 6 different lengths and tailored fragments of peptides (ceratotoxin A, pleurocidin, PGQ, cecropin P1, cecropin A, and SMAP-29) on a plate to observe the binding affinity against *E. coli*. They found that two tailored fragments obtained significantly higher binding efficiency compared to their complete length of peptides. Azmi et al. (2015) exposed *L. monocytogenes* to the different fragments of peptide functionalized gold substrates and found high capture affinity of Gram-positive bacteria towards the peptide Lue 10. In the case of leucocin A, both full-length peptide and fragmented peptide (Leu10) demonstrated similar binding affinity to *L. monocytogenes* whereas other fragments of Leu A displayed a lower affinity for the same bacteria. The authors postulated that the binding affinity of peptide fragments varied due to the helical conformation associated with the length of peptides. Therefore, the length of peptide sequences could substantially influence the affinity of AMPs for capturing bacteria.

Etayash et al. (2013) reported that the peptide 24 AA Leu A immobilized on a gold surface exhibited differential binding affinities towards several Gram-positive bacteria while no binding variances were observed against a fragment of a similar 14 AA Leu A peptide as shown in Figure 2.6 (a-f). These binding variances could be attributed to the short length of peptide, which is not efficient for recognizing the targeted bacterial membrane-bound receptor. In another study conducted by this group (Etayash et al., 2014b), the gold surface

was conjugated with AMP 37 Leu A and incubated with 5 different Gram-positive bacteria (*Carnobacterium divergens, Staphylococcus aureus, Enterococcus faecalis*, *L. monocytogenes* 19116 and *L. monocytogenes* 43256) as shown in Figure 2.6 (g-h). Interestingly, significant binding variances were observed for individual bacteria while pathogenic *L. monocytogenes* showed the highest binding affinity. In addition, they also observed that the C-terminal peptide

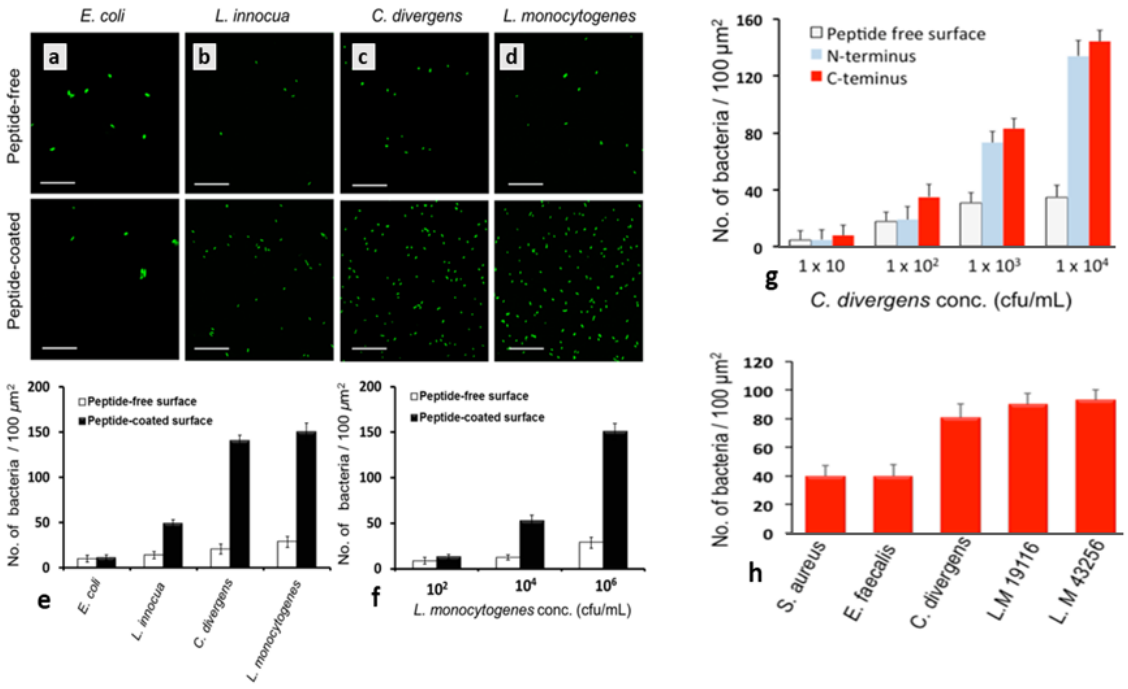

Figure 2.6 The bacteria capture efficiency (average number) of peptide (24AA LeuA) coated and peptide free surfaces against different bacteria such as *Listeria innocua*, *Escherichia coli*, *Listeria monocytogenes*, and *Carnobacterium divergens* at 10^6 CFU/mL (a-e), the different concentration *L. monocytogenes* (10^2 - 10^6 CFU/mL) against peptide 24AA LeuA (f), bacteria capture efficiency (average number) by AMP of LeuA, the *Carnobacterium divergens* (10^1-10^4 CFU/mL) capture efficiency by the peptide (N or C terminal) coated and uncoated gold surfaces (g), the capture efficiency of C-terminal peptide against different bacteria (*Staphylococcus aureus*, *Enterococcus faecalis Carnobacterium divergens*, *Listeria. monocytogenes* 191116, *Listeria monocytogenes* 43256) at 10^3 CFU/mL (h) (Etayash et al., 2013; Etayash et al., 2014b).

obtained higher bacteria binding efficiency compared to the N-terminal peptide (LeuA). Besides, the long peptides obtained higher bacteria capture efficiency compared to the fragmented length of similar peptide sequences.

2.7 AMP used as ligands in biosensing

AMPs have been tethered on the surface of biosensors for capturing bacteria for some time (de Miranda et al., 2017; Jiang et al., 2015). Furthermore, bacteria can be captured on the surface of biosensors using the AMP-bacteria premix technique as presented in Figure 2.7a (Pardoux et al., 2020). In this method, AMPs are captured on the surface of bacteria by electrostatic and hydrophobic interactions between peptides and bacterial envelopes. The surface tethering technique has been widely used to capture bacteria on the surface of a biosensor as shown in Figure 2.7b (Humblot et al., 2009; Mannoor et al., 2010). In this technique, several physical and chemical (*i.e.,* covalent interaction) methods have been used to immobilize AMPs on the surface of a biosensor (Eddy et al., 2010; Jiang et al., 2015). In the case of physical methods, the number of AMP polymer layers can be designed flexibly, which allows for controlling peptide loading on the solid surface (Costa et al., 2018). However, the charge diffusion could

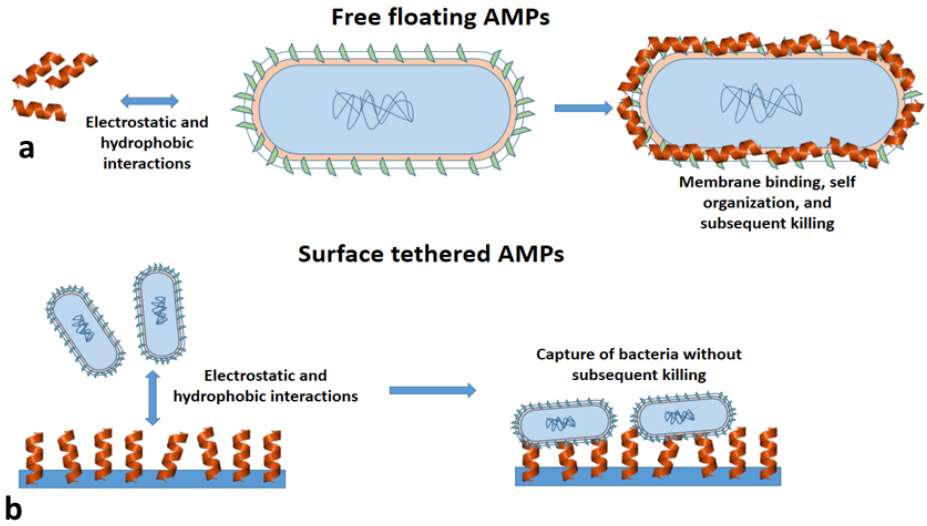

Figure 2.7 Techniques for capturing bacteria on the surface of biosensors substrates, AMP-bacteria pre-mix technique (a), surface tethering technique (b) (Pardoux et al., 2020).

be interrupted due to the polymer surfaces (Sanchez-Gomez and Martinez-de-Tejada, 2017) and thus this technique is not efficient for charge sensitive biosensors. Alternatively, the covalent based immobilization of AMPs on biosensor surfaces is the most used technique to tether peptides on biosensor surfaces as it is more effective compared to physical immobilizations (Andrade et al., 2015; Bagheri et al., 2009). The covalent methods of peptide

immobilization on biosensors surface are summarized in Table 2.5. In the covalent method, the AMPs can be functionalized with several spacers (*i.e.,* thiol) containing reactive groups to immobilize the peptides on the biosensor surface as

Table 2.5 An overview of the covalent based AMP tethering techniques on the biosensor's substrates.

Name	Immobilization technique	Length	Structure	References
Magainin I	Cysteine terminated peptide was covalently (directly) immobilized on the gold electrode surface	23	α-Helix	(Mannoor et al., 2010)
Clavanin A	The peptide was covalently immobilized with EDC-NHS activated cysteine thiol	37	α-Helix	(de Miranda et al., 2017)
Plantaracin 17 C	The peptide was covalently immobilized with EDC-NHS activated (3-mercaptoproyl) trimethoxy silane (MPTS) thiol	17	α-Helix	(Guralp et al., 2015)
Magainin I	The peptide was covalently immobilized with EDC-NHS activated 11-mercaptoundecanoic acid	23	α-Helix	(Humblot et al., 2009)
Colicin V	The peptide was covalently immobilized with EDC-NHS activated cysteine thiol	-	α-Helix	(Jiang et al., 2015)
Magainin I	The peptide was covalently immobilized with EDC-NHS activated 6-mercapto-1-hexanol	23	α-Helix	(Li et al., 2015)
Magainin I	The peptide was covalently immobilized with EDC-NHS activated ferrocene	23	α-Helix	(Li et al., 2014)
Clavanin A	The peptide was covalently immobilized with EDC-NHS activated cysteine thiol	37	α-Helix	(Andrade et al., 2015)

presented in Figure 2.8. In covalent based coupling, one of the most effective approaches is to immobilize peptides on the biosensor surfaces through the reactive groups present on the self-

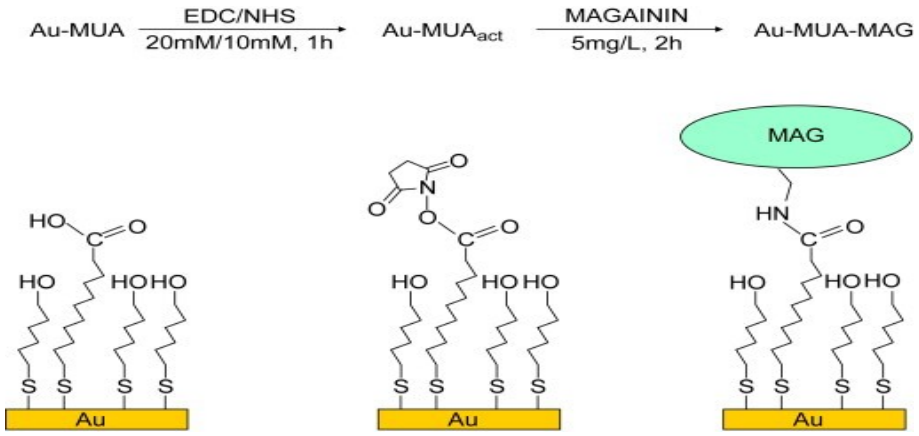

Figure 2.8 An overview of the covalently immobilized peptide on biosensor surface; 1st, absorption of thiols on the electrode surface; 2nd, activation of -COOH group presence in thiols by EDC/NHS coupling reagents; 3rd, covalent immobilization of peptide on electrode surface through the activated thiols (Humblot et al., 2009).

assembled monolayer (SAM). The SAM can be functionalized with several reactive coupling reagents (Sanchez-Gomez and Martinez-de-Tejada, 2017). The length of the carbon chain present in the SAM is more effective for reacting with AMPs (Stassen et al., 2017). Polymer resins, especially polyethylene glycol (PEG), containing reactive groups corresponding to several peptides is another common approach for covalently immobilizing AMPs (Abshar Hasan et al., 2020). In general, PEG allows faster immobilization, which can substantially increase peptide and bacteria interactions leading to the enhancement of the performance of biosensors (Karimzadeh et al., 2018). However, in the PEG-based peptide, there is a possibility of polymer degradation due to the chain cleavage reactions, hence AMPs can be designed from one to several carbons, by considering which disassociate from the sensor surfaces (Zoppe et al., 2017).

2.8 Application of AMP for detecting pathogenic bacteria

Several recent studies have shown that AMP could be used as bioreceptors for selectively detecting bacteria using biosensing techniques. For instance, Kulagina et al. (2005) detected pathogenic *S. typhimurium* and *E. coli* O157 using a fluorescence biosensor anchored with AMP Magainin I. In their subsequent study (Kulagina et al., 2006), they functionalized salinized glass surfaces using different AMPs such as cecropin A, magainin I, parasin, polymyxin B, and polymyxin E, and observed differential cell capture efficiencies for *S.*

typhimurium and *E. coli* O157. They also observed that the non-pathogenic *E. coli* did not interact with most of the peptides. Their results clearly show that AMPs could be used as bio-recognition elements for selective detection of bacteria even at species level. Furthermore, they investigated the efficiency of AMPs for detecting several bacteria such as *Brucella melitensis* and *Coxiella burnetii*, where they observed maximum binding affinity of *B. melitensis* by the bactenecin, polymyxin B and polymyxin E functionalized surface, while no binding affinity was observed for magainin I functionalized surface (Kulagina et al., 2007). Therefore, this study further strengthens the selectivity of AMPs to distinguish pathogens closely related species. The application of AMPs in biosensors for pathogenic bacteria detection is summarized in Table 2.6.

Mannoor et al. (2010) designed an AMP (magainin I) based microelectrode impedimetric biosensor to detect Gram-negative bacteria. In their study, they successfully detected low concentrations of pathogenic *E. coli* (10^3 CFU/mL). Interestingly, they observed that the pathogenic *E. coli* generated a higher signal compared to the non-pathogenic *E. coli*, which suggested the possibility of strain level bacteria detection using this technique. In another study, Etayash et al. (2014a) used leucocin A, which is known as class IIa bacteriocins for detecting Gram-positive bacteria, and they successfully detected *L. monocytogenes* at a concentration of 10^3 CFU/mL. Albanese et al. (2019) designed an AMP (nisin) anchored biosensor where they compared binding affinities between N and C terminal peptides, and subsequently, they investigated the detection efficiency of *L. innocua*, *E. coli* O157 by AMP-functionalized electrochemical sensor. In their study, the C-terminus peptide successfully detected low concentrations of *L. innocua*. Lillehoj et al. (2014) designed an AMP-anchored impedimetric micro-sensor for detecting pathogenic bacteria, where the sensor detected pathogenic *P. aeruginosa* and *Streptococcus mutans* at a concentration of 10^5 CFU/mL. In another study, Dong and Zhao (2015) developed an AMP-based impedimetric biosensor for detecting *E. coli* O157. In their study, they effectively detected very low concentrations of pathogenic *E. coli* (4×10^2 CFU/mL) in water samples.

Table 2.6 AMPs used as bio-recognition elements for bacterial detection.

AMP	Detected Bacteria	LOD (CFU/mL)	Sample type	Transducer	Detection time	Reference
Magainin I	*E. coli* O157:H7; *S. typhimurium*	1.6×10^5; 6.5×10^4	PBS	Fluorescens spectroscopy	70 min	(Kulagina et al., 2005)
Ceropin A, Parasin I	*E. coli* O157:H7; *S. typhimurium*	1×10^5; 5×10^5	PBS	Fluorescens spectroscopy	-	(Kulagina et al., 2006)
Magainin I	*E. coli* O157:H7; *S. typhimurium*	10^3	PBS	EIS	15 min	(Mannoor et al., 2010)
Leucocin A	*L. monocytogenes*; *S. aureus*	10^3	10% milk spiked	EIS	20 min	(Etayash et al., 2014a)
Clvanin A	*K. pneumoniae*; *E. fecalis*; *E. coli*; *B. subtilis*	10^2 10^2 10^3 10^3	-	EIS	-	(Andrade et al., 2015)
Magainin I	*E. coli* O157	10^3	PBS	EIS	90 min	(Li et al., 2014)
Colicin V	*E. coli*	10^3	Water	EIS	15 min	(Jiang et al., 2015)
Leucocin A	*L. monocytogenes*	10	Seawater	EIS	60 min	(Lv et al., 2018)
Bactenecin	*Brucella melitensis*	5×10^4	-	Fluorescens spectroscopy	-	(Kulagina et al., 2007)
Magainin I	*E. coli O157*	5.0×10^2	Water, fruit and vegetable juice spiked	SPR	40 min	(Zhou et al., 2018)

Some studies have shown that very low LOD can be obtained by AMP-conjugated biosensors. For instance, D'Souza et al. (2018) detected 10 CFU/mL of *L. monocytogenes* using an AMP pair based sandwich technique. In an another study, Albanese et al. (2019) detected 1.5 CFU/mL of *Listeria innocua* using an AMP (nisin) functionalized electrochemical sensor. It has also been reported that the AMP-based colorimetric biosensor can detect 13 CFU/mL of *E. coli* O157 (Qiao et al., 2017b). These results are promising to apply the AMP-based biosensors in the practical field. However, in most cases, the LODs are reported by solely considering dilution factors rather than comparing with positive or negative

control samples such as other bacterial strains. Besides, in some studies (Li et al., 2015; Mannoor et al., 2010; Qiao et al., 2017a), the detection time is reported based on final read-out of biosensing results. However, the detection time should recognize the whole process including sample preparation to final results or the time of individual stages to better assesses the LODs in the context of realistic conditions, where the target bacteria would exist with other bacterial strains.

2.9 Semiconductor optical (photoluminescence) sensors

In semiconductor materials, electrons can move from the valance (Ev) to the conduction band (Ec) due to the absorption of a photon with the energy equal or exceeding the band gap energy (Ahmad et al., 2017; Sharma et al., 2014). PL is a radiative recombination of excited valance band holes and conduction band electrons that happens once electrons migrate from conduction to the valance band (Pathak et al., 2016). The non-radiative recombination of electrons and holes occurs due to the diffusion exchange of minor carriers within the thin surface layer. The surface recombination velocity (SRV) is generally determined by the condition of surface which dominates the non-radiative recombination rate. The non-radiative and radiative recombination of holes and electrons are illustrated in Figure 2.9. The recombination rate is inversely proportional to the minority carrier lifetime (τ) which can be

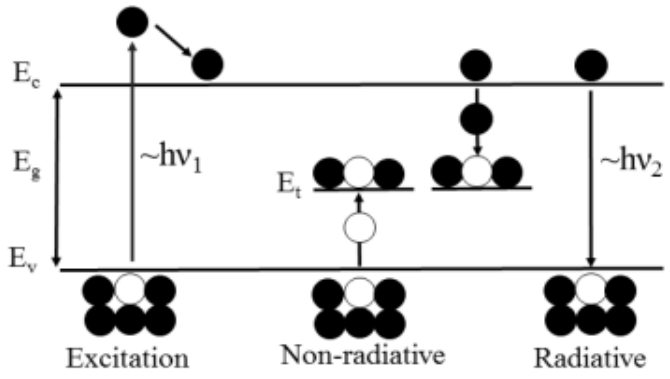

Figure 2.9 Schematic diagram of the surface recombination processes in GaAs. The absorption of photons at higher energy than band gap energy of GaAs stimulates electrons and elevates them into the conduction band. The diffusion movement of minority carriers leads to non-radiative recombination while radiative recombination is associated with the direct transition of electrons from the excited conduction band to the valance band (Marshall, 2011).

defined by the reciprocal terms of non-radiative and radiative recombination as expressed in Eq. 2.1. For n-type semiconductor, the radiative and non-radiative recombination rates can be expressed by the Eq. 2.2 and 2.3, respectively. In case of p-type semiconductors, the radiative and non-radiative recombination rates can be expressed using similar equations (Yacobi, 2003),

$$\frac{1}{\tau} = \frac{1}{\tau_r} + \frac{1}{\tau_{nr}} \tag{2.1}$$

$$r_r = \tau_r^{-1} \approx \beta\,(n_0 + \Delta n) = \beta n \tag{2.2}$$

$$r_{nr} = \tau_{nr}^{-1} = \sigma_p v_{th,p} N_t \tag{2.3}$$

In Eq. 2.2, β represents the radiative recombination rate (Lambert et al., 1990), n_0 represents the equilibrium majority carrier (*i.e.,* electrons) concentration, and Δn represents the photo-generated excess concentration.

The recombination theory given by Shockley-Read-Hall (Shockley and Read Jr, 1952) is expressed in equation 2.3, where the $v_{th,p}$, σ_p, and N_t represent the minority carrier thermal velocity (cm/s), minority carrier (*i.e.,* holes) capture cross section (cm^2), and trap density (cm^{-3}), respectively. The PL intensity can be computed through the internal quantum efficiency (γPL) which can be defined in terms of non-radiative and radiative recombination rates (Yacobi, 2003). According to Eq. 2.4, the intensity of PL varies with the changes in non-radiative or radiative recombination rates which are at crucial metric in PL-based semiconductor sensors:

$$\gamma_{PL} = \frac{r_r}{r_r + r_{nr}} \tag{2.4}$$

The signal of PL based biosensors is associated with the variations of non-radiative and radiative electron-hole recombinations. Figure 2.10 illustrates the band bending occurring at

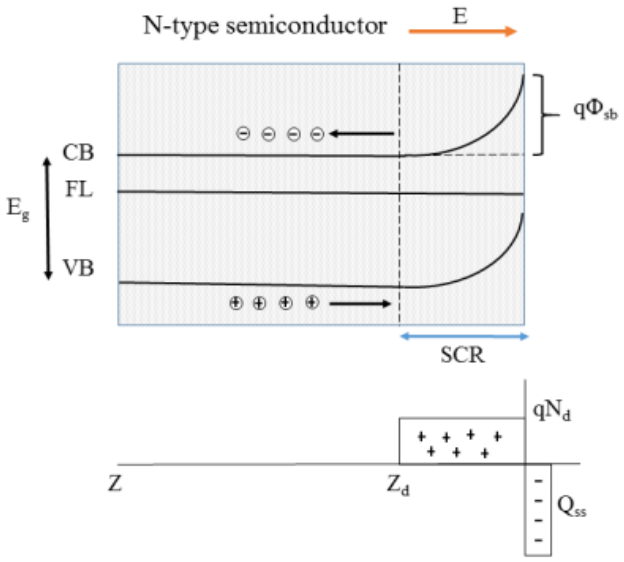

Figure 2.10 Schematic diagram of the near-surface band structure in n-type semiconductors. The photo-excited minority carriers (⊕) are moved towards the surface due to diffusion. This diagram indicates the built-in electric field (E), surface barrier height (qΦsb), space charge region (SCR), space charge density (qNd), surface charge density (Qss), depletion depth (Zd), ionized donors (+), surface trapped charge (-), Fermi level energy (FL), and conduction/valance bands (CB/VB) (Marshall, 2011).

N-type semiconductor surfaces. This diagram also represents the built-in electric field (E), surface barrier height ($q\Phi_{sb}$), space charge region (SCR), space charge density (qN_d), surface charge density (Q_{ss}), depletion depth (Z_d), ionized donors (+), surface trapped charge (-), valance/conduction/bands (CB/VB) and Fermi level energy (FL).

In PL-based sensors, analytes can be immobilized either on the surface directly, or on the surface coated with a transducer film. Transducer films are employed to functionalize the surface of semiconductors and to change the PL intensity by affecting surface conditions of the biosensing device. The behaviour of PL monitored DIP of GaAs/AlGaAs can be explained according to Aithal and Dubowski (2018) as presented in Figure 2.11a. In this study, GaAs/AlGaAs (wafer 10-150) was irradiated using a spatially homogenized beam of a 532 nm light emitting diode (LED) at a power density of 70 $mWcm^{-2}$ and different duty cycles (DCs) to investigate the average photocorrosion rate of samples. The DC is defined as (time of light on)/ (time of light on + time of light off). Two prominent PL intensity maxima

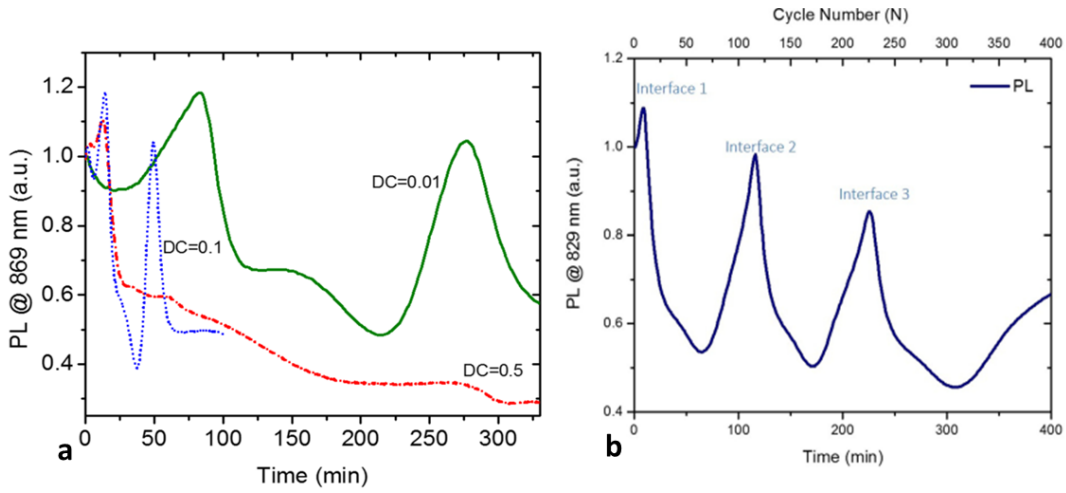

Figure 2.11 Temporal PL plots for a GaAs/AlGaAs nanoheterostructures irradiated with a 532 nm LED at 70 mW cm^{-2} using different duty cycles (a), the PL signal of GaAs/$Al_{0.35}Ga_{0.65}As$ nanoheterostructures photocorroded with 625 nm and 25 mW/cm^2 of power density (b) (Aithal and Dubowski, 2018; Aithal et al., 2017).

appear at 80 and 275 min for DC=0.01 and at 15 and 50 min in the case of DC=0.1 while a single peak at 12 min was observed for DC=0.5. The number of PL maxima observed at low duty cycles (DC = 0.1 and 0.01) are correlated with the number of GaAs–$Al_{0.35}Ga_{0.65}As$ interfaces revealed in the process of digital photocorrosion. Furthermore, the region of a slowed down PL decay is observed for DC = 0.01 at ~125–140 min, and for DC = 0.1 at ~25–40 min which can be attributed to the reduced rate of photocorrosion for the 10 nm thick $Al_{0.35}Ga_{0.65}As$ layer. For DC = 0.5, a single maximum occurred at ~12 min suggesting an accelerated photocorrosion rate with the inability of observing higher order PL maxima. An example of digital photocorrosion (DIP) monitored with PL signal in a similar GaAs/$Al_{0.35}Ga_{0.65}As$ nanoheterostructure is shown in Figure 2.11b (Aithal et al., 2017). In this case, the GaAs/AlGaAs sample was irradiated with a 625 nm LED delivering power of 25 $mWcm^{-2}$. The intermittent photo-irradiation of the sample with DC=0.5 revealed the formation of three intense PL maxima (indicated as interfaces 1-3) due to the oxidation and dissociation of the oxidized material. Each individual maximum observed in this case corresponds to the photocorrosion front passing the GaAs-AlGaAs interface. Since the rate of photocorrosion depends on the number of minority carriers present and arriving at the surface of a semiconductor (holes in the case of n-type material), the immobilization of an electrically active biomolecule at the surface of a GaAs/AlGaAs sample could affect the photocorrosion rate of such a sample.

The PL monitored DIP process of GaAs/AlGaAs nanoheterostructure has been employed for detecting electrically charged analytes, such as bacteria (Aziziyan et al., 2016; Nazemi et al., 2017). A schematic illustration of the DIP process of an n-type GaAs/AlGaAs nanoheterostructure monitored with the PL signal is presented in Figure 2.12a. The formation of the PL maximum is associated with the transition from GaAs-electrolyte to AlGaAs-electrolyte. According to the Figure 2.12b, once the semiconductor sample is exposed in a liquid environment to photons with the energy exceeding the GaAs bandgap, the built-in electric potential separates photo-excited electrons (e^-) and holes (h^+) in the depletion region of the semiconductor (Aziziyan et al., 2016; Nazemi et al., 2017). The holes (h^+), driven by the electric surface potential, arrive at the electrolyte/semiconductor interface and induce formation of surface oxides. Among those oxides, Ga_2O_3 is relatively stable in water (Choi et al., 2002; Ruberto et al., 1991), but is easily dissolvable in an ammonia environment. The reaction of the photocorrosion process for GaAs can be expressed by Eq. 2.5:

$$GaAs + 2H_2O + 6h^+ \rightarrow \ Ga^{3+} + HA_SO_2 + 3H^+ \qquad (2.5)$$

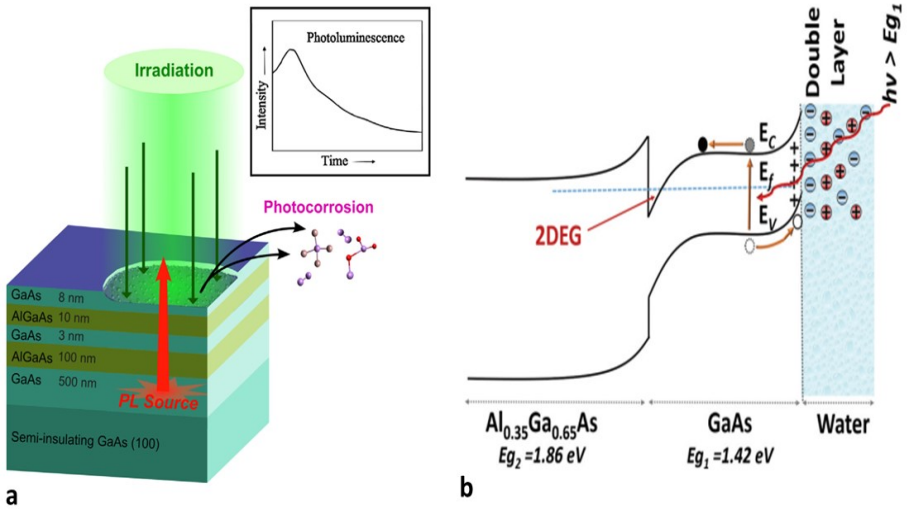

Figure 2.12 Cross sectional view of the GaAs/AlGaAs heterostructure, the inset represents the PL spectrum at 869 nm for GaAs/AlGaAs cap (a), a schematic diagram of the photocorrosion process (b) (Aziziyan et al., 2016).

Generally, the formation of Ga_2O_3 reduces the number of surface defects responsible for non-radiative recombination of electron-hole pairs, thus this leads to the enhanced intensity of the PL signal emitted by the semiconductor (Aziziyan et al., 2020; Passlack et al., 1995). The

rate of photocorrosion and time to form PL intensity maxima can be delayed or accelerated with the exposure of GaAs/AlGaAs biochips to electrically charged molecules. In this way, the measurement of PL is an attractive option for *in situ* monitoring of the presence of charged molecules, such as bacteria immobilized at the semiconductor surface (Aziziyan et al., 2016). In general, the membrane of bacteria in pH higher than 4 is negatively charged, probably due to presence of excessive concentration of carboxyl and phosphate groups than the amino acids in their membranes (Aziziyan et al., 2016; Poortinga et al., 1999). Furthermore, the molecular interaction between bacteria and bioreceptors repels negative ions on the surface of semiconductors. Consequently, the formation of PL intensity maxima can be delayed due to the discharge of negative ions or electrostatic interaction between negatively charged bacteria and the semiconductor surface (Nazemi et al., 2015; Poortinga et al., 1999).

In a recent study, Aziziyan et al. (2016) detected *L. pneumophila* by utilizing a PL based DIP technique as presented in Figure 2.13. In this study, they observed that the enhancement in the PL intensity of GaAs semiconductor biochips is directly correlated with the concentration of negatively charged targeted analytes (*L. pneumophila* bacteria) as shown in Figure 2.13a. They monitored the position of PL intensity maxima for different concentrations of *L. pneumophila* exposed GaAs/AlGaAs nanoheterostructure biochips as

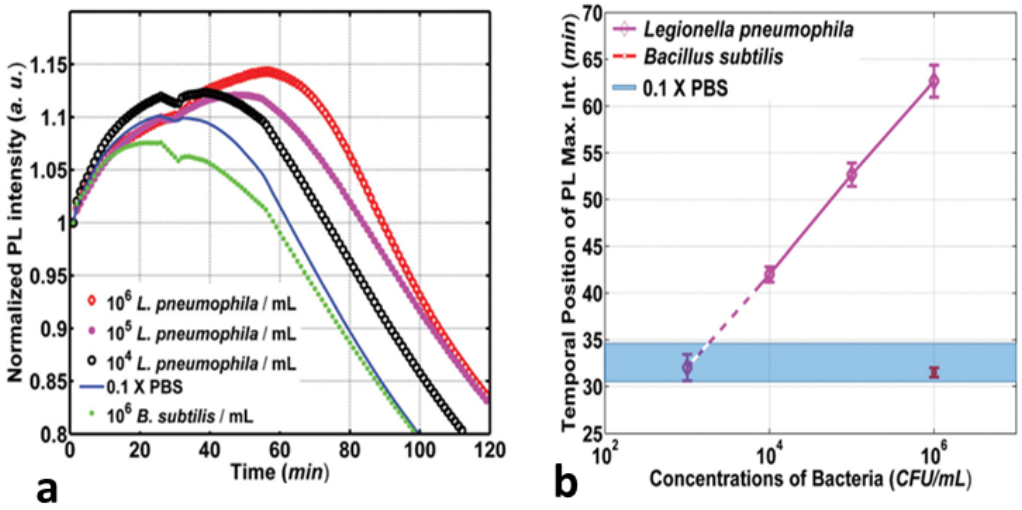

Figure 2.13 The temporal behaviour of PL signals from antibody functionalized biochips (J0150) exposed to different concentrations of *L. pneumophila* (a), and the PL maxima *vs* time for repeated runs (b) (Aziziyan et al., 2016).

shown in Figure 2.13b. It was clearly observed that the increasing number of bacteria immobilized on the surface of GaAs/AlGaAs biochips reduced the photocorrosion rate and delayed formation of PL maxima related to the transition from the electrolyte-GaAs to the electrolyte-AlGaAs interface. The results suggest that the PL monitored DIP process could be considered a promising method for detecting other pathogens in a water environment.

2.10 Methods applied to GaAs surface characterization and monitoring bacterial attachment

2.10.1 Fourier-transform infrared spectroscopy analysis

Fourier transform infrared spectroscopy (FTIR) is an analytical tool for characterizing various chemicals and materials especially surface functionalized samples as it is highly sensitive to the surface chemistry (Baer et al., 2010; Khan et al., 2018). A schematic diagram of FTIR (Bruker Vertex 70v) is presented in Figure 2.14. In transmission mode, IR radiation in a defined range of wavenumbers passes through a sample and some of the radiation is absorbed at specific wavenumbers by the sample while some reaches the detector (Haas and Mizaikoff, 2016). The molecular fingerprint of the tested sample is created through the transmission and

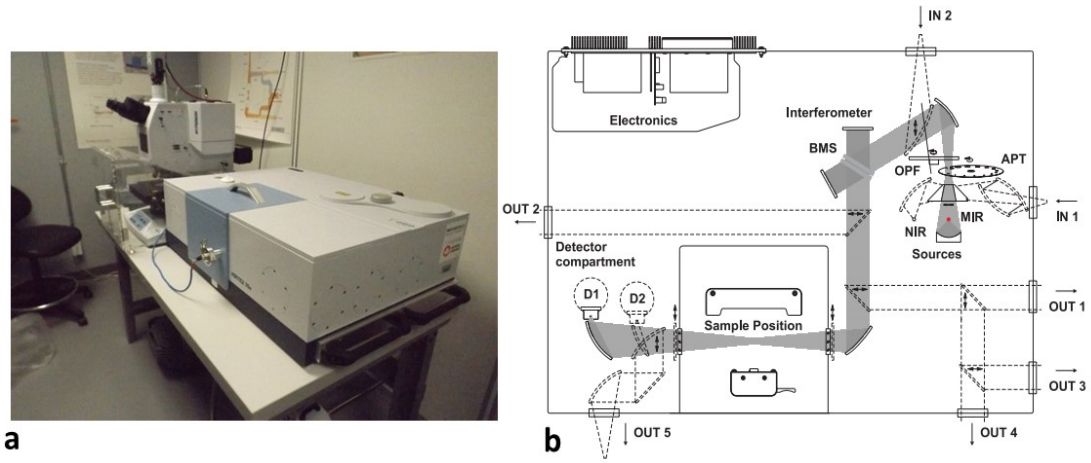

Figure 2.14 Schematic diagram of the Bruker Vertex 70v FTIR (a), and the optical path for transmission measurements (b); D1: standard detector; D2: optional detector; BMS: beam splitter; OPF: optical filter wheel.

absorption (Baer et al., 2010). As fingerprints are characteristic of chemical groups and atomic bindings, the analysis of FTIR spectra is a unique way of identifying the presence of specific chemicals on the surface of investigated samples (Haas and Mizaikoff, 2016). In addition, the intensity/area of peaks in the spectrum can be correlated with the amount of material present in the sample. The FTIR-based characterization technique is attractive due to its monolayer sensitivity and non-destructive character providing precise results without external calibration. In this project, a Bruker Vertex 70v FTIR system as presented in Figure 2.14 was used to evaluate functionalization of GaAs and GaAs/AlGaAs samples.

2.10.2 Atomic force microscopy analysis

AFM could also be applied to characterize the surface functionalized materials through the measurement of sample roughness as denoted by the root mean square (σ_{RMS}). AFM is considered as one of the powerful techniques for nanoscale measurement and characterization of sample surface (Nguyen-Tri et al., 2020). A picture of the AFM instrument employed in this research is shown in Figure 2.15. The crucial point of AFM sample characterization is that the specimens must be immobilized to prevent potential displacement induced by the force of cantilever (Dufrêne, 2002). Furthermore, the sample characterization process with AFM is time consuming and thus the throughput is quite slow. AFM can be conducted in different modes, such as tapping, contact and non-contact as presented in Figure 2.16. In the contact mode, the tip of the cantilever is dragged across the surface of samples, and images are taken according to the deflections of cantilever. A number of sample surfaces such as insulators and semiconductors trap electrostatic charges which can contribute to the additional attractive forces between the sample and probe. In the non-contact mode, the sample surface is not touched by the cantilever tip that hovers very close (~50-150 Angstrom) over the surface and the images are taken based on the changes of frequency or amplitude of the oscillations (Eslami and Caputo, 2021). Unlike contact mode, the attractive forces from the samples are substantially weaker than the forces used by contact (Magonov et al., 1997). In the case of tapping mode, the tip oscillates up and down at the close distance of sample surfaces (Garcia, 2020). However, the much higher amplitude of oscillations with higher risk of damaging the

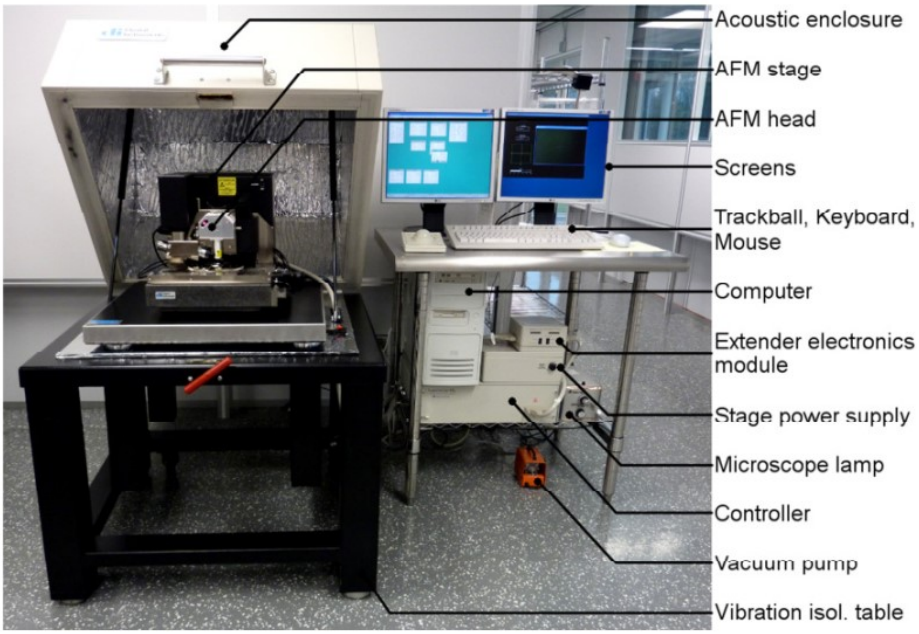

Figure 2.15 A picture of the Veeco Dimension 3000 AFM.

sample surface are observed for this technique compared to the non-contact mode (Eslami and Caputo, 2021; Magonov et al., 1997). Thus, the imaging of fragile and soft

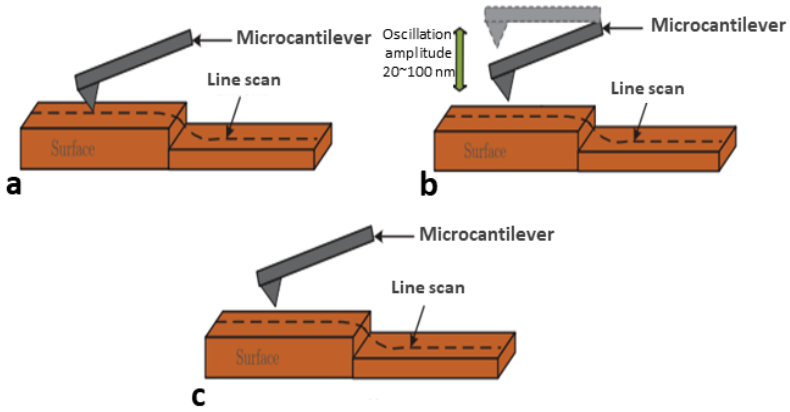

Figure 2.16 A schematic diagram for different modes of AFM operation: contact (a), tapping (b), non-contact (c) (Rana et al., 2016).

such as delicate biological samples should be carried out in the non-contact mode (Yang et al., 2007). In this project, a Veeco Dimension 3000 AFM system (Figure 2.15) was used to investigate the surface functionalization of GaAs samples.

2.10.3 Optical microscopy

Optical microscopy provides a simple and inexpensive way of visualizing surface attached bacteria (Gopinath et al., 2014). This method is the fastest way to determine the number of bacteria attached on the solid surfaces. However, the surface should be optically clear and planar for properly visualizing or counting bacteria. Moreover, the viability of bacteria cannot be determined through this method. Very small pleomorphic bacteria and particles that resemble the bacteria are very difficult to differentiate with this method leading to the high error of bacteria counting. However, the application of some software, especially imageJ, can significantly reduce the counting error by subtracting particles that resemble the bacteria. In this project, Zeiss infinity 2 optical/light microscopy with a 10x wide-field eye piece and objective lenses of 5x - 100x was used to visualize bacteria on the GaAs surfaces.

2.10.4 Scanning electron microscope analysis

Scanning electron microscopy (SEM) allows generating highly magnified bacteria image for observing adhesion of bacteria on surfaces with good detail (Karcz et al., 2012). In this microscopic technique, the sample surface is scanned by electron beam and surface morphology is characterized based on interaction of electrons and sample. However, chemical fixation is required for imaging soft bodied organism such as bacteria. This technique is time consuming and unable to provide information related to the viability. Moreover, a number of sample treatment steps are required for visualizing bacteria through this technique, such as metallization. In this project, a Hitachi S-4700 (Japan) SEM microscopy with a magnification of 40k is used to visualize bacteria attached on the surface of GaAs.

Chapter 3. Avant-propos

Auteurs et affiliations:

M. Amirul Islam: Étudiant au doctorat, Université de Sherbrooke, Faculté de génie, Département de génie électrique et informatique.

Walid M. Hassen: Assistant de recherche, Université de Sherbrooke, Faculté de génie, Département de génie électrique et informatique.

Azam F. Tayabali: Professeur associé, Laboratoire de biotechnologie, Bureau de la science et de la recherche en santé environnementale, Direction générale de la santé environnementale et de la sécurité des consommateurs, Centre de santé environnementale, Santé Canada

Jan J. Dubowski: Professeur, Université de Sherbrooke, Faculté de génie, Département de génie électrique et informatique.

Titre français: Biocapteur à base de GaAs/AlGaAs fonctionnalisé par peptide antimicrobien warnericin RK pour une détection hautement sensible et sélective de *Legionella pneumophila*

Date d'acceptation: 12 novembre 2019

État de l'acceptation : version finale publiée

Revue: Biochemical Engineering Journal

Référence: M. A. Islam, W. M. Hassen, A. F. Tayabali, J. J. Dubowski, "Antimicrobial warnericin RK peptide functionalized GaAs/AlGaAs biosensor for highly sensitive and selective detection of *Legionella pneumophila*" Biochemical Engineering Journal, vol. no. 154, pp. 1-5, 2019.

Contribution au document: Ce chapitre décrit le développement d'un biocapteur DIP GaAs/AlGaAs à base de warnericin RK (PAM) pour la détection sensible et sélective de *L. pneumophila* en milieu aqueux. Le biocapteur conçu a démontré une détection efficace de *L. pneumophila* dans des échantillons d'eau faiblement concentrés (10^3 UFC/mL). Cette limite de

détection est comparable ou même 10 fois inférieure à celle reportée en cas de détection directe de *L. pneumophila* en utilisant la même méthode de transduction (DIP GaAs/AlGaAs), des transducteurs optiques ou électrochimiques mais en utilisant des anticorps comme molécules de reconnaissances. Cette bioarchitecture basée sur le PAM ouvre la voie au remplacement des immunobiocapteurs qui pourraient souffrir d'une faible sensibilité et reproductibilité en raison que la production des anticorps de mammifères est dépendante des animaux en plus de la possibilité de variation d'un lot à un autre.

Résumé français:

La détection de la bactérie pathogène *Legionella pneumophila* (*L. pneumophila*) par des méthodes de culture n'est pas efficace pour prévenir les épidémies de la maladie du légionnaire. Le principal problème est le délai relativement long pour l'obtention des résultats ainsi que dans certains cas l'incapacité d'assurer la croissance de bactéries viables mais non cultivable. L'une des stratégies pour pallier à ces problèmes consiste à développer des biocapteurs fonctionnalisés avec des anticorps de mammifères conçus pour capturer les bactéries. Cependant, les anticorps de mammifères sont connus pour souffrir de la variabilité des lots produits et d'une stabilité limitée, ce qui réduit l'usage et la constance des immunobiocapteurs. Pour tenter de résoudre ce problème, nous avons exploré l'usage des peptides antimicrobiens (PAM) pour la capture de *L. pneumophila* avec des biopuces de GaAs/AlGaAs. Des analyses de spectroscopie infrarouge à transformée de Fourier ont démontré que les peptides étaient bien immobilisés de manière covalente sur les terminaisons -COOH du l'acide mercaptohexadécanoïque (MHDA) formant une monocouche auto-assemblée à la surface de la biopuce de GaAs/AlGaAs. Les groupements COOH ont été préalablement activées par le 1-éthyl-3-(-3-diméthylaminopropyl) et le carbodiimide/N-hydroxysuccinimide (EDC/NHS) Les interactions entre le PAM (warnericin RK) et *L. pneumophila*, *E. coli*, *B. subtilis* et *P. fluorescens* ont été évaluées en termes de couverture de surface (nombre de bactéries par unité de surface de biopuce), par microscopie à fluorescence et un biocapteur à photocorrosion digitale de GaAs/AlGaAs. Nous avons constaté que le peptide warnericin RK présentait une affinité ~4 fois plus élevée envers *L. pneumophila* qu'aux autres bactéries étudiées. De plus, un niveau de détection aussi bas que 10^3 UFC/mL était possible avec l'architecture proposée. Nous soutenons qu'un biocapteur basé sur le PAM

warnericin RK AMP offre une alternative intéressante aux dispositifs à base d'anticorps pour la détection de *L. pneumophila*.

Chapter 3. Antimicrobial warnericin RK peptide functionalized GaAs/AlGaAs biosensor for highly sensitive and selective detection of *Legionella pneumophila*

3.1 Abstract

Detection of pathogenic *Legionella pneumophila* (*L. pneumophila*) by culture-based methods is not efficient in predicting Legionnaires' disease. The main problem is the relatively slow time-to-result and the inability of some culture media to support the growth of viable bacteria. One strategy to alleviate these issues is developing biosensors functionalized with mammalian antibodies designed to capture bacteria. However, mammalian antibodies are known to suffer from batch-to-batch variations, as well as limited stability, which reduce the consistent utility of antibody-based biosensors. In an attempt to address this problem, we investigated antimicrobial peptides (AMPs) for capture of *L. pneumophila* with GaAs/AlGaAs biochips. Fourier-transform infrared spectroscopy measurements revealed that the peptides were covalently immobilized on the 1-ethyl-3- (-3-dimethylaminopropyl) carbodiimide/N-hydroxysuccinimide (EDC/NHS) activated -COOH terminals of mercaptohexadecanoic acid (MHDA) self-assembled monolayer functionalized GaAs surface. The efficiency of the specific interaction between the peptide and *L. pneumophila*, *E. coli*, *B. subtilis* and *P. fluorescens* was investigated with fluorescence microscopy and a digital photocorrosion GaAs/AlGaAs biosensor. We found that the warnericin RK peptides exhibited ~4 times greater binding affinity towards *L. pneumophila* than to the other bacteria investigated. Furthermore, detection levels as low as 10^3 CFU/mL were possible with the proposed biosensor architecture. We argue that a biosensor based on warnericin RK AMP peptides offers an attractive alternative solution to antibody-based devices towards detection of *L. pneumophila*.

Key words: Antimicrobial peptides, Warnericin RK, *Legionella pneumophila*, GaAs/AlGaAs biosensor, Binding affinity

3.2 Introduction

Biosensor-based detection of *Legionella pneumophila* (*L. pneumophila*) is relatively fast, requires minimal technical knowledge for the user, and can be adapted as potentially portable devices (Hoyos-Nogués et al., 2018). In the past few years, a variety of biosensing methods, such as optical (Manera et al., 2013), piezoelectric (Hoyos-Nogués et al., 2018) and electrochemical (Li et al., 2012) have been proposed to detect *L. pneumophila*. Recently, photoluminescence (PL) monitored using a GaAs/AlGaAs digital photocorrosion (DIP) biosensor has proven attractive for rapid and sensitive detection of *E. coli* (Nazemi et al., 2015) and *L. pneumophila* (Aziziyan et al., 2016) bacteria.

The efficiency of bio-recognition elements is crucial to the operation of biosensors (Elakkiya and Matheswaran, 2013). Several bio-recognition elements such as antibodies, carbohydrates, aptamers, peptides have been widely used for capturing bacteria on the biosensor surface (Hoyos-Nogués et al., 2018). Among these, antibodies are commonly used since they can be selected to be highly specific to the target (Etayash et al., 2013). However, antibody-based biosensors suffer from instability and non-specificity to pathogens under harsh environments (Mannoor et al., 2010). Furthermore, antibodies are prone to batch-to-batch variation (Voskuil, 2014), which may result in inconsistent biosensor calibration. Recently, studies have shown that antimicrobial peptides (AMPs) could be employed as bio-recognition elements as an alternative to antibodies (de Miranda et al., 2017; Etayash et al., 2013). AMPs have been extensively investigated for their antibacterial action towards *Bacillus cereus*, *Pseudomonas aeruginosa*, and *Staphylococcus aureus* (Geitani et al., 2019; Han et al., 2017) as well as for *L. pneumophila* (Birteksoz-Tan et al., 2019; Verdon et al., 2009). However, to the best of our knowledge, a dedicated study has not been conducted to detect *L. pneumophila* using AMP functionalized biosensors. AMPs contain multiple domains that bind with specific bacterial or fungal cell envelope moieties (Mannoor et al., 2010). The stability of AMPs is considerably higher than that of typical globular proteins, especially antibodies (Etayash et al.,

2014b; Mannoor et al., 2010). Therefore, AMPs could be considered as a replacement of typical polyclonal antibody-based biosensing architectures.

The warnericin RK peptide is highly active against *L. pneumophila* (Verdon et al., 2011). Although the exact interaction between peptide and bacteria is not clearly understood, it has been proposed that the peptide may attach to the target cell surface through electrostatic interaction between the positively charged peptide and the negatively charged bacteria, followed by the specific interactions of the peptide with a specific but as yet unknown surface membrane component. According to Verdon et al. (2008), warnericin RK and delta-lysin I display the same antibacterial spectra, which is largely restricted to the *Legionella* genus. In further analyses (Verdon et al., 2011), the authors observed that the warnericin RK range of antimicrobial activity is due to the presence of phosphatidylcholines (30% content) lipid on the surface of *Legionella* membrane. However, in a different study, Marchand et al. (2011) found that the amino acid residues at position 14 for warnericin RK were of major importance for bactericidal as well as lytic activities to *L. pneumophila*.

Prompted by the intriguing prospect of employing AMP for *L. pneumophila* biosensing, we functionalized a GaAs/AlGaAs DIP biosensor with this moiety and investigated its capacity to detect *L. pneumophila*. We demonstrate that the investigated biosensing architecture offers both sensitivity and selectivity to detect *L. pneumophila* in a water environment.

3.3 Experimental section

3.3. 1 Materials and reagents

The undoped GaAs (001) chips (WV 23084) used for the FTIR measurements were obtained from Wafer Technology LTD (Washington, USA). GaAs chips (G108K21530237) used for the bacterial coverage study were obtained from AXT Inc. (Fremont, USA). The D3422 GaAs/$Al_{0.35}Ga_{0.65}As$ chips used for the digital photocorrosion (DIP) experiments were obtained from CPFC (Ottawa, ON, Canada). Semiconductor grade isopropanol, acetone and OptiClear were purchased from Fisher Scientific (Ottawa, Canada), ACP (Montréal, Canada) and, National Diagnostics (Mississauga, Canada), respectively. The ethanol (Anhydrous) was

purchased from Commercial Alcohols Inc. (Brampton, Canada). The 28% of NH_4OH (ammonium hydroxide) used for removing oxide from the GaAs samples was obtained from Anachemia (Richmond, Canada). The MHDA (16-Mercaptohexadecanoic acid) thiol was purchased from Sigma-Aldrich (Oakville, Canada). The buffer (phosphate buffered saline, PBS) solution (10X, pH 7.4), polyclonal antibodies (Ab) specific to *L. pneumophila* were purchased from Sigma (Oakville, Canada) and ViroStat, Inc. (Portland, ME), respectively. Green fluorescent *Legionella pneumophila* JR32 was provided by the Faculty of Agricultural and Environmental Sciences, Department of Natural Resource Sciences, McGill University (Ste- Anne de Bellevue, Québec, Canada), *E. coli* ATCC 25922 and *Bacillus subtilis* ATCC 60514 were obtained from the Department of Biology, Université de Sherbrooke (Quebec, Canada) and *Pseudomonas fluorescens* ATCC 13525 was purchased from Cedarlane (Burlington, ON, Canada). The intention behind this bacterial selection, in addition to *L. pneumophila*, was to investigate the response of warnericin RK AMP to microbial representatives that are abundantly found in natural and industrial water environments. The warnericin RK AMPs were purchased from GenScript (Piscataway, USA).

3.3.2 Sample preparation

The samples prepared for Fourier-transform infrared (FTIR) absorption and bacteria surface coverage measurements were cut from an undoped GaAs (100) bulk wafer (WV 23084). The DIP biochips were prepared using an undoped wafer comprising stack of GaAs/$Al_{0.35}Ga_{0.65}As$ nanoheterostructures (Wafer D3422) for monitoring PL. The cross-sectional view of the wafer is presented in Figure 3.1 and the biofunctionalization process of the chip with attachment of *L. pneumophila* is presented in Figure 3.2. The 2 mm x 2 mm chips were cleaned following the previously established procedure (Aziziyan et al., 2016; Nazemi et al., 2015) in an ultrasonic bath using acetone, OptiClear, acetone, and isopropanol sequentially for 5 min each and blown dry with high purity compressed nitrogen gas. Thereafter, the samples were etched in NH_4OH for 2 min at room temperature for removing native oxides from the surface of GaAs and immediately dipped in the degassed ethanol. Following this step, the etched samples were immersed in 1 mM of (mercaptohexadecanoic acid) MHDA thiol for 20 h. After the thiolation step, the biochips were sonicated in deoxygenated ethanol for 1 min and rinsed with

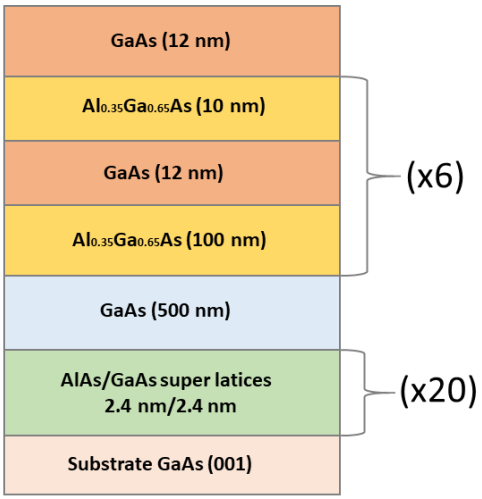

Figure 3.1 Schematic view of the GaAs/AlGaAs biochip cross-section (Wafer D3422).

degassed ethanol to remove unbound molecules. Thereafter, the thiolated samples were incubated for 30 min in the 0.4 M EDC – 0.1 M NHS (1:1) solution to activate -COOH terminals. Following this procedure, the samples were immerged for 1 h in 0.1 mg/mL of warnericin RK AMP synthesized by GenScript Corporation, Piscataway, USA. The functionalized samples were incubated with *L. pneumophila*, JR32 *E. coli* ATCC 25922,

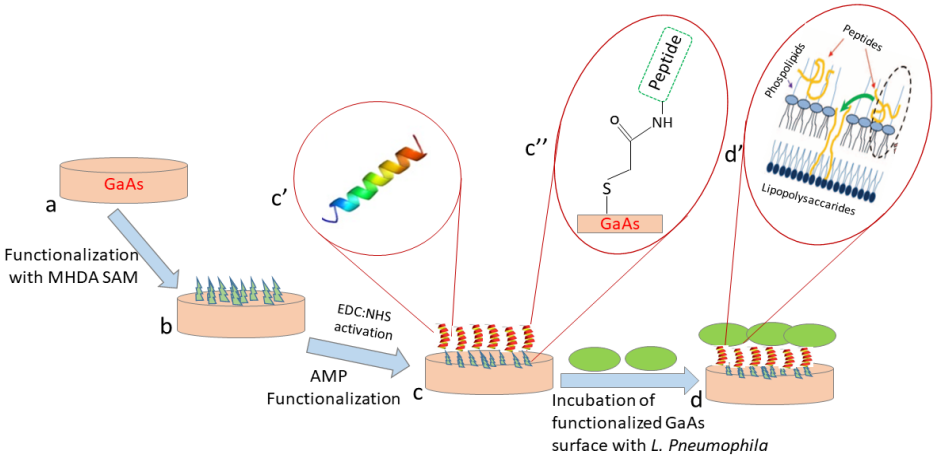

Figure 3.2 The bio-recognition mechanism of AMP, non-functionalized GaAs wafer (a), functionalized with MHDA SAM (b), AMP functionalized following the EDC/NHS step (c), globular structure of AMP (c'), MHDA-peptide hybrid (c''), attachment of bacteria to peptide (d), interaction between peptide and bacterial cell membrane (d') (Etayash et al., 2014b; Moghaddam et al., 2015).

Bacillus subtilis ATCC 60514 (*B. subtilis*) and *Pseudomonas fluorescens* ATCC 13525 (*P. fluorescens*) at 10^6 CFU/mL, each, for 2h. The biofunctionalization procedure of the biochip GaAs surface was carried out in the same manner as that employed for the biofunctionalization of the bulk GaAs (001) samples described above.

3.3.3 Optical microscopy analysis

The density of immobilized bacteria on the surface of GaAs was evaluated under an Optical microscopy (Nikon Instruments, Inc.). The optical microscopy images were taken using 200X magnification. The images were taken from three different regions of each sample surface for statistical analysis purpose. The cell surface coverage was calculated using the ImageJ software. All experiments were repeated 3 times for statistical analysis of optical microscopy data.

3.3.4 Field emission scanning electron microscopy analysis

The GaAs surface immobilized *L. pneumophila* cells were visualized with a field emission scanning electron microscope (FE-SEM, Hitachi S-4700, Japan). The microbes attached to the GaAs/MHDA/EDC-NHS-AMP surface (see the bacteria attachment procedure in Section 3.2) were rinsed with increasing concentrations of ethanol 30%, 50% and 100% sequentially for 5 min each and dried with nitrogen gas (Islam et al., 2017). Thereafter, the samples were coated with gold to a thickness of 10 nm. The bacteria were visualized by FE-SEM operating at 3 kV with 40k magnification.

3.3.5 Fourier-transform infrared spectroscopy analysis

The FTIR data were collected using a Bruker Optics Hyperion 2000 FTIR system. The spectra were recorded with resolution at 4 cm^{-1}, and an individual spectrum was averaged over 1000 scans. The FTIR data were recorded using a N_2 chilled HgCdTe (mercury cadmium telluride) IR detector. The sample cleaned by the afore-mentioned method using organic solvents (acetone, Opti-Clear, acetone, isopropanol, and ethanol) followed by removing oxides (28% NH_4OH) was used as a background reference.

3.3.6 Photoluminescence measurements

The photonic detection of bacteria was based on PL monitor DIP of GaAs/AlGaAs biochips carried out at room temperature using a custom designed quantum semiconductor photonic biosensor (QSPB) reader as described by Nazemi et al. (2015). The biochips were irradiated at 660 nm by a light emitting diode (LED). The PL signal was recorded by charged-couple device (CCD) camera. A power density of ~17 mW/cm^2 was employed to observe the photocorrosion of the investigated biochips. All experiments were repeated 3 times for statistical analysis of PL data. The photocorrosion of an AMP functionalized biochip immersed in 0.1 x PBS without bacterial exposure was considered as a reference sample.

3.4 Results and Discussion

3.4.1 Fourier-transform infrared spectroscopy analysis

The molecular conformation of the peptide binding architecture on the surface of GaAs was evaluated by collecting FTIR absorption spectroscopy spectra (Figure 3.3 and Table 3.1). The intense bands recorded at 2919 cm^{-1} and 2850 cm^{-1}, as shown in Figure 3.3 (a-b), are assigned

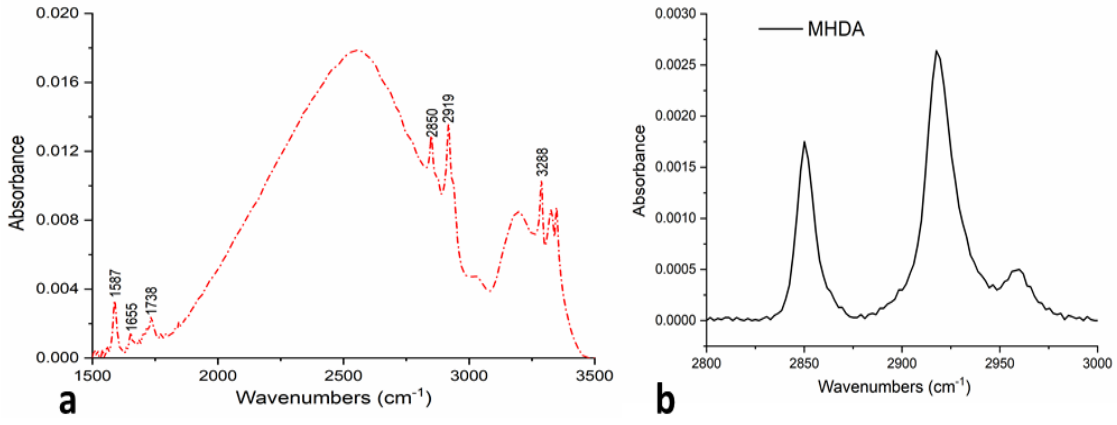

Figure 3.3 FTIR spectrum of a MHDA/EDC-NHS/AMP biofunctionalized GaAs (001) chip (a), FTIR spectrum of -CH_2 asymmetric (2919 cm^{-1}) and symmetric vibrations (2850 cm^{-1}) for MHDA-SAM (b).

to the -CH_2 asymmetric and symmetric vibrations, respectively. The observed FTIR characteristics of these two vibrations suggest the formation of high quality MHDA SAMs (Huang et al., 2013). The absorbance bands at 1655 cm^{-1}, 1587 cm^{-1}, 1738 cm^{-1} and 3288 cm^{-1}

are assigned to the amide I, amide II, amide III and amide A bands of AMP, respectively (Etayash et al., 2013; Etayash et al., 2014b; Forsting et al., 2017). Similarly, the peptide immobilized through the C-terminal with free N-terminal region shows a characteristic peak at 1655 cm^{-1} (Ami et al., 2014; Barbosa et al., 2017). The band observed at 1738 cm^{-1} is the C=O stretching mode of lateral chain functions and of some hydrolysed ester functions (Humblot et al., 2009).

Table 3.1 FTIR absorbance bands corresponding to the assigned functional groups.

Absorbance bands (cm^{-1})	Corresponding bonds	Reference
1587	Amide II (N-H banding)	(Rai et al., 2016)
1655	Amide I bond (C=O stretching)	(Ami et al., 2014), (Barbosa et al., 2017)
1738	Amide II, C=O stretching lateral chain function	(Humblot et al., 2009), (Doiron et al., 2018)
2850	CH_2 symmetric stretching	(Humblot et al., 2009), (Etayash et al., 2014b)
2922	CH_2 asymmetric stretching	(Humblot et al., 2009), (Etayash et al., 2014b)
3288	Amide A	(Forsting et al., 2017)

The peaks at 1655 cm^{-1} and 1738 cm^{-1} suggest the presence of a characteristic helical conformation of the surface-conjugated peptide (Barbosa et al., 2017; Doiron et al., 2018). Furthermore, the peak at 1587 cm^{-1} is likely related to the presence of the N-H bending mode for Amide II (Rai et al., 2016). These results suggest that the investigated peptide bound covalently on the EDC-NHS activated MHDA SAM. We note that, as expected, the peptide related absorbance peaks have not been observed for the MHDA/EDC-NHS modified GaAs unexposed to AMP.

3.4.2 Interaction of bacteria with the warnericin RK functionalized GaAs (001) surface

To evaluate the attachment/binding efficiency of warnericin RK, the AMP functionalized GaAs chips were incubated for 1h with 10^6 CFU/mL of either *L. pneumophila*, *E. coli*, *B. subtilis* or *P. fluorescens* as presented in Figure 3.4. The non-functionalized GaAs surface (Figure 3.4a) captured a small number of *L. pneumophila* compared to the warnericin RK functionalized surface (Figure 3.4b). Furthermore, the low capture efficiency of *E. coli*, *B.*

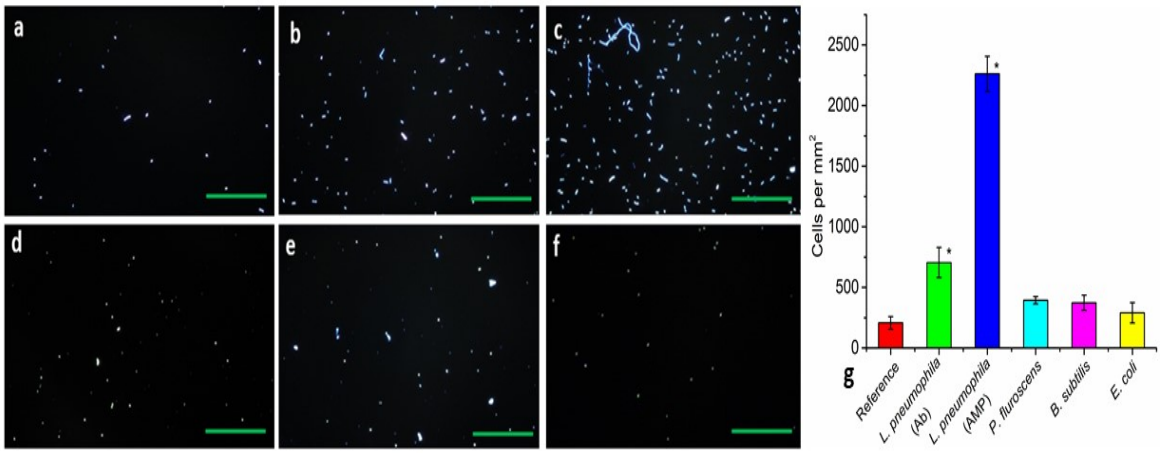

Figure 3.4 The attachment efficiency of *L. pneumophila* to the non-functionalized (a), antibody functionalized (b), AMP functionalized (c) surface of GaAs, and the attachment efficiency of the AMP functionalized GaAs surface for *P. fluorescens* (d), *B. subtilis* (e), and *E. coli* (f); averaged surface coverage for different bacteria (g). The asterisks indicate significantly different values compared to reference ($p<0.05$) as determined by the Students T-test (n=3). The scale bar corresponds to 100 µm.

subtilis and *P. fluorescens* by the warnericin RK AMP functionalized GaAs is well illustrated in Figs. 3.4c-f. The average number of quantified bacteria, as summarized in Figure 3.4g, shows that the peptide-coated surface captured ~2261, ~394, ~373, and ~290 cells/mm^2 of *L. pneumonphila*, *E. coli*, *B. subtilis* and *P. fluorescens*, respectively, while the peptide-free surface (*i.e.*, background) exhibited ~207 cells/mm^2. Thus, these results illustrate a 5-6 times greater capture efficiency of the warnericin RK functionalized GaAs surface of the biochip towards *L. pneumophila* than to *E. coli*, *B. subtilis* and *P. fluorescens*. The variation of binding efficiency could be attributed to the specificity of peptide bacteria interactions (Berjeaud et al., 2016; Etayash et al., 2014b).

In the present study, the warnericin RK functionalized surface of GaAs was found to be highly specific to *L. pneumophila* probably due to the presence of the unique lipid

composition of the *L. pneumophila* bacterial membrane (Marchand et al., 2011). An example of FE-SEM image for *L. pneumophila* is shown in Figure 3.5. Verdon et al. (2011) investigated the sensitivity of the warnericin RK to *L. pneumophila* and found that the presence of branched-chain fatty acids on the surface of bacteria play a crucial role for the sensitivity of bacteria to these peptides. Furthermore, *L. pneumophila* contains high proportions (30%) of phosphatidylcholines (PCs) that are conventionally prevalent in

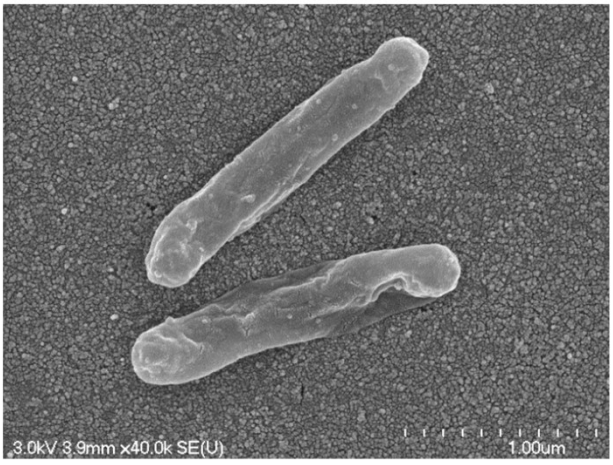

Figure 3.5 An example of FESEM micrograph for determining *L. pneumophila*.

eukaryotic cells (Verdon et al., 2011). As such, these lipids are very specific to the *Legionella* genus (Berjeaud et al., 2016), and may explain the strong interaction observed between warnericin RK and the *Legionella* bacterial membrane.

3.4.3 Detection of *L. pneumophila* with DIP GaAs/AlGaAs biosensor

An example of a series of temporal PL plots collected for the GaAs/AlGaAs DIP biochips exposed to *L. pneumophila* solutions in the range from 10^3 to 10^6 CFU/mL at 0.1x PBS, and the calibration plot obtained from 3 repetitions are presented in Figure 3.6 (a-b) and Table 3.2, respectively. Delayed positions of PL maxima were observed with increasing concentrations of bacteria, which is consistent with the response of a DIP GaAs/AlGaAs biochip exposed to negatively charged bacteria suspended in a water environment (Aziziyan et al. 2016; Nazemi et al. 2017). The limit of detection at 10^3 CFU/mL has been estimated based on the time dependent positions of PL maxima determined for 3 independent runs with an error nearest to

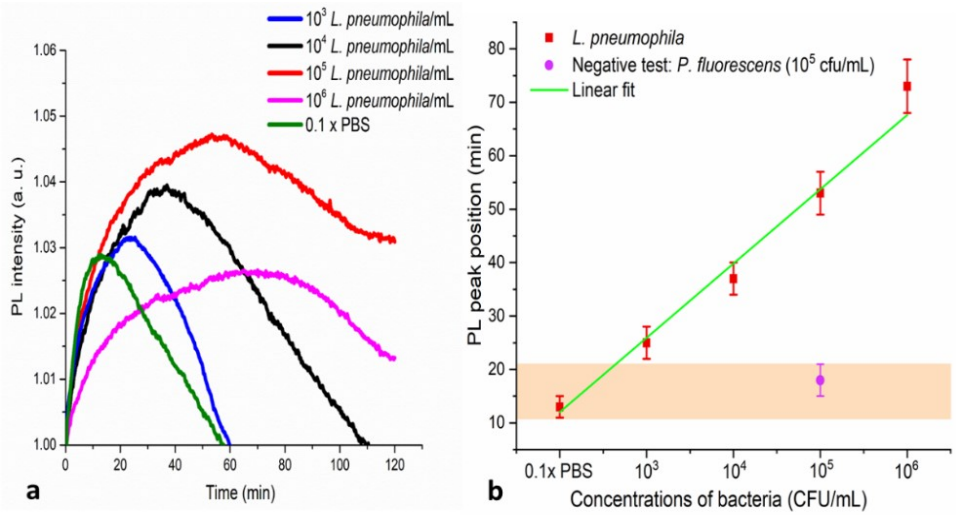

Figure 3.6 Normalized PL intensity for MHDA/EDC-NHS/AMP functionalized GaAs/AlGaAs DIP biochips (wafer D3422) exposed at 0.1 x PBS to different concentrations of *L. pneumophila* (a), PL peak positions *vs*. different concentrations of *L. pneumophila* bacteria (b). The PL peak positions obtained for *L. pneumophila* were statistically different compared to either 0.1x PBS and *P. fluorescens* treated surface ($p<0.05$) as determined by the Students T-test (n=3).

that of the positions of PL maxima for 3 independent reference runs in a 0.1x PBS solution. Although the specificity of this method warrants extensive future research, the results demonstrate that the sensitivity of a warnericin AMP-functionalized *L. pneumophila* biosensor is by one order of magnitude better than that reported for an antibody-based DIP biosensor (Aziziyan et al., 2016) while comparable to that of DIP detected *L. pneumophila* decorated with sodium dodecyl sulphates (SDS) (Aziziyan et al., 2020), as well to some other recently published results as shown in Table 3.3.

Table 3.2 PL maxima obtained for different concentrations of *L. pneumophila*

Bacteria	Concentrations	PL maxima (min)
PBS	0.1 x	13 ± 15%
L. pneumophila	10^3	25 ± 12%
L. pneumophila	10^4	37 ± 8%
L. pneumophila	10^5	53 ± 8%
L. pneumophila	10^6	73 ± 7%
P. fluorescens	10^5	18 ± 16%

It is important to note that antibodies have been widely used as bio-recognition elements for bacterial detection solely based on their specific interaction with bacterial

antigens. However, apart from the specificity, the design of the detection architecture should include other practical considerations. In electrochemical (Hoyos-Nogués et al., 2018) and PL based biosensors (Aziziyan et al., 2016), the excessive distance of the antibody from the sensing surface could decrease the detection performance due to reduced electrostatic interaction and/or inefficient charge transfer between the biosensor and analytes. Furthermore, antibodies might not demonstrate stable performance in harsh environments. In contrast,

Table 3.3 Immunosensor based detection of *L. pneumophila*.

Type of bioreceptors	LOD	Linear range (CFU/mL)	Reference
Anti-*L. pneumophila* polyclonal antibodies	10^4 CFU/ mL	10^3 - 10^6 CFU/ mL	(Aziziyan et al., 2016)
Anti-*L. pneumophila* antibodies	10^4 CFU/9 mL	10^3 - 10^4 CFU/9 mL	(Bedrina et al., 2013)
Antibody (Ab) was linked to the poly (dopamine)	10^4 CFU/ mL	-	(Martín et al., 2015)
L. pneumophila LPS specific Ab	10^1 CFU/ mL	10^1 – 10^3 CFU/9 mL	(Lin et al., 2007)
SDS-decorated *L. pneumophila*	10^3 CFU/mL	10^2 – 10^4 CFU/mL	(Aziziyan et al., 2020)
AMP	10^3 CFU/ mL	10^3 – 10^6 CFU/mL	This study

AMPs could offer attractive biosensing solutions, as their small molecular size allows for efficient charge transfer, and they exhibit high stability compared to typical mammalian antibodies (Dong and Zhao, 2015; Wilson et al., 2019). Furthermore, AMPs can be manufactured with high reproducibility (Hoyos-Nogués et al., 2018). The specific detection of *L. pneumophila* with a warnericin RK biosensor as reported here should not be surprising in view of some recent studies claiming the highly selective nature of AMPs-based biosensors. For instance, Hossein-Nejad-Ariani et al. (2018) reported the high binding affinity of a Leucocin A (Leu A) functionalized gold microelectrode to *Listeria monocytogenes* in comparison to 4 other bacteria. In another study, Mannoor et al. (2010) observed that a gold electrode functionalized with magainin I (AMP) permitted ~4-fold higher binding affinities to the *E. coli* O157:H7 compared to other bacteria (*i.e., E. coli* ATCC 35218 and *Listeria Monocytogenes*). To the best of our knowledge, the present study demonstrates for the first

time the attractive application of warnericin RK AMP for highly selective detection of *L. pneumophila* with a photonic biosensor.

3.5 Conclusions

The present study investigated the application of AMP for direct *in situ* detection of *L. pneumophila* in a water environment. The molecular orientation of the warnericin RK AMP on the GaAs (001) surface was examined using FTIR analysis, which indicated covalent interaction of AMP with the GaAs surface. The specificity experiments demonstrated that *L. pneumophila* was captured with ~5-fold greater binding affinity than JR32 *E. coli* ATCC 25922, *Bacillus subtilis* ATCC 60514, and *Pseudomonas fluorescens* ATCC 13525. Detection sensitivity of the biosensor was demonstrated between 10^3 – 10^6 CFU/mL. The lower detection limit of 10^3 CFU/mL was one order of magnitude better than that previously reported with an antibody-based GaAs/AlGaAs DIP biosensor (Aziziyan et al., 2016). Our results provide evidence for the attractive application of a warnericin RK AMP biofunctionalized DIP biosensor for highly sensitive and specific detection of *L. pneumophila* in water samples, and pave the way towards the development of a robust biosensor operating in harsh environments.

3.6 Acknowledgements

This research was supported by the Natural Sciences and Engineering Research Council of Canada Strategic Partnership Grant (NSERC SPG-2016-494057) and the NSERC Discovery Grant (RGPIN-2015-04448). The fabrication of GaAs/AlGaAs wafers was subsidized by CMC Microsystems (Kingston, Canada). The authors are indebted to Prof. E.H. Frost for helpful discussions and Dr. K. Moumanis for technical assistance.

Chapter 4. Avant-propos

Auteurs et affiliations:

M. Amirul Islam: Étudiant au doctorat, Université de Sherbrooke, Faculté de génie, Département de génie électrique et informatique.

Walid M. Hassen: Assistant de recherche, Université de Sherbrooke, Faculté de génie, Département de génie électrique et informatique.

Azam F. Tayabali: Professeur associé, Laboratoire de biotechnologie, Bureau de la science et de la recherche en santé environnementale, Direction générale de la santé environnementale et de la sécurité des consommateurs, Centre de santé environnementale, Santé Canada

Jan J. Dubowski: Professeur, Université de Sherbrooke, Faculté de génie, Département de génie électrique et informatique.

Titre français: Le peptide antimicrobien warnericin RK un court ligand modifié par la cystéine pour une détection hautement sensible de *Legionella pneumophila*

Date d'acceptation: 14 décembre 2020

État de l'acceptation : version finale publiée

Revue: ACS Omega

Référence: M. A. Islam, W. M. Hassen, A. F. Tayabali, J. J. Dubowski, "Short ligand, cysteine modified warnericin RK antimicrobial peptides favour highly-sensitive detection of *Legionella pneumophila*" ACS Omega, vol. no. 6, pp. 1299-1308, 2020.

Contribution au document: Dans ce chapitre, une bioarchitecture à base de PAM modifié avec la cysteine (Cys-WRK) a été proposée pour construire un biocapteur DIP GaAs/AlGaAs pour améliorer la sensibilité de détection de *L. pneumophila*. Le biocapteur proposé a détecté avec succès la *L. pneumophila* à une concentration de 2 x 10^2 UFC/mL avec une assez satisfaisante spécificité. L'application de Cys-WRK AMP pour la fonctionnalisation des

biocapteurs DIP à base de GaAs fournit un moyen alternatif permettant d'éliminer l'étape de 20 heures requise pour la formation de la monocouche auto-assemblée (MAA) de MHDA et l'activation ultérieure du groupement -COOH du MHDA par l'EDC/NHS nécessaire pour attacher à la suite le PAM via sa terminaison amine. En optant vers l'usage du Cys-WRK, nous avons pu avoir une bioarchitecture d'environ 2 nm comparé à 15 nm en cas d'usage du MHDA ainsi que réduire le temps d'analyse à seulement 3h (préparation d'échantillon comprise). Réduisant les étapes de fonctionnalisation, pourrait permettre l'obtention de résultats plus reproductibles ceci en plus qu'une couche de fonctionnalisation plus courte faciliterait le transfert de charge entre les bactéries et la surface du biocapteur. Ainsi, les architectures à base de PAM à chaîne courte offrent une détection rapide, sensible et spécifique de *L. pneumophila* et serait mieux adaptées aux transducteurs sensibles aux charges électriques, tels que les biocapteurs DIP.

Résumé français: Les méthodes basées sur la culture pour la détection de *Legionella pneumophila* sont excessivement lentes et souvent inadéquates. Le problème a été résolu avec diverses technologies de biodétection utilisant une variété de ligands pour la capture spécifique de bactéries. Cependant, le succès limité de l'application d'anticorps de mammifères, d'aptamères et de sondes à base d'acide nucléique pour la biodétection a suscité un intérêt croissant pour l'exploration d'architectures alternatives, telles que celles basées sur les peptides antimicrobiens (PAM) dèjà connus pour leurs propriétés thérapeutiques attrayantes. Nous rapportons en l'utilisation satisfaisante de la warnericin RK modifiée par la cystéine pour le développement d'un biocapteur hautement sensible à *L. pneumophila* basé sur la photocorrosion numérique de nanohétérostructures GaAs/AlGaAs. Le remplacement de la procédure relativement lourde couramment appliquée pour la fixation d'anticorps aux monocouches auto-assemblées (MAA) d'acide mercaptohexadécanoïque à terminaison COOH (MHDA) a permis une réduction significative de la distance entre les bactéries capturées et la surface du biocapteur. Une conséquence importante de cette approche est la limite de détection attractive de *L. pneumophila* estimée à 2 x 10^2 UFC/mL. La bactérie cible ont été capturée quatre fois plus efficacement que *P. fluorescens*, *B. subtilis* et *E. coli*, ce qui rend un tel biocapteur prometteur pour la surveillance environnementale de *Legionella pneumophila*.

Chapter 4. Short ligand, cysteine modified warnericin RK antimicrobial peptides favor highly sensitive detection of *Legionella pneumophila*

4.1 Abstract

Culture-based methods for the detection of *Legionella pneumophila* (*L. pneumophila*) are prohibitively slow and frequently inadequate. The problem has been addressed with biosensing technology that employs a variety of ligands for the specific capture of bacteria. However, the limited success of the application of mammalian antibodies, aptamers, and nucleic acid-based probes for sensitive biosensing has generated growing interest in exploring alternative biosensing architectures, such as those based on antimicrobial peptides (AMP) that are known for their attractive therapeutic applications. We report on the successful employment of cysteine modified warnericin RK AMP for the operation of a highly sensitive biosensor of *L. pneumophila* based on digital photocorrosion of GaAs/AlGaAs nanoheterostructures. The replacement of the relatively cumbersome procedure commonly applied for the attachment of antibodies to COOH-terminated mercaptohexadecanoic acid (MHDA) self-assembled monolayers (SAM) has allowed for a significant reduction in the distance at which bacteria are immobilized above the biosensor surface. An important consequence of this approach is the attractive limit of detection of *L. pneumophila* estimated at 2 x 10^2 CFU/mL. The target bacteria were captured four times more efficiently than *P. fluorescens*, *B. subtilis*, and *E. coli*, which is highly promising for environmental monitoring.

Keywords: Cysteine modified warnericin RK, *Legionella pneumophila*, Antimicrobial peptides, Digital photocorrosion biosensor, GaAs/AlGaAs nanoheterostructures, Photoluminescence

4.2 Introduction

Rapid detection of pathogenic bacteria in a water environment remains a challenging issue (Ashbolt, 2004; Etayash et al., 2014b). Of particular interest are rapid, portable, non-labor intensive, yet cost-attractive tools for detection of pathogens (Rodrigues Ribeiro Teles et al.,

2010). The culture based, colony-counting methods have been widely used to detect bacteria (Hameed et al., 2018), but they are labour and time intensive (Hameed et al., 2018; Jayan et al., 2019). For instance, *Legionella pneumophila* (*L. pneumophila*) may require up to 10 days of incubation for visible detection of colonies (Keserue et al., 2012). Alternatively, polymerase chain reaction (PCR) based detection (Mothershed and Whitney, 2006) or matrix-assisted laser desorption ionization time-of-flight (MALDI-TOF) spectroscopy (Jeverica et al., 2018) could both provide relatively fast and accurate detection. However, the need for highly trained personnel and sophisticated lab requirements are the main constraints of these techniques (Buchan and Ledeboer, 2014; Singhal et al., 2015). The biosensor-based detection methods of pathogenic bacteria have gained attention due to their potential to offer relatively fast, portable and easy-to-handle solutions (Hoyos-Nogués et al., 2018). In that context, various types of *L. pneumophila* biosensors have been investigated ranging from optical (Meneghello et al., 2017; Yoo and Lee, 2016) and piezoelectric (Gupta and Kakkar, 2020; Miranda-Castro et al., 2007) to electrochemical (Laribi et al., 2020; Mobed et al., 2019). However, to the best of our knowledge, an economically attractive method for automated monitoring of water reservoirs for the presence of pathogenic bacteria has yet to be developed. Recently, photoluminescence (PL) based detection of *E. coli* has proven to be rapid and relatively sensitive (Nazemi et al., 2015). In this technique, the sensitivity of PL varies with the presence of electrically charged molecules (*i.e.* proteins, viruses and bacteria) on the surface of semiconductor nanoheterostructures that have the potential for the realization of a regenerable system designed for automated data collection (Aziziyan et al., 2020; Nazemi et al., 2015).

L. pneumophila is a pathogenic waterborne bacterium, predominantly found in man-made artificial water reservoirs, *i.e.,* spas and cooling towers (Berjeaud et al., 2016; Guyard and Low, 2011). Humans who are accidentally exposed may develop a pulmonary infection known as Legionnaire's disease (Berjeaud et al., 2016; Marchand et al., 2011). In 2006, more than 6000 cases were reported in Europe, 400 of them fatal (Marchand et al., 2011). Of the 60 reported *Legionella* species, 85-90% are associated with Legionnaire's disease (Verdon et al., 2008). Therefore, the detection of *L. pneumophila* in water reservoirs has emerged as a public health priority. Culture based methods have been commonly applied for the detection of *L. pneumophila* (Ballard et al., 2000; Dusserre et al., 2008), however, they are time consuming techniques. In addition to a multi-day delayed detection, some viable but non-culturable

bacteria could not be detected with these techniques. The PCR-based method can address most of the aforementioned problems, but the requirement of trained personnel and sophisticated laboratory facilities limit the application of this technique (Hameed et al., 2018). Biosensor-based detection of *L. pneumophila* has the potential to alleviate these deficiencies.

The efficiency of bio-recognition elements is crucial in order that biosensor technology be able to offer a selective, sensitive and accurate measurement of the target (Elakkiya and Matheswaran, 2013; Ramanavičius et al., 2006). Numerous bio-recognition elements, such as antibodies (Ab), carbohydrates, aptamers, peptides, as well as combinations of these, have been widely explored in different biosensing platforms (Hoyos-Nogués et al., 2018). Among them, Ab have been considered as an attractive option since they can be highly specific towards the antigenic target (Etayash et al., 2013; Mannoor et al., 2010). However, Ab suffer from lack of stability, especially under extreme environmental conditions, such as high/low pH and elevated temperatures (Mannoor et al., 2010), and they often require additional conjugating compounds, such as neutravidin, biotin or avidin (Aziziyan et al., 2016). These conjugations increase the number of interfaces which could affect the reproducible performance of a biosensor. Recently, some studies have shown that antimicrobial peptides (AMPs) could be reasonable candidates for bio-recognition in biosensing platforms (de Miranda et al., 2017; Dong and Zhao, 2015; Etayash et al., 2013). The multiple molecular niches of an AMP seem partially responsible for the strong interaction with bacteria and fungi surface moieties (Mannoor et al., 2010). Furthermore, it has been reported that some cationic AMPs could maintain their activity in harsh environments, even after boiling and autoclaving (Friedrich et al., 1999; Rydlo et al., 2006). The considerably superior stabilities of AMPs over those of typical globular proteins (Mannoor et al., 2010; Rydlo et al., 2006) justify the AMP research expected to lead to the replacement of typical Ab-based biorecognition elements.

In the past few years, several AMPs such as magainin I (Kulagina et al., 2005), Clavanin A (Andrade et al., 2015) and polymyxin B (Kulagina et al., 2006)[40] have been investigated as bio-recognition probes, with some AMPs demonstrating a highly specific recognition capacity. Mannoor et al. (2010) reported that a gold electrode functionalized with magainin I AMP showed differential binding affinity to the pathogenic bacterial strains of *E. coli* and *Salmonella* at 10^7 CFU/mL. Another study reported that a gold microelectrode

functionalized with Leucocin A (Leu A) exhibited high binding affinity to *Listeria monocytogenes* (Hossein-Nejad-Ariani et al., 2018). It has been reported that warnericin RK is a membrane active peptide which shows high specificity to *L. pneumophila* (Marchand et al., 2015). However, the exact interaction between peptide and bacterium is not clearly understood. It has been proposed that initially, the peptide attaches to the target cell surface due to a general electrostatic interaction with negatively charged bacteria. This initial association is followed by a specific interaction of the peptide with a specific, yet unidentified, *L. pneumophila* membrane moiety (Verdon et al., 2011). It has also been reported that the selectivity of warnericin RK to *L. pneumophila* might be related to the fatty acid composition of the cell membrane (Verdon et al., 2011).

In our recent study (Islam et al., 2020), we employed a digital photocorrosion (DIP) biosensor biofunctionalized with a 16-mercaptohexadecanoic acid (MHDA) linker for interfacing warnericin RK AMP, which allowed detection of *L. pneumophila* at 10^3 CFU/mL. Given that a DIP biosensor is sensitive to the flow of electric charge between the biosensor and immobilized bacteria, we hypothesized that a short-linker biosensor, consisting also of a reduced number of interfaces, could exhibit a significantly enhanced sensitivity. Thus, we report here on the operation of an innovative DIP biosensor comprising cysteine-modified RK AMP (Cys-AMP) designed for rapid detection of *L. pneumophila*. A successful investigation was also carried out by demonstrating a negligible specificity of the biosensor towards *P. fluorescens*, *B. subtilis* and *E. coli*.

4.3 Experimental section

4.3.1 Materials and reagents

Undoped, double side-polished GaAs (001) chips (Wafer WV 23084, Wafer Technology Ltd, Washington, USA) were used for measuring bacteria capture efficiency. GaAs/$Al_{0.35}Ga_{0.65}As$ nanoheterostructure wafers (Canadian Photonics Fabrication Centre, Ottawa, Ontario, Canada) were used for monitoring the DIP process of biofunctionalized chips. The details for employing GaAs/AlGaAs nanoheterostructures in DIP biochips have been reported elsewhere (Aziziyan et al., 2016; Nazemi et al., 2015). Semiconductor grade isopropanol, acetone and

OptiClear were purchased, respectively, from Fisher Scientific (Ottawa, Canada), National Diagnostics (Mississauga, Canada), and ACP (Montréal, Canada). Anhydrous ethanol was purchased from Commercial Alcohols Inc. (Brampton, Canada). Ammonium hydroxide (28% of NH_4OH) used for removing oxides from the GaAs surface was purchased from Anachemia (Richmond, Canada). Phosphate buffered saline solution (PBS; 10X, pH 7.4) and 16-Mercaptohexadecanoic acid (MHDA) thiol were purchased from Sigma-Aldrich (Oakville, Canada) and ViroStat, Inc. (Portland, ME), respectively. Anti-*L. pneumophila* polyclonal Ab were purchased from ViroStat, Inc. Green fluorescent *L. pneumophila* JR32 was obtained from the Faculty of Agricultural and Environmental Sciences, McGill University (Ste-Anne de Bellevue, Québec, Canada). *Bacillus subtilis* ATCC 60514 and *Escherichia coli* ATCC 25922 were obtained from the Department of Biology, Université de Sherbrooke (Quebec, Canada), and *Pseudomonas fluorescens* ATCC 13525 was purchased from Cedarlane (Burlington, Ontario, Canada). Cys-AMPs (GenScript, Piscataway, USA) were employed to achieve robust functionalization of GaAs/AlGaAs chips thus taking advantage of the strong affinity of sulphur towards Ga and As (Voznyy and Dubowski, 2009).

4.3.2 Biofunctionalization of Gallium Arsenide (GaAs) chip surface

Bulk GaAs (001) chips, 2 mm x 2mm, were used for carrying out Fourier-transform infrared spectroscopy (FTIR), x-ray photoelectron spectroscopy (XPS), atomic force microscopy (AFM) and bacteria capture efficiency measurements. The samples of bulk GaAs and GaAs/AlGaAs nanoheterostructures were cleaned in ultrasonic baths of acetone, OptiClear and isopropanol for 5 min each, and then dried with high purity nitrogen gas (Lacour et al., 2016; Sharma et al., 2016). Thereafter, native oxides present on the surface of the samples were removed with 28% NH_4OH (2 min at room temperature), followed by immediate dipping of the samples in degassed ethanol, and rinsing with copious amounts of degassed DI water. Different concentrations of peptide solutions (2-100 μg/mL) were prepared for functionalizing the GaAs and GaAs/AlGaAs chips. To investigate the stability of the proposed biosensor, aliquots of peptide solution (50 μg/mL) were stored at room temperature for up to 30 days. Functionalization was achieved by immersing cleaned samples in peptide solution for 1h. The functionalized chips were sonicated in degassed DI water for 1 min, and immediately rinsed with degassed DI water in order to remove non-immobilized peptides.

4.3.3 Preparation of bacteria

E. coli, P. fluorescens and *B. subtilis* were obtained from fresh cultures in a Luria-Bertani (LB) medium. *L. pneumophila* serogroup 1 (SG1) was cultured in a buffered charcoal yeast extract agar (BCYE), supplemented with isopropyl thio-β-galactoside (IPTG) and L-cysteine. Subsequently, several colonies of *L. pneumophila* were transferred to 0.1x PBS, and concentration of bacteria was determined by OD_{600nm} measurement (0.1 OD 600_{nm} corresponds to 6.4 x 10^7 *L. pneumophila*/mL). Serial dilutions were carried out in 0.1x PBS to achieve the test concentrations.

4.3.4 Biosensor architecture

Following the removal of native oxides from the surface of GaAs/AlGaAs chips, the samples were immersed for 1 hour in Cys-AMPs suspended in DI water. Subsequently, a 1 min sonication in degassed DI water was applied to remove non-immobilized peptides. However, it was found that light rinsing with DI water was sufficient to remove weakly bonded (physisorbed) peptides, which may be important for the future development of a procedure for automated biofunctionalization. The biofunctionalized chips, typically less than 60 min from their fabrication, were exposed to different suspensions of bacteria. Figure 4.1 illustrates the process of a biosensor fabrication. Notice that the strong interaction of warnericin RK AMP with *L. pneumophila* is expected to result in the rapid breaking of the bacterial outer

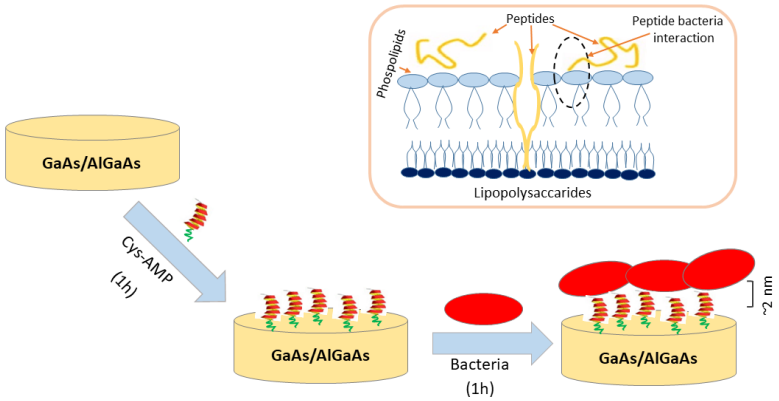

Figure 4.1 Cysteine-modified warnericin RK antimicrobial peptide-based architecture of a *L. pneumophila* biosensor employing GaAs/AlGaAs nanoheterostructure chips. The inset illustrates the proximity of interaction between bacterial cell membrane and peptides.

membrane as illustrated by the inset in Figure 4.1. It is important to note that the entire detection procedure of this biosensor could be completed within ~2 hours, including the biofunctionalization step, as compared to the more than 20 hours required by a biosensor employing an alkanethiol self-assembled monolayer (as shown in Figure 4.2). Furthermore, of potential importance to the operation of charge sensitive sensors (DIP, electrochemical or field-effect devices) is the remarkably short, 2 nm distances between the biochip surface and bacteria immobilized with the Cys-AMP architecture, which could affect the process of charge

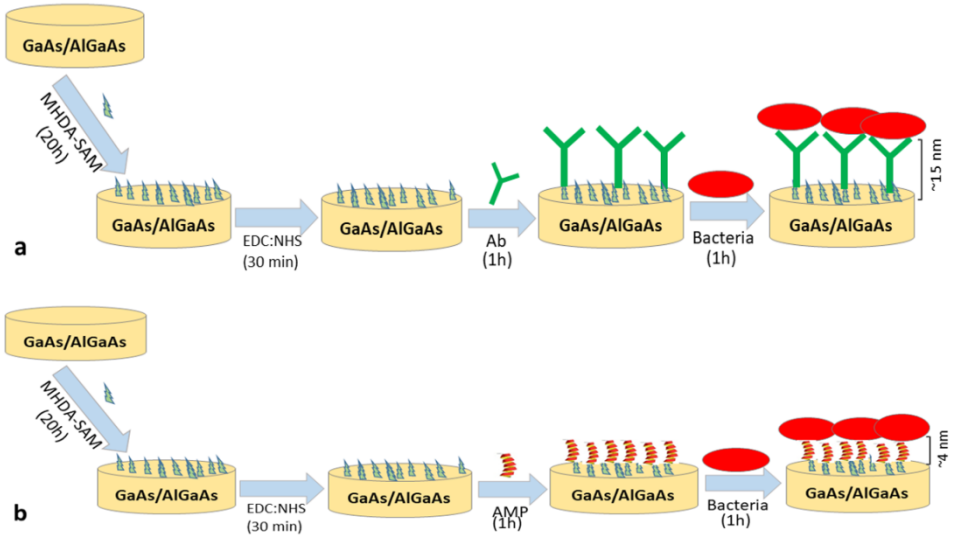

Figure 4.2 Schematic representation of antibody and AMP based bio-functionalization architectures for capturing *L. pneumophila* on GaAs/AlGaAs surface, GaAs/AlGaAs-MHDA-Ab (a), GaAs/AlGaAs-MHDA-AMP (b).

transfer. In the case of anti-*L. pneumophila* Ab functionalization, the etched samples (after being treated with 28% NH_4OH) was immersed in 1mM of MHDA thiol in 10 mL of deoxygenated ethanol for 20h. After the thiolation, the functionalized chips were sonicated in degassed ethanol for 1 min and immediately rinsed with degassed ethanol in order to remove non-immobilized thiols. Thereafter, the -COOH terminals of thiolated samples were activated using 0.4 M EDC: 0.1 M NHS (1:1) solution for 30 min and immediately rinsed with DI water. Then, the samples were incubated in 100 µg/mL of anti-*L. pneumophila* polyclonal Ab for 1h. Finally, both AMP and Ab functionalized samples were incubated with heat killed *L. pneumophila* at 10^6 CFU/mL for 1h. The GaAs/$Al_{0.35}Ga_{0.65}As$ nanoheterostructures were used

for the fabrication of 2 mm x 2 mm DIP biochips functionalized by following the aforementioned protocols.

4.3.5 Fourier-transform infrared spectroscopy analysis

The FTIR absorption spectroscopy measurements were collected using a Bruker Optics Hyperion 2000 FTIR system. The spectra were collected with a resolution at 4 cm^{-1}, and individual spectra were averaged over 1000 scans. All FTIR data were recorded with a liquid N_2 chilled HgCdTe (mercury cadmium telluride) IR detector. A reference GaAs sample was obtained by consecutive cleanings in ultrasound baths with OptiClear, acetone, isopropanol, acetone, and ethanol (5 min each), and then etched with a 28% NH_4OH solution.

4.3.6 Atomic force microscopy analysis

Topographic images of functionalized GaAs samples were taken with an atomic force microscope (AFM, Shimadzu Instruments, SPM - 9700, Japan) operating at room temperature (~25±2 ^oC). The root mean square (σ_{RMS}) surface roughness was calculated based on scans collected from 5 μm × 5 μm surface areas of the investigated samples. Images were analyzed using AFM Gwyddion software (version 2.53).

4.3.7 X-ray photoelectron spectroscopy analysis

XPS spectra were recorded with a Kratos Analytical AXIS (Ultra DLD XPS) spectrometer employing an Al Kα source (1486.6 eV) operating at 150 W. The XPS data were obtained with a 60° take-off angle with respect to the surface normal. The carbon signals were measured and fitted using Casa XPS software for both bulk GaAs and GaAs/AlGaAs biochip samples. The binding energy reference to adventitious C 1s peak at 284.8 eV positioned the As $3d_{5/2}$ peak at 40.8 eV, which was subsequently used as a nominal calibration.

4.3.8 Contact angle measurements

The water hydrophilicity of the peptide functionalized GaAs surface was determined at room temperature using commercial static water contact angle measurement equipment (KRÜSS DSA30). The GaAs surface was exposed to a 10-μL droplet of Milli-Q water and after 5 s, the contact angle of the GaAs-water interface was calculated.

4.3.9 Optical microscopy analysis

Optical microscopy (Nikon Instruments, Inc.) was used to determine the density of immobilized bacteria on the biochip surface. The images were taken at 200X magnification in three different regions of each sample surface. All experiments were repeated at least three times. The bacteria surface coverage was calculated using ImageJ software (Grishagin, 2015).

4.3.10 Photoluminescence measurements

The detection of bacteria was carried out at room temperature with a DIP GaAs/AlGaAs biosensor whose PL was measured with a quantum semiconductor photonic biosensing (QSPB) reader described elsewhere (Aithal et al., 2017; Aziziyan et al., 2016). Reference measurements and bacteria coated biochips were irradiated with 5-s pulses delivering 17 mW/cm^2 each, in every 20-s period, using a light emitting diode (LED) operating at a wavelength of 660 nm. The PL signal and images of the biochips collected *in situ* were recorded with a charge-coupled device (CCD) camera. Experiments were carried out in a 0.1X PBS solution, and runs without bacteria were used to obtain reference signal. All experiments were repeated at least 3 times.

4.4 Results and discussion

4.4.1 Functionalization of GaAs/AlGaAs biosensors

The immobilization of peptides on the surface of GaAs was evaluated by FTIR analysis as presented in Figure 4.3 (for a detailed list of peak positions see Table 4.1). The FTIR absorbance spectra have been normalized as presented in Figure 4.3 (a-b). The absorbance band at 1235 cm^{-1} was assigned to amide III, while the band at 1519 cm^{-1} could be assigned to amide II (de Campos Vidal and Mello, 2016; Munje et al., 2017). The absorbance at 1540 cm^{-1} and 1655 cm^{-1} is characteristic for C=O stretching of amide I (Akrami et al., 2016; Ami et al., 2014). The intense bands at 2922 cm^{-1} and 2850 cm^{-1} observed in Figure 4.3a are typical of CH_2 asymmetric and symmetric vibrations, and are related to the thiol groups of peptides reported in the literature (Etayash et al., 2013; Etayash et al., 2014b). The absorbance bands at 1653 cm^{-1} and 1587/1734 cm^{-1} were assigned to amide I and amide II, respectively

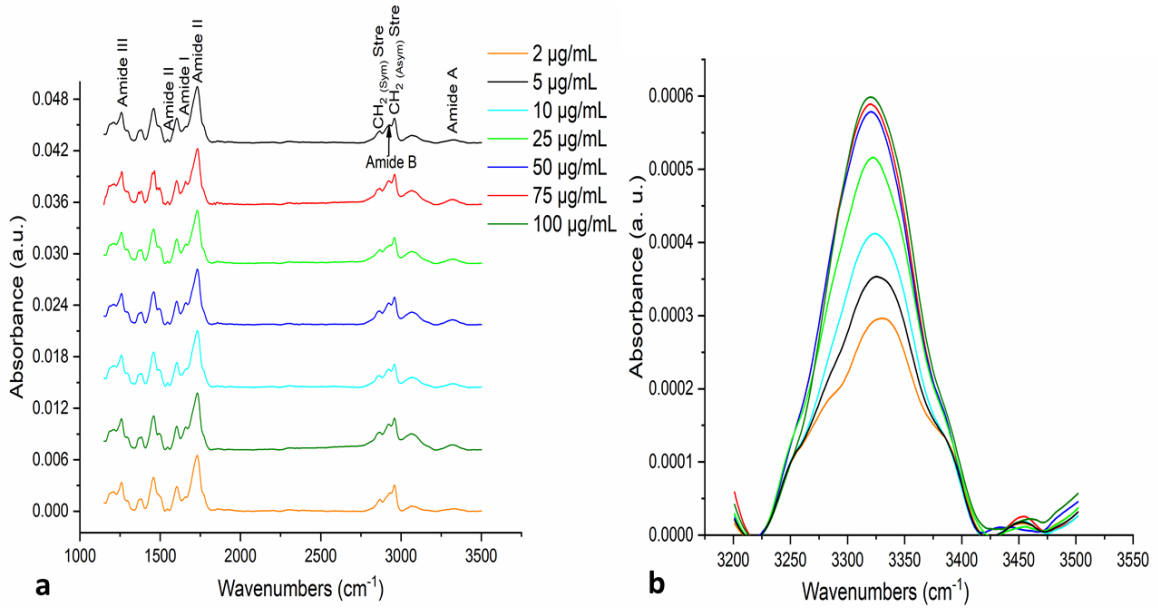

Figure 4.3 Representative FTIR absorbance spectra of thiol and peptide related peaks (a), and amide A absorbance spectra collected for different peptide concentrations (b).

(Forsting et al., 2017; Humblot et al., 2009). Similarly, the peptide immobilized at the C-terminal with a free N-terminal region shows a characteristic peak at 1653 cm^{-1} (Ami et al., 2014; Barbosa et al., 2017). Furthermore, the band observed at 1734 cm^{-1} corresponds to C=O stretching of lateral chain functions and some hydrolysed ester functions (Doiron et al., 2018; Humblot et al., 2009). The intense peaks at 1653 cm^{-1} and 1734 cm^{-1} suggest a helical conformation (Ami et al., 2014; Barbosa et al., 2017; Doiron et al., 2018). Furthermore, the band at 1587 cm^{-1} suggests the presence of an N-H bond for amide II (Rai et al., 2016), while the band at 3324 cm^{-1} could be assigned to amide A (Dinesh et al., 2015; Jeevithan et al., 2014). Therefore, the amide related peaks in the FTIR spectra (1235, 1519, 1587, 1653, 1734, 3324 cm^{-1}) confirm the successful immobilization of peptides on the surface of GaAs via cysteine linker of peptide. It is noticeable that the peaks of a similar intensity were observed in Figure 4.3a for amide I, II, III of different concentration peptides, while the amide A intensity varied with the increasing concentration of peptide as presented in Figure 4.3b. The peak intensity increased with the increasing concentrations of peptide until 50 µg/mL, thereafter the peak intensity did not correlate with higher peptide concentrations. Hence, the 50 µg/mL could be considered as the optimum peptide concentration for GaAs functionalization.

Table 4.1 FTIR absorbance bands corresponding to the assigned functional groups.

Absorbance bands (cm^{-1})	Corresponding bonds	Reference
1235	Amide III	(de Campos Vidal and Mello, 2016)
1519 – 1738	Amide II	(Munje et al., 2017), (Rai et al., 2016)
1655 - 1670	Amide I	(Ami et al., 2014), (Barbosa et al., 2017)
2850 - 3070	CH_2 symmetric and asymmetric stretching	(Humblot et al., 2009), (de Campos Vidal and Mello, 2016)
1519	Amide II	(Munje et al., 2017)
1540	N-H bending	(Akrami et al., 2016)
1587	Amide II (N-H banding)	(Rai et al., 2016)
1655	Amide I bond (C=O stretching)	(Ami et al., 2014), (Barbosa et al., 2017)
1738	Amide II, C=O stretching lateral chain function	(Humblot et al., 2009), (Doiron et al., 2018)
1750	Ester C=O stretching	(Munje et al., 2017)
1770, 1828	C=O stretching	(Guler and Sarac, 2016)
2850	CH_2 symmetric stretching	(Humblot et al., 2009), (de Campos Vidal and Mello, 2016)
2922	CH_2 asymmetric stretching	(Humblot et al., 2009), (de Campos Vidal and Mello, 2016)
3324	Amide A	(Dinesh et al., 2015), (Jeevithan et al., 2014)

The AFM evaluation of Cys-AMP functionalized GaAs surface topography is illustrated in Figure 4.4, while the corresponding σ_{RMS} values are plotted in Figure 4.5. The micrograph in Figure 4.4a presents a freshly etched GaAs surface, and Figure 4.4 (b-h) demonstrate the roughness of the GaAs surface functionalized with peptides of different

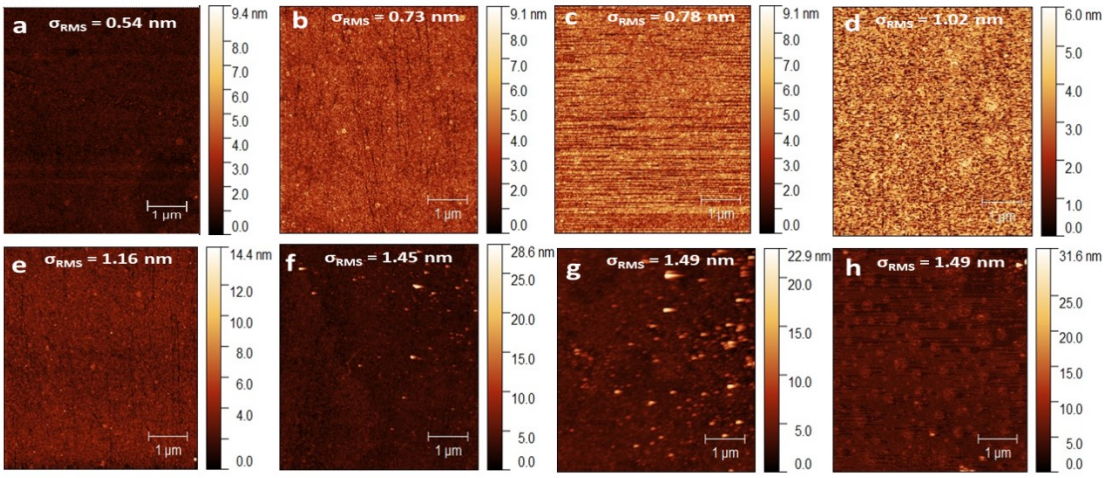

Figure 4.4 Representative AFM micrographs of GaAs reference surface (a), and peptide-coated GaAs at 2 µg/mL (b), 5 µg/mL (c), 10 µg/mL (d), 25 µg/mL (e), 50 µg/mL (f), 75 µg/mL (g), and 100 µg/mL (h).

concentrations. As shown in Figure 4.4a, the freshly etched GaAs surface is characterized by σ_{RMS} = 0.54 nm, which is consistent with the previously published results (Aziziyan et al., 2019). Following exposure to peptides at concentrations of 2, 5, 10, 25, 50, 75 and 100 µg/mL, the GaAs surface was characterized by σ_{RMS} of 0.73, 0.78, 1.02, 1.16, 1.45, 1.49 and 1.49 nm,

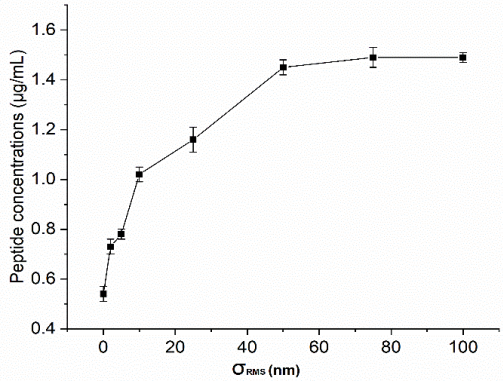

Figure 4.5 The root-mean-square roughness (σ_{RMS}) values of the GaAs surface exposed to peptide solutions of different concentrations.

respectively (Figure 4.4b-h). A comparable surface roughness is observed for GaAs exposed to 50 and 100 µg/mL of peptides, which is consistent with the saturation effect, also recorded with the FTIR measurements (Figure 4.3b). Clearly, the concentration of peptides at 50 μg/mL appears optimal for the functionalization of the GaAs surface. Figure 4.6a illustrates the dependence of the water contact angle of the GaAs surface on the concentration of peptides

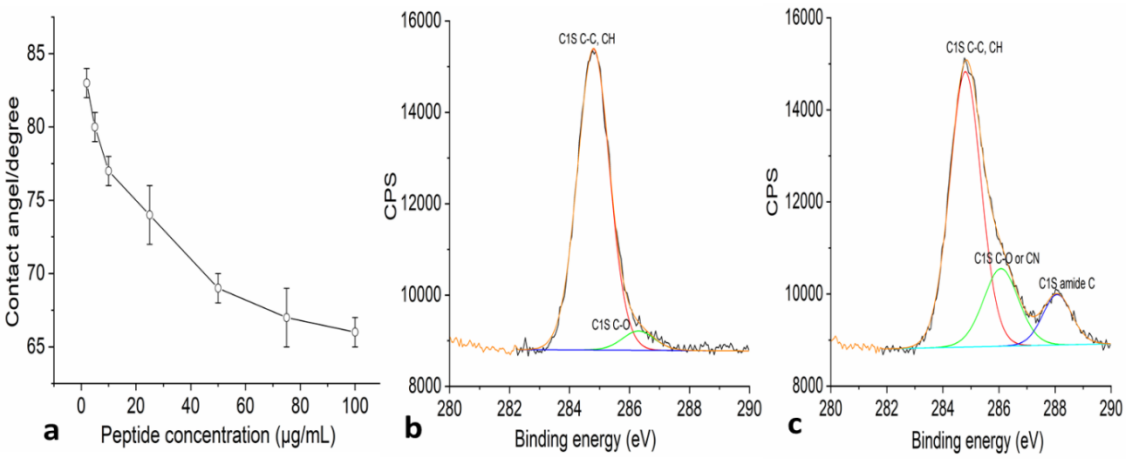

Figure 4.6 Water contact angle of the GaAs surface exposed to different concentrations of cysteine-modified peptides (a), and representative XPS spectra in the C1s absorption region for the uncoated GaAs (b), and exposed to 50 µg/mL of a peptide solution (c). The error bars in Figure 4a represent standard deviations of 3 repetitions.

employed for functionalization. The contact angle values decreasing from 83 to 66° were observed for surfaces functionalized with peptides at 2, 5, 10, 25, 50, 75 and 100 μg/mL. Note that the oxidized surface of GaAs is characterized by contact angles exceeding 90° (Gocalinska et al., 2011). The increased hydrophilicity of GaAs following the deposition of peptides is consistent with the results of Date et al. (2013) who showed that the air bubble angles decreased substantially with increasing concentrations of peptides on the gold surface.

XPS data for bare and peptide functionalized (50 µg/mL) GaAs surfaces are presented in Figure 4.6 (b-c). The C1s spectra for both functionalized and non-functionalized samples were observed at 284.8 eV, ascribed to C–H and C–C bonds (Wang et al., 2016). The peak at 286.3 eV could be assigned to the carbon atoms of the C=O or C–N (Fears et al., 2013; Oger et al., 2019) or to the O=C–N (Soylemez et al., 2016; Wang et al., 2016). The amide related peak at 288.08 eV (Corrales-Ureña et al., 2020; Soylemez et al., 2016), observed only for the functionalized sample, confirms the presence of peptide.

4.4.2 Surface coverage with bacteria

Representative optical micrographs of the GaAs surface functionalized with different concentrations of Cys-AMP and exposed to an *L. pneumophila* suspension at 10^6 CFU/mL are

shown in Figure 4.7 (a-h), while the capture efficiencies are summarized in Figure 4.7i. The uncoated (reference) surface of GaAs was able to capture ~72 bacteria/mm^2, whereas peptides at 2, 5, 10, 25, 50, 75 and 100 µg/mL yielded 217, 301, 394, 1009, 1868, 1920, and 2011 average bacteria/mm^2, respectively. The captured bacteria steadily increased with the concentration of peptide to 50 µg/mL, thereafter demonstrating a tendency towards saturation.

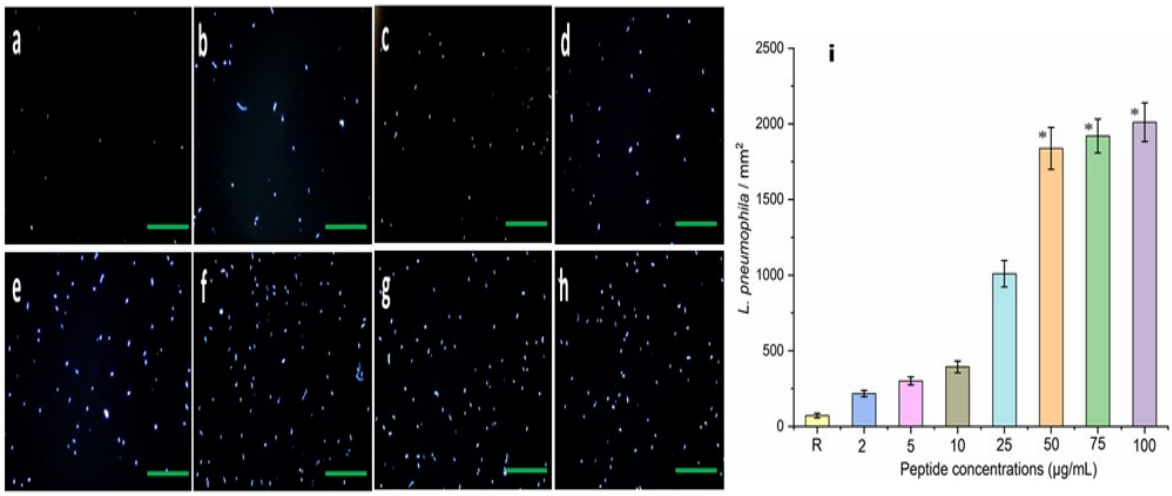

Figure 4.7 Representative optical micrographs of *L. pneumophila* captured on the GaAs surface using several concentrations of peptides: reference (a), 2 µg/mL (b), 5 µg/mL (c), 10 µg/mL (d), 25 µg/mL (e), 50 µg/mL(f), 75 µg/mL (g), 100 µg/mL (h), and density of captured *L. pneumophila* on the reference (R) and peptide functionalized GaAs surfaces (i). The asterisks indicate significantly different values compared to the reference ($p<0.05$) as determined by the Students T-test (n=3). The scale bar corresponds to 100 µm.

To evaluate the specificity of peptide towards *L. pneumophila*, a series of tests were carried out against the non-target *P. fluorescens*, *B. subtilis*, and *E. coli* bacteria at 10^6 CFU/mL with the GaAs chips functionalized with either peptides cysteine modified warnericin RK (Cys-WRK) AMP or anti-*L. pneumophila* Ab. The representative micrographs of the biochip surfaces are shown in Figure 4.8 and resulting bacterial capture efficiencies are illustrated in the Figure 4.9. The Cys-WRK AMP functionalized biochips captured *L. pneumophila*, *B. subtilis*, *P. fluorescens*, and *E. coli*, on average, at 2018, 477, 331 and 216 bacteria/mm^2, respectively. This compared with the ability of anti-*L. pneumophila* Ab functionalized biochips to capture the same bacteria, on average, at 742, 217, 186, 165 bacteria/mm^2, respectively. These results clearly demonstrate that RK AMP peptide and, as expected, anti-*L. pneumophila* Ab-coated GaAs surfaces captured *L. pneumophila* more

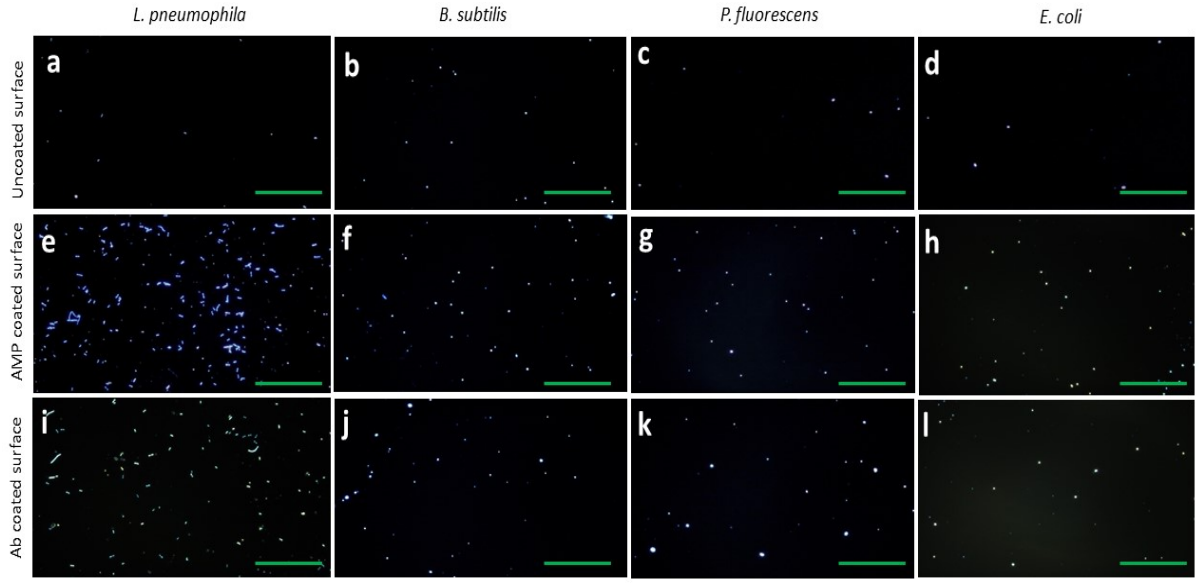

Figure 4.8 Representative optical micrographs of different bacteria on GaAs surfaces functionalized with AMP at 50 µg/mL (a-f), and Ab at 50 µg/mL (g-l). The scale bar corresponds to 100 µm.

efficiently compared to other bacteria. Notably, the cysteine-modified RK AMP functionalized GaAs biochips captured *L. pneumophila* at least 4 times more efficiently than the other investigated bacteria.

A number of studies have evaluated binding affinity, as well as interaction between peptide and bacteria on the surface of biosensor substrates. For instance, Etayash et al. (2013) observed that 24AA LeuA-conjugated gold substrate exhibited high binding specificity towards gram-positive bacteria, while lower specificity was observed for short length peptide 14AA LeuA. In another study (Etayash et al., 2014b), gold substrates functionalized with 37AA LeuA were incubated with four different bacteria (*i.e., E. coli*, *Listeria innocua*, *Coronabacterium divergens*, *Listeria monocytogenes*) and it was found that the *Listeria monocytogenes* demonstrated the highest binding efficiency compared to other bacteria. Recent studies have reported that *L. pneumophila* sensitivity towards warnericin could be due to the lipid composition of the bacterial membrane. Verdon et al. (2011) investigated the sensitivity of *L. pneumophila* to warnericin RK and found that the presence of branched-chain fatty acids on the surface of the bacteria play a crucial role in the sensitivity of the bacteria to the peptide. *Legionella* contains unusually high amounts of phosphatidylcholine (30%), which are predominantly present in eukaryotic cells only (Conover et al., 2008). Furthermore,

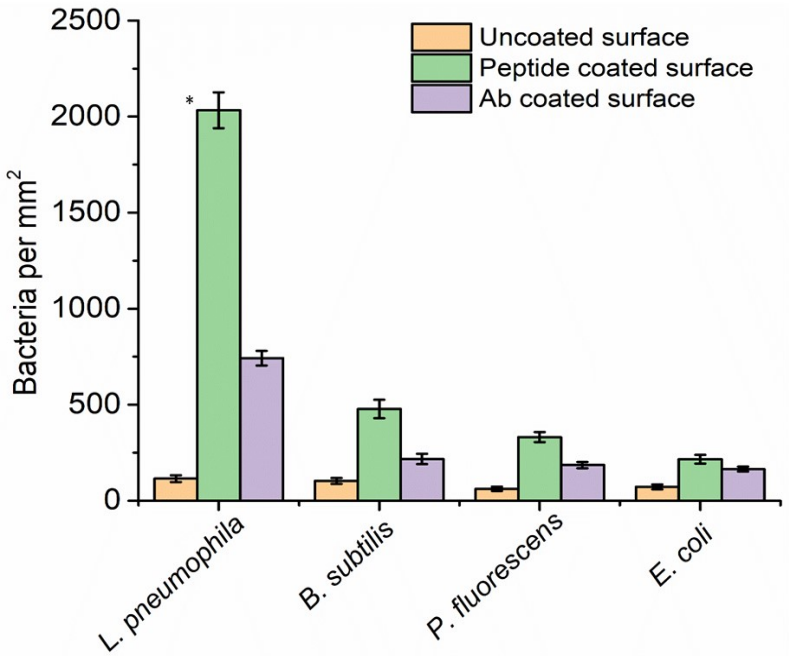

Figure 4.9 Summary of the results indicating that a cysteine-modified warnericin AMP biosensor captured *L. pneumophila* 4 times more efficiently than the other investigated bacteria. The asterisks indicate significantly different values compared to reference ($p<0.05$) as determined by the Students T-test (n=3). The scale bars correspond to 10 µm.

phosphatidylcholine is not typically present in other bacterial cell membranes (Berjeaud et al., 2016; Conover et al., 2008). A number of *Legionella* -specific peptides have been reported (Berjeaud et al., 2016; Verdon et al., 2011). Of these, only 3 peptides, warnericin RK being one of them, were found to be specific towards *L. pneumophila* serogroups 1, 3, 5 and 6 (Berjeaud et al., 2016). Therefore, the results obtained here, in agreement with previous reports, suggest that the innovative warnericin RK-conjugated GaAs-based biosensor could be an attractive system for specific detection of *L. pneumophila*.

4.4.3 Detection of *L. pneumophila*

Detection of *L. pneumophila* was carried out with the PL effect employed for monitoring DIP of GaAs/AlGaAs nanoheterostructures. The PL scans of the Cys-AMP functionalized biochips exposed to different concentrations of *L. pneumophila* are shown in Figure 4.10. The PL maxima were observed at 15, 20, 27, 34, 46, 57 and 76 min for 0, 10^2, 5 x 10^2, 10^3, 10^4, 10^5 and 10^6 CFU/mL of *L. pneumophila*, respectively. The details of this experiment are summarized in Table 4.2. Under optimized conditions, the PL maximum at 20 min obtained

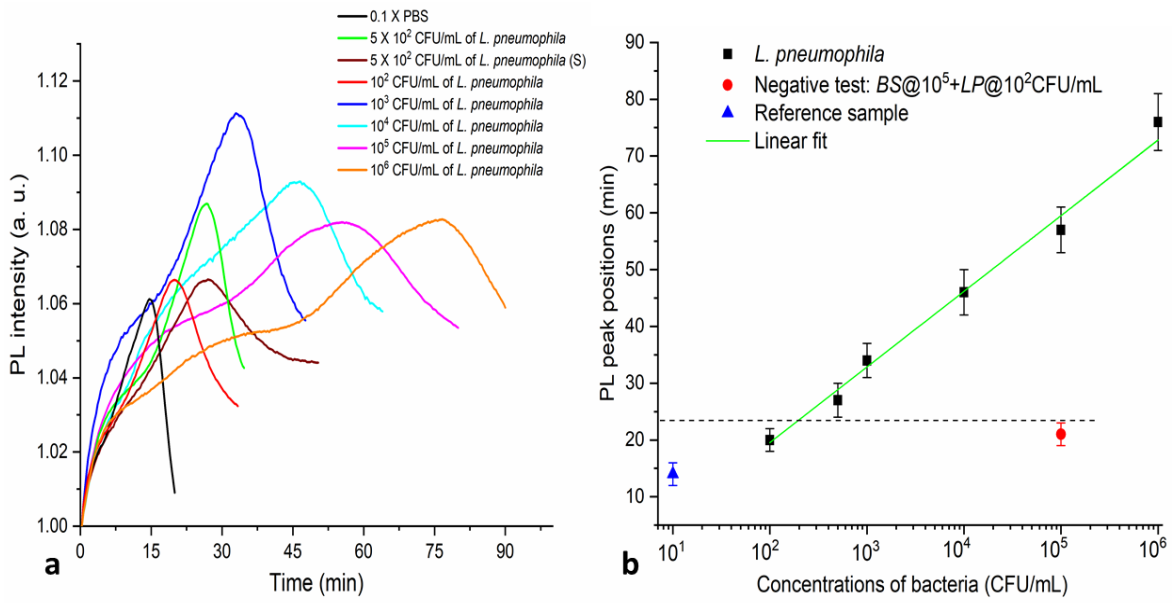

Figure 4.10 Normalized PL intensity of AMP functionalized GaAs/AlGaAs DIP biochips (wafer D3422) exposed to different concentrations of *L. pneumophila* in 0.1 x PBS (a), PL peak positions *vs*. different concentrations of *L. pneumophila* (b). The PL peak positions obtained for *L. pneumophila* are statistically different compared to either 0.1x PBS (reference), 10^2 CFU/mL of *L. pneumophila* or the negative control test for *B. subtilis* + *L. pneumophila* exposed surfaces ($p<0.05$), as determined by the Student's t-test (n=3). The dashed line highlights the biosensing resolution of the device against peak positions of the negative test and the results obtained for *L. pneumophila* suspension at 10^2 CFU/mL.

for a bacterial suspension at 10^2 CFU/mL is slightly delayed from the 15-min maximum observed for the reference sample. At the same time, the 21-min PL maximum observed for the mixed suspension of *B. subtilis* at 10^5 CFU/mL and *L. pneumophila* at 10^2 CFU/mL suggests that the limit of detection of the biosensor is at ~2 x 10^2 CFU/mL. The delayed positions of PL maxima revealed for the growing concentrations of *L. pneumophila* are consistent with the sensitivity of DIP GaAs/AlGaAs nanoheterostructures to the presence of bacteria immobilized on the biosensor surface. In this system, the rate of photocorrosion of GaAs/AlGaAs nanoheterostructures is delayed due to the charge transfer between bacteria and the semiconductor, as reported previously (Aziziyan et al., 2020; Nazemi et al., 2017). A mixed suspension of *B. subtilis* at 10^5 CFU/mL with *L. pneumophila* at 10^2 CFU/mL was used as a negative control to demonstrate the specificity of a proposed biosensor. When mixed together, the bacteria showed a PL maximum at 21 min, whereas *L. pneumophila* alone at 10^5 CFU/mL yielded a PL maximum at 57 min, which suggests that the PL maxima were not

Table 4.2 PL maxima obtained for the reference (PBS) run and different concentrations of *L. pneumophila* (all experiments repeated for at least 3 times).

Bacteria	Concentrations (CFU/mL)	PL maxima (min)
PBS	0.1 x	15 ± 13%
L. pneumophila	10^2	20 ± 10%
L. pneumophila	5 x 10^2	27 ± 11%
L. pneumophila	5 x 10^2(S)	27 ± 9%
L. pneumophila	10^3	34 ± 9%
L. pneumophila	10^4	46 ± 9%
L. pneumophila	10^5	57 ± 7%
L. pneumophila	10^6	76 ± 7%
B. subtilis + *L. pneumophila*	$10^5 + 10^2$	21 ± 13%

affected in a measurable manner by the presence of non-target bacteria. We also observed that inter-experimental (different biochips) errors for determining PL maxima varied less than 13%, which indicated a relatively highly reproducible detection. Furthermore, the reproducible response of the biosensor was demonstrated for GaAs/AlGaAs chips functionalized with

Table 4.3 Immunosensor based detection of *L. pneumophila*.

Type of bioreceptors	LOD	Linear range (CFU/mL)	Reference
Anti-*L. pneumophila* polyclonal antibodies	10^4 CFU/ mL	10^3 - 10^6 CFU/ mL	(Aziziyan et al., 2016)
Anti-*L. pneumophila* antibodies	10^4 CFU/9 mL	10^3 - 10^4 CFU/9 mL	(Bedrina et al., 2013)
Antibody (Ab) was linked to the poly (dopamine)	10^4 CFU/ mL	-	(Martín et al., 2015)
Lipopolysaccharide (LPS) specific Ab	10^1 CFU/ mL	10^1 – 10^3 CFU/9 mL	(Lin et al., 2007)
SDS-decorated *L. pneumophila*	10^3 CFU/mL	10^2 – 10^4 CFU/mL	(Aziziyan et al., 2020)
AMP	10^3 CFU/mL	10^3 – 10^6 CFU/mL	(Islam et al., 2020)
Cys-AMP	2x10^2 CFU/ mL	10^2 – 10^6 CFU/mL	This study

peptide solutions stored at room temperature for 30 days. The related PL scan, collected for *L. pneumophila* at 5 x 10^2 CFU/mL (sample S), revealed the PL maximum position at 27 min, which is similar to that obtained for the fresh peptide solution. A summary of several recent studies reporting on biosensing of *L. pneumophila* has been provided in Table 4.3. Aziziyan et

al. (2016) detected 10^4 CFU/mL of *L. pneumophila* using an Ab functionalized GaAs/AlGaAs DIP biosensor. In their subsequent study,[21] they improved the detection limit to 10^3 CFU/mL by decorating bacteria with sodium dodecyl sulphate (SDS). However, a decoration step of bacteria with SDS increases the complexity of a detection protocol and, thus, it may not be entirely advantageous in comparison to the simple process of detecting *L. pneumophila* with a Cys-AMP based biosensor.

4.5 Conclusions

This study has demonstrated the innovative concept of a cysteine-modified warnericin RK antimicrobial peptide (Cys-AMP) architecture for construction of a biosensor for rapid detection of *L. pneumophila* in an aqueous environment. The biosensing architecture was employed for functionalization of GaAs/AlGaAs nanoheterostructure biosensors operating on the principle of a digital photocorrosion. The role of peptide concentration on the efficiency of capturing *L. pneumophila* was investigated with FTIR, AFM, XPS, and water contact angle measurements. The absorbance band peaks related to peptide, observed at 1653 cm^{-1} (amide I), 1734 cm^{-1}/1538 cm^{-1} (amide II) and 3324 cm^{-1} (amide A), confirmed the chemisorption of peptide on the GaAs surface. Our results showed that 50 µg/mL of Cys-AMP was the optimum concentration as determined by maximum capture of *L. pneumophila* visualized with optical microscopy. The detection sensitivity of the developed biosensor was investigated in the range of 10^2 to 10^6 CFU/mL of *L. pneumophila,* with the limit of detection estimated at 2 x 10^2 CFU/mL. Thus, the investigated GaAs/AlGaAs nanoheterostructure DIP biosensors demonstrate functionality which is attractive for the rapid and direct detection of *L. pneumophila* present in a water environment at a relatively low concentration. The specificity of the biosensor was rated against *P. fluorescens*, *B. subtilis*, and *E. coli* abundantly found in samples of the environmental water. The Cys-AMP functionalized GaAs biochips showed a capture efficiency of over 4 times greater for *L. pneumophila* compared to the other investigated bacteria. The important consequence of the proposed Cys-AMP biosensing architecture is that it requires a relatively short time for completion, which may be found attractive for the operation of other biosensors of *L. pneumophila* compatible with the thiolation procedure. Furthermore, the short length of the employed ligand could potentially

result in an enhanced charge transfer between bacteria and the biochip surface, thus leading to an enhanced performance of charge sensing biosensors.

4.6 Acknowledgements

This project has been supported by the Natural Sciences and Engineering Research Council of Canada (NSERC) Strategic Partnership Grant No. SPG-2016-494057, and the NSERC Discovery Grant RGPIN-2015-04448. The fabrication of GaAs/AlGaAs wafers was subsidized by CMC Microsystems (Kingston, Canada). MAI acknowledges the B2X scholarship from the Fonds de Recherche sur la Nature et les Technologies du Québec (FRQNT). The authors are indebted to Prof. E.H. Frost and Dr. K. Moumanis for helpful discussions.

Chapter 5. Avant-propos

Auteurs et affiliations:

M. Amirul Islam: Étudiant au doctorat, Université de Sherbrooke, Faculté de génie, Département de génie électrique et informatique.

Walid M. Hassen: Assistant de recherche, Université de Sherbrooke, Faculté de génie, Département de génie électrique et informatique.

Ishika Ishika: Étudiante au doctorat, Université de Sherbrooke, Faculté de génie, Département de génie électrique et informatique.

Azam F. Tayabali: Professeur associé, Laboratoire de biotechnologie, Bureau de la science et de la recherche en santé environnementale, Direction générale de la santé environnementale et de la sécurité des consommateurs, Centre de santé environnementale, Santé Canada

Jan J. Dubowski: Professeur, Université de Sherbrooke, Faculté de génie, Département de génie électrique et informatique.

Titre français: Détection sélective des sérogroupes 1 et 5 de *Legionella pneumophila* avec un biocapteur à photocorrosion digitale utilisant une interaction en sandwich peptide antimicrobien -anticorps

Date d'acceptation: 2 février 2022

État de l'acceptation : version finale publiée

Revue: Biosensors

Référence: M. A. Islam, W. M. Hassen, I. Ishika, A. F. Tayabali, J. J. Dubowski, "Selective detection of *Legionella pneumophila* serogroup 1 and 5 with a digital photocorrosion biosensor using antimicrobial peptide-antibody sandwich strategy" Biosensors, vol. no. 12 *(105)*, pp. 1-14, 2022.

Contribution au document: Dans ce chapitre, une architecture de biodétection hybride est construite impliquant la warnericin RK AMP pour capturer *L. pneumophila* et la décoration des bactéries capturées avec des anticorps pour augmenter la sensibilité et la sélectivité du biocapteurs. Le biocapteur proposé a permis une détection sensible et sélective des *L. pneumophila* SG1 et 5 dans des échantillons d'eau à raison de 50 UFC/mL sans pré-concentration. De plus, le biocapteur conçu a détecté sélectivement 100 UFC/mL de *L. pneumophila* SG1 (responsable de plus de 85 % des épidémies de maladies liées à *L. pneumophila*) et 5 à partir d'échantillons qui simulent l'eau de tour de refroidissement. Le capteur proposé est prometteur pour résoudre le possible problème concernant les spectres de spécificités relativement larges des PAMs envers les bactéries. Par cette configuration de détection, une charge négative supplémentaire provenant d'anticorps qui décorent les bactéries a considérablement amélioré la sensibilité de notre biocapteur DIP et cette configuration pourrait être mise en œuvre pour les autres capteurs sensibles à la charge des cibles. Cette méthode a le potentiel d'offrir une détection hautement spécifique et sensible de *L. pneumophila* ainsi que d'autres bactéries et virus pathogènes.

Résumé français:

La détection rapide de *Legionella pneumophila* (*L. pneumophila)* est d'une importance majeure pour un suivi en continue de ses concentrations dans les sources d'eau et prévenir ainsi des possibles éclosions de la maladie du Légionnaire. Dans ce but, nous avons amélioré la biodétection de *L. pneumophila* par le biais de la photocorrosion digitale d'une biopuce fonctionnalisée par le warnericin RK, un peptide antimicrobien (PAM) qui va capturer les bactéries qui seront à la suite exposée à des anticorps polyclonaux (pAb) anti-*Légionnelle*. En effet, la warnericin permet une efficacité de capture des *Légionnelles* supérieure à celles des anticorps ou aptamères. L'usage des anticorps pour la détection en sandwich de *L. pneumophila* a permis à la fois d'améliorer la sensibilité de notre capteur à base de DIP grâce aux charges négatives des IgG ainsi que de permettre une détection sélective de *L. pneumophila* SG1 validée par une faible réponse du biocapteur au SG5.

Chapter 5. Selective detection of Legionella pneumophila serogroup 1 and 5 with a digital photocorrosion biosensor using antimicrobial peptide-antibody sandwich strategy

5.1 Abstract

Rapid detection of *Legionella pneumophila* (*L. pneumophila*) is important for monitoring the presence of these bacteria in water sources and prevents transmission of the Legionnaires' disease. We report improved biosensing of *L. pneumophila* with a digital photocorrosion (DIP) biosensor functionalized with an innovative structure of cysteine-modified warnericin antimicrobial peptides for capturing bacteria that are subsequently decorated with anti-*L. pneumophila* polyclonal antibodies (pAb). The application of peptides for operation of a biosensing device has been dictated by the peptides higher capture efficiency of bacteria compared to the capture of the other traditional ligands, such as those based on antibodies or aptamers. At the same time, the significantly stronger affinity of pAb decorating *L. pneumophila* serogroup-1 (SG-1) compared to serogroup-5 (SG-5) allowed selective detection of *L. pneumophila* SG-1 at 50 CFU/mL. The results suggest that the attractive sensitivity of the investigated sandwich method is related to the flow of extra electric charge between pAb and a charge sensing DIP biosensor. The method has the potential to offer highly specific and sensitive detection of *L. pneumophila* as well as other pathogenic bacteria and viruses.

Keywords: Cysteine modified warnericin RK; Antimicrobial peptides; Anti-*Legionella pneumophila* polyclonal antibody; Digital photocorrosion biosensor; GaAs/AlGaAs nanoheterostructures.

5.2 Introduction

Rapid detection of pathogenic *Legionella pneumophila* (*L. pneumophila*) in water environments is a key challenge in preventing related illness outbreaks (Pinel et al., 2021; Reuter et al., 2020). Presently, culture based methods are widely used and considered gold standard techniques for detecting pathogenic *L. pneumophila* (Nocker et al., 2020). However,

these approaches are both labour intensive and time consuming (Kim and Choi, 2020), typically taking up to ~10 days to quantify growing bacterial colonies (Fricke et al., 2020). Other techniques, such as polymerase chain reaction (PCR) and matrix-assisted laser desorption/ionization time-of-flight (MALDI-TOF) spectroscopy provide accurate and relatively fast detection (Váradi et al., 2017). However, the requirement of highly trained personnel and sophisticated laboratory equipment are the main constraints for wide application of these techniques (Rajapaksha et al., 2019). Therefore, research interests have been directed to avail cost effective, fast, portable, and less labor-intensive tools for detecting *L. pneumophila* (Chambers et al., 2021; Mobed et al., 2019; Reuter et al., 2020).

Numerous immunosensors investigated for the detection of *L. pneumophila* are listed in Table 5.1. These sensors undoubtedly offer specific and rapid detection of bacteria; however operation of most of them is restricted to laboratory settings due to the need for instrumentation that is not suitable for field applications and sophisticated stepwise biochemical protocols. For instance, Park et al. (2010) have reported a DNA biosensor for specific detection of *L. pneumophila*, but the extraction of DNA from bacteria is associated with a number of processing steps, resulting in laborious and costly analysis. Whole cell *L. pneumophila* biosensors have frequently been investigated based on electrochemical impedance spectroscopy (EIS) (Laribi et al., 2020; Li et al., 2012), surface plasmon resonance (SPR) (Manera et al., 2013) and colorimetric detection (Albalat et al., 2014; Nuthong et al., 2018) as presented in Table 5.1. EIS biosensors have received significant attention due to their sensitivity and cost-effectiveness (Jafari et al., 2019). However, the drifting of the electrochemical signal related to changes of buffer chemistry affects the performance and reproducibility of such devices (Vogiazi et al., 2019). SPR biosensors have some advantages related to label-free detection, sensitivity, and applicability to real-time kinetic measurements (Lin et al., 2007). However, SPR biosensors are also sensitive to temperature variations and require special temperature-stabilized chambers (Huang et al., 2012). Colorimetric paper-based biosensors (Nuthong et al., 2018; Sadsri et al., 2020) are potentially attractive due to their ability to monitor the presence of specific pathogens by detecting change in colors distinguishable with the naked eye. However, the major limitation of colorimetric assays is their low sensitivity since it is often difficult to transform biochemical reactions into measurable color changes (Sadsri et al., 2020). An innovative biosensing method based on

Table 5.1 Immunosensors proposed for the detection of *L. pneumophila*.

Detection technique	Substrate for immobilization	Bioreceptors	Detection Source	Time for Result	Limit of detection (CFU/mL)	Reference
SPR	Au	mAb	PBS	2h 20 min	10^2	(Oh et al., 2003)
EIS	Au	mAb	PBS	-	10^1	(Laribi et al., 2020)
Microelectrode array	Si	Antibody	PBS	-	10^5	(Lei and Leung, 2012)
EIS	Au	Antibody	PBS	-	2×10^2	(Li et al., 2012)
Amperometric sensor	Carbon	pAb	PBS	3h	10^4	(Martín et al., 2015)
SPR	Au	mAb	PBS	-	10^1	(Lin et al., 2007)
SPR	Au	pAb	PBS	30 min	10^3	(Manera et al., 2013)
Colorimetric	Gold nanoparticles	Nucleic Acid	DI water	60 min	124	(Nuthong et al., 2018)
DIP	GaAs/AlGaAs	pAb	PBS	42 min	10^4	(Aziziyan et al., 2016)
DIP	GaAs/AlGaAs	pAb/SDS	PBS	70 min	10^3	(Aziziyan et al., 2020)

mAb: Monoclonal antibody, pAb: Polyclonal antibody

digital photocorrosion (DIP) of GaAs/AlGaAs semiconductor nanoheterostructures has been recently introduced for rapid detection of *L. pneumophila* (Aziziyan et al., 2016; Hassen et al., 2016). The method is sensitive to charge transfer between semiconductors and immobilized biomolecules, and decorating *L. pneumophila* with negatively charged sodium dodecyl sulphate (SDS) permitted detection at 10^3 CFU/mL with polyclonal antibody (pAb) functionalized DIP biochips (Aziziyan et al., 2020).

The functioning of *L. pneumophila* biosensors have frequently been based on the application of Ab as bacteria recognizing ligands (Li et al., 2012; Wunderlich et al., 2016). The limitation of this approach is largely related to the dependency on animal-based production, which is prone to batch-to-batch variations (Byrne et al., 2009). Furthermore, the interaction of bacteria with Ab favours free liquid space (3D method) compared to the interaction with Ab immobilized on a biochip surface (2D method) (Choinière et al., 2019), while the orientation of Ab immobilized on the surface might also influence the capture of

bacteria (Hiep et al., 2010; Shen et al., 2017), There also has been growing interest in exploring antimicrobial peptides (AMP) as binding moieties designed for capturing bacteria on biosensor surfaces (Hoyos-Nogués et al., 2016; Mannoor et al., 2010). The AMP ligands can be obtained by employing synthetic processes (de Miranda et al., 2017; Dong and Zhao, 2015; Etayash et al., 2013), some cationic AMPs maintain strong affinity even after exposure to extreme environmental conditions, such as autoclaving and boiling (Etayash et al., 2014a; Mannoor et al., 2010). Thus, the increased stability of AMP in comparison to that of typical globular proteins, such as Ab, is potentially advantageous for biosensing applications (Etayash et al., 2014b; Mannoor et al., 2010). We have explored warnericin RK AMP for application in a DIP biosensor and demonstrated rapid detection of *L. pneumophila* at 10^3 CFU/mL (Islam et al., 2020). In a follow up to publication (Islam et al., 2021), we reported that a cysteine-modified warnericin RK AMP (Cys RK AMP) biosensing architecture increased limit of detection to 200 CFU/mL.

However, the relatively broad specificity spectrum of AMP towards different bacteria raised the question about specificity of the proposed biosensor, especially for detection of *L. pneumophila* serogroup 1 (SG1) that is responsible for over 85% of *L. pneumophila* related disease outbreaks (Berjeaud et al., 2016). To address this question, we have investigated the sandwich approach involving pAb for decorating captured *L. pneumophila*. We have also verified that the applied pAb exhibited four times greater capture efficiency of *L. pneumophila* SG1 than that of *L. pneumophila* SG5, and confirmed with the DIP biosensing results reported in this work.

5.3 Experimental section

5.3.1 Materials and reagents

The chips (2 mm x 2 mm) were cut from a 5 cm diameter wafer comprising a stack of GaAs and $Al_{0.35}Ga_{0.65}As$ layers grown on the GaAs (001) substrate (CMC Microelectronics, Kingston, Canada). More details about this wafer and the mechanisms of digital photocorrosion of GaAs/AlGaAs nanoheterostructures were published somewhere else (Aithal et al., 2017; Aziziyan et al., 2019). The application of a GaAs/$Al_{0.35}Ga_{0.65}As$ nanoheterostructure for building DIP biosensors was discussed earlier (Aithal and Dubowski,

2018; Aziziyan et al., 2016; Aziziyan et al., 2019; Nazemi et al., 2015). The results reported in this paper were obtained by recording DIP of the topmost pair of GaAs (12 nm thick) and AlGaAs (10 nm thick) layers. Undoped double-sided polished GaAs (001) wafer (WV 23084) purchased from Wafer Technology Ltd. (Washington, USA) was used to investigate biofunctionalization and evaluate bacteria capture efficiency. High quality (semiconductor grade) acetone, isopropanol, anhydrous ethanol and OptiClear were purchased, from National Diagnostics (Mississauga, Canada), Fisher Scientific (Ottawa, Canada), and ACP (Montréal, Canada), respectively. The 28% ammonium hydroxide (NH_4OH) was purchased from Anachemia (Richmond, Canada). Phosphate buffered saline (PBS; pH 7.4) at 10X, Luria-Bertani (LB) medium, isopropyl thio-β-galactoside (IPTG) and chloramphenicol were all purchased from Sigma-Aldrich (Oakville, Canada). BCYE agar medium was obtained from VWR (Ontario, Canada). Polyclonal Abs (anti-*L. pneumophila*) were purchased from ViroStat, Inc., catalog number 6051 prepared against the *L. pneumophila* SG1, ATCC 33152. The green fluorescent (GFP) *L. pneumophila* JR32 was kindly donated by Pr. Faucher from the Faculty of Agricultural and Environmental Sciences, McGill University (Ste-Anne de Bellevue, Québec, Canada). Green fluorescent *Escherichia coli* K12 BW25113 (GFP *E. coli*) was obtained from the Department of Microbiology and Infectiology of the Université de Sherbrooke (UdeS) Faculty of Medicine (Sherbrooke, QC, Canada), *Bacillus subtilis* ATCC 6051 (*B. subtilis*) was obtained from the Department of Biology of the UdeS Faculty of Sciences (Sherbrooke, QC, Canada), and *Pseudomonas fluorescens* ATCC 13525 (*P. fluorescens*) was purchased from Cedarlane (Burlington, ON, Canada). The following, cysteine modified AMPs: Cysteine-warnericin (Cys-WRK), Cysteine phenol-soluble modulins (Cys-PSM) and Cysteine-H2U (Cys-H2U) were synthesized by GenScript, Piscataway, USA and employed for the functionalization of GaAs or GaAs/AlGaAs chips targeting *L. pneumophila*.

5.3.2 Biofunctionalization of GaAs chips

The procedure of biochip preparation is schematically illustrated in Figure 5.1. The 2 mm x 2 mm GaAs chips (bulk or GaAs/AlGaAs nanoheterostructures) were cleaned by successive dipping in acetone, OptiClear and isopropanol for 5 min under ultra-sonication and then dried with highly pure compressed nitrogen gas (Lacour et al., 2016; Sharma et al., 2016).

Thereafter, native oxides present on the surface of samples were removed by immersion in 28% NH_4OH for 2 min at room temperature, followed by rinsing with degassed ethanol and subsequently degassed de-ionized (DI) water. Then, individual samples were incubated in

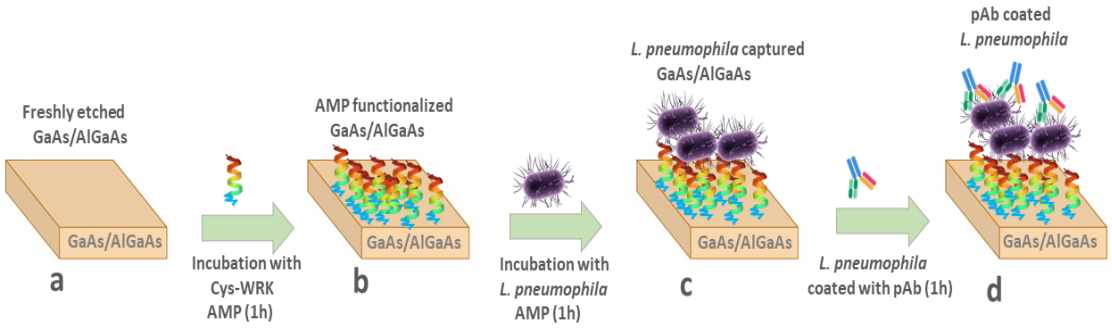

Figure 5.1 Schematic diagram of biosensor development, freshly etched GaAs/AlGaAs nanoheterostructures (a), adsorption of thiolated AMPs on GaAs/AlGaAs (b), immobilization of bacteria on AMP functionalized GaAs/AlGaAs (c), immobilization of anti-*L. pneumophila* pAb on the surface of bacteria (d).

each thiolated AMP solutions (50 µg/mL) for 1h to allow the Cys-AMPs attachment to the GaAs surface through the formation of covalent bound between Ga or As atoms and the cysteine sulphur (S). The functionalized chips were sonicated in degassed DI water for 1 min, and immediately rinsed with degassed DI water to remove non-covalently bonds peptides, and subsequently incubated in bacterial suspensions for 1h. Bacterial-bound chips were rinsed with DI water to remove unbound or loosely bound bacteria. The bacteria decoration step with anti-*L. pneumophila* pAb was completed by incubation with 100 µg/mL anti-*L. pneumophila* pAb for 30 min. This concentration of pAb is considered sufficient to saturate bacteria in a reproducible fashion.

5.3.3 Preparation of bacteria

Cultures of *P. fluorescens*, *E. coli,* and *B. subtilis* were grown in Luria-Bertani (LB) medium. Cultures of green fluorescent *L. pneumophila* SG1 and non-fluorescent SG5 were grown in buffered charcoal yeast extract agar (BCYE) medium with L-Cysteine. For the SG1 strain, the medium was supplemented with isopropyl thio-β-galactoside (IPTG) to induce the production of the green fluorescent protein (GFP) and chloramphenicol to maintain the plasmid encoding

for the GFP. After growth, a few colonies were placed in 0.1x PBS and concentrations were determined by optical density measurements at 600 nm (OD_{600} nm).

5.3.4 Capture Efficiency of *L. pneumophila* SG1 and SG5 with pAb functionalized GaAs

The pAb were prepared against whole cells of a *L. pneumophila* SG1 strain (Yamaguchi et al., 2017). However, the cross-reactivity is expected for various *L. pneumophila* serogroups due to the polyclonal character of these Ab. To evaluate the affinity of the used pAb against the *L. pneumophila* SG1 and SG5, freshly cleaned and oxide-etched GaAs chips were functionalized for 20 h using a 1mM of mercaptohexadecanoic acid (MHDA) solution in degassed ethanol. To capture Abs, the samples were incubated for 30 min in 1-ethyl-3-(-3-dimethylaminopropyl) and carbodiimide/N-hydroxysuccinimide (EDC-NHS) solution (0.4 M-0.1 M). This allowed for activation of the -COOH terminal group of MHDA. Following washing with DI water, the samples were exposed for 1h to the anti-*L. pneumophila* pAb at 100 µg/mL in 1x PBS that bind through their amine group to the activated -COOH. To saturate the unreacted -COOH groups, the chips were exposed for 1 h at pH 8 in a 1M of ethanolamine solution. Following 3-times washing with 1x PBS, the samples were exposed for 1 h to either *L. pneumophila* SG1 or SG5 suspensions in 1x PBS at 10^6 CFU/mL. Finally, the samples were washed with DI water and imaged by optical microscopy to determine bacterial surface coverage.

5.3.5 Processing of cooling tower water for biosensing experiments

For biosensing experiments, 10 mL of cooling tower (CT) water from the Université de Sherbrooke was filtered through a 0.22 µm syringe filter. The retained matter was washed in triplicate with 10 mL of DI water. Finally, the filter was backwashed using 10 mL of 0.1x PBS to collect the CT suspended matter. The backwashed samples were spiked with *L. pneumophila* SG1 or SG5 employed for the exposure of AMP functionalized GaAs/AlGaAs chips designed for capturing bacteria.

5.3.6 Optical microscopy analysis

The surface density of bacteria immobilized on GaAs bulk samples was determined by optical microscopy imaging (Zeiss Instruments, Inc.). The images were captured under 200X magnification from at least three different regions of individual samples to show the distribution bacteria. The experiments were repeated three times for statistical analysis. ImageJ software was used to subtract particles and enumerate bacterial surface coverage.

5.3.7 PCR measurements

DNA of *L. pneumophila* SG1 and SG5 were extracted from the AMP-functionalized GaAs biochip for conducting PCR experiments. AMP coated GaAs wafers were exposed to 10^6 CFU/mL of *L. pneumophila* SG1 and SG5 for 1h. The bacteria captured by GaAs were heated for 80 °C for 30 min with the quick DNA extract solution kit. Thereafter, the DNA containing supernatants were centrifuged for 5 min at 10000 RPM and 5 µL of solution was taken for the PCR reaction. Standard real time PCR protocol was followed for conducting PCR reactions (35 cycles) using qPCR Illumina machine (Bookout and Mangelsdorf, 2003). The *mip* gene specific forward primer (5'-TTGTCTTATAGCATTGGTGCCG-3') and reverse primer (5'-CCAATTGAGCGCCACTCATAG-3') were used for the reactions. The PCR fluorescence values at 35 cycles were considered to compare the variation.

5.3.8 Photoluminescence measurements

The detection of bacteria was carried out at room temperature using a quantum semiconductor photonic biosensing reader (QSPB-1) described previously (Aithal and Dubowski, 2018). The reference and bacteria-coated biochips were irradiated with a light emitting diode (LED) at 660 nm. Photocorrosion was monitored by measuring photoluminescence (PL) of intermittently irradiated biochips (5 s irradiation in 20 s total period) with an intensity homogenized beam delivering power density of ~17 mW/cm^2 to the biochip surface. All experiments were repeated at least 3 times for statistical analysis. The experiments carried out in a 0.1x PBS solution (without bacteria) were used to obtain the reference measurements.

5.3.9 Statistical Analysis

Statistical analyses were performed using Graphpad Prism™ (Graphpad Software, San Diego, CA, USA). Bacterial capture and RT-PCR data were evaluated by two-way analysis of variance (ANOVA) followed by post-hoc analysis using Tukey's Multiple Comparison Test. For Bacterial capture, bacteria and AMP coating were independent variables. Serogroup and AMP coating were independent variables for quantitative measurement of the *mip* gene by RT-PCR. Capture efficiency of *L. pneumophila* SG1 versus SG5 was tested using an unpaired Student's T-test. For biosensor experiments, peak PL values were compared to no-bacteria controls using 1-way ANOVA followed by Tukey's (pristine water) or Dunnett's (water originated from cooling tower) multiple comparison tests. In all analyses, a $p<0.05$ was considered statistically different.

5.4 Results and discussion

5.4.1 Bacteria capture efficiency by peptide coated surfaces

To evaluate the specificity of the AMPs used for *L. pneumophila* capture, a series of experiments were conducted by exposing GaAs bulk samples functionalized with Cys-WRK, Cys-PSM or Cys-H2U to *L. pneumophila,* while negative control runs were collected for *B. subtilis*, *P. fluorescens* and *E. coli* suspensions at 10^6 CFU/mL. The background signal was measured by exposing bare GaAs to the investigated bacteria. The bacterial capture efficiencies (bacteria/mm^2) are presented in Figure 5.2 (examples of optical microscopy

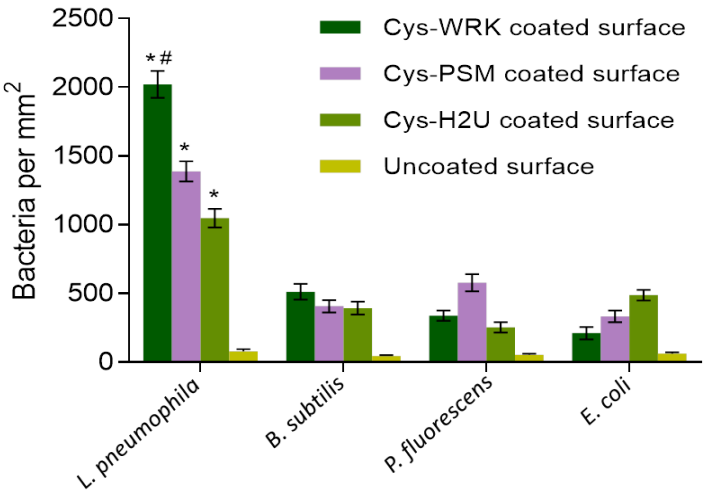

Figure 5.2 Bacterial capture efficiency enumerated by optical microscopy following conjugation of different peptides with GaAs chips. Cysteine-modified warnericin AMP biosensor captured *L. pneumophila* 4 times more efficiently than the other investigated bacteria. Error bars represent standard error of the mean for five separate experiments. Statistical differences were measured by 2-way ANOVA followed by Tukey's multiple comparison test with different bacteria and coatings as variables affecting capture efficiency. The asterisk (*) indicates significantly different values of *L. pneumophila* compared to reference bacteria ($p<0.0001$). The hash (#) indicates significantly different values for *L. pneumophila* on Cys-WRK compared to other coatings ($p<0.05$).

images for each case are shown in Figure 5.3 while the size of bacteria was confirmed by 500X magnification as presented in Figure 5.4). The average density of bacteria captured by the Cys-WRK peptide functionalized GaAs were 2021, 338, 512 and 211 bacteria/mm^2 for *L. pneumophila*, *P. fluorescens*, *B. subtilis*, and *E. coli*, respectively. Furthermore, it can also be

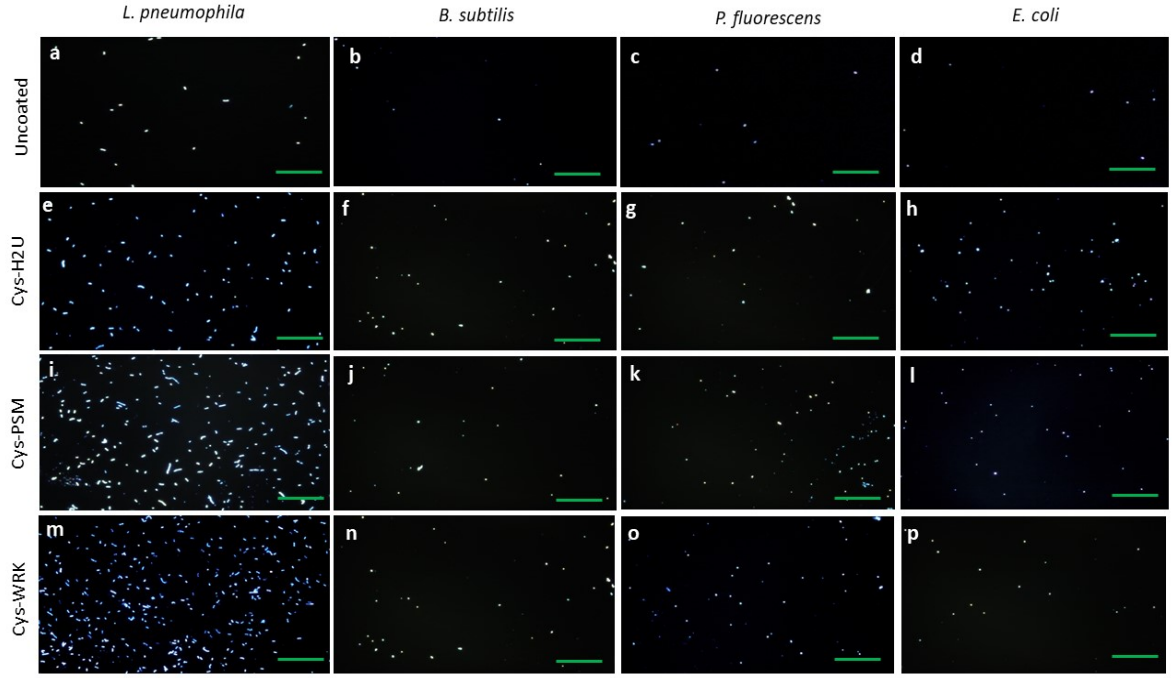

Figure 5.3 Representative optical micrographs (200x magnification) of different bacteria on uncoated and different AMP (50 µg/mL) functionalized surfaces of GaAs. The scale bar corresponds to 100 µm.

seen that Cys-WRK captured 1.5 to 2 times more *L. pneumophila* (2021 bacteria/mm^2) compared to the Cys-H2U and Cys-PSM based biosensor architectures. These results illustrate that the investigated peptides bind *L. pneumophila* more efficiently than the other investigated bacteria, consistent with earlier reports (Marchand et al., 2015; Marchand et al., 2011; Verdon et al., 2008). Furthermore, the Cys-WRK AMP has a significantly higher binding affinity

towards *L. pneumophila* than the other investigated peptides. This superior performance in capturing *L. pneumophila* could be related to the lipid composition of the *L. pneumophila* membrane. For instance, it has been reported Verdon et al. (2011) that the presence of branched-chain fatty acids, such as C15:0, C 16:0 and C 17:0 on the surface of *L. pneumophila*

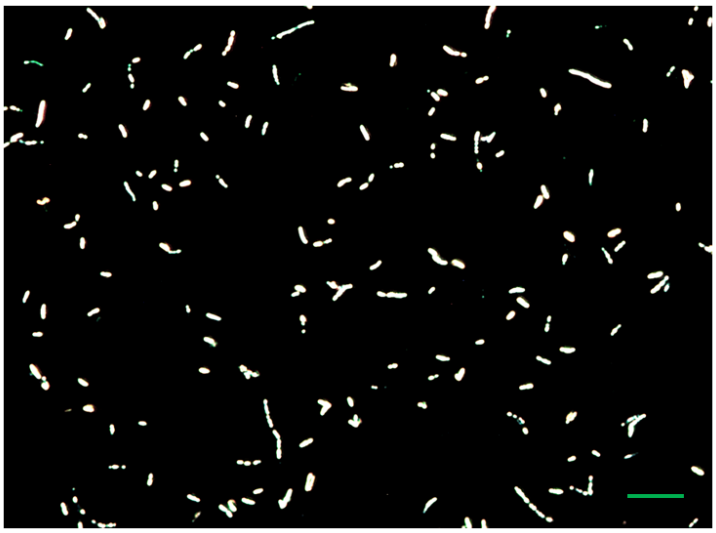

Figure 5.4 An example of optical micrograph at 500x magnification for determining *L. pneumophila*. The scale bar corresponds 15 µm.

is associated with bacterial specificity of warnericin RK AMP. Another study has suggested that the large presence (30%) of phosphatidylcholine, also known as lecithin, on the outer membrane of *Legionella* leads to a specific interaction with the Cys-WRK peptide (Conover et al., 2008; Hindahl and Iglewski, 1984). Marchand et al. (2015) reported that two specific amino acids present in Cys-WRK sequence at the 4^{th} and 17^{th} position are also associated with the specific interaction between peptide and *L. pneumophila.* Nevertheless, more study is required to elucidate further the reasons for enhanced specific interaction between Cys-WRK peptide and *L. pneumophila* bacteria.

5.4.2 Reactivity of *L. pneumophila* pAb against *L. pneumophila* SG1 and SG5

Figure 5.5 represents the surface coverage of the pAb functionalized GaAs chips showing the number of captured *Legionella* at 785/mm^2 (dense pattern) and 192/mm^2 (light pattern) in the case of SG1 and SG5, respectively. Thus, for the same tested concentrations (10^6 CFU/mL) of

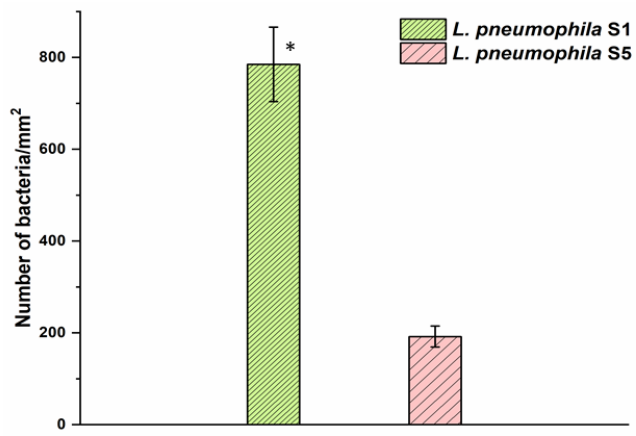

Figure 5.5 The capture efficiency of *L. pneumophila* SG1 and SG5 with pAb functionalized GaAs surface. Error bars represent standard error of the mean from three separate experiments. The asterisk indicates significantly different values compared to the reference as determined by the Student's t test ($n = 3$, $p < 0.05$).

both *Legionella* serogroups, the binding efficiency of the pAb was around 4 times greater for SG1 compared to SG5 serogroup. The higher affinity of pAb towards *L. pneumophila* SG1 could be attributed due to the fact that the preparation of these ligands was based on the interaction with the whole cell of that strain (Yamaguchi et al., 2017). However, it is important to note that the *L. pneumophila* strains used here were isolated from different environments showing distinct genetic backgrounds (Sousa et al., 2018). The lipopolysaccharide (LPS) characteristic and the phenotype of the used strains to produce these pAb could explain why more capture was observed in the case of the *L. pneumophila* SG1 strains. It is worth mentioning that working with large concentrations of bacteria allowed statistically validation of results by conducting microscopic enumeration of bacteria. In the case of weakly concentrated bacterial suspensions, the enumeration of bacteria would carry excessively large errors as the capture efficiency of the biofunctionalized chips is below 1%. Thus, we have not attempted to conduct macroscopic enumeration of bacteria for suspension at ≤ 100 CFU/mL discussed later in this report.

5.4.3 Reactivity of *L. pneumophila* SG1 and SG5 against Different Peptides

The reactivity of *L. pneumophila* SG1 and SG5 against AMP coated GaAs surface was tested using the PCR technique. The related PCR fluorescence data presented in Figure 5.6a (real-time amplification plots) and 5.6b (maximum fluorescence value) show a significant

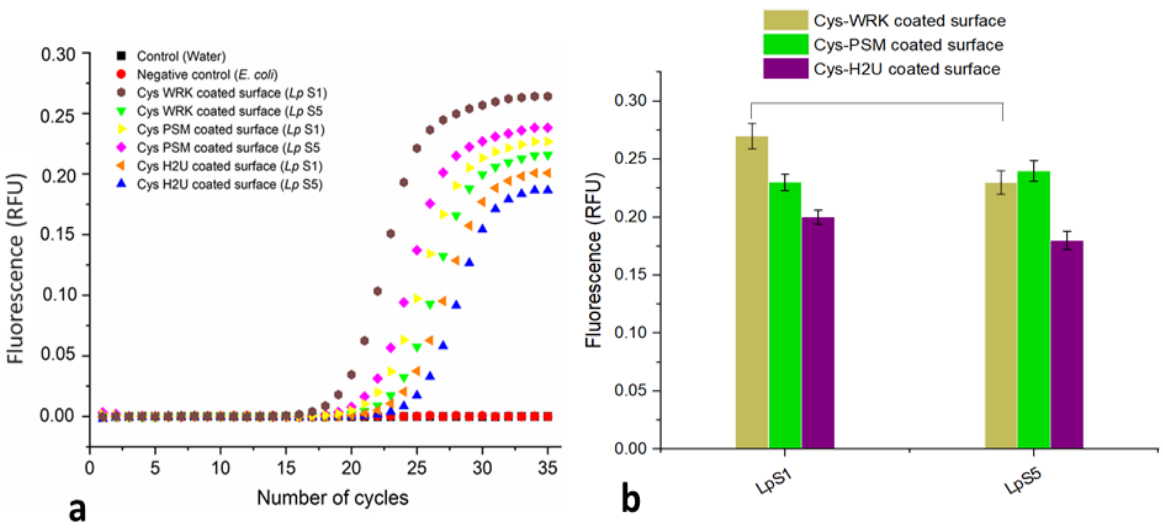

Figure 5.6 The real-time PCR amplification curves (relative fluorescence units, RFU) for *L. pneumophila* SG1 and *L. pneumophila* SG5 captured by different peptide-functionalized GaAs (a), quantitative PCR results (relative fluorescence units, RFU) for *L. pneumophila* SG1 and *L. pneumophila* SG5 captured by peptide-functionalized biosensors (b). Error bars represent standard error of the mean from three separate experiments. Statistical differences were measured by 2-way ANOVA followed by Tukey's multiple comparison test with *L. pneumophila* serogroups and coatings as variables affecting amplification of the *mip* gene. The horizontal lines between bars indicate significantly different values between serogroups ($p<0.05$).

difference between fluorescence intensities corresponding to *L. pneumophila* SG1 and SG5 for the Cys-WRK coated surface while insignificant differences were observed for other peptides. The results suggest that the Cys-WRK coated GaAs offers certain levels of specificity for selective capture of *L. pneumophila* SG1. However, as can be seen Figure 5.2, some other microbes also could be bound by this peptide. Therefore, the selectivity offered by Cys-WRK AMP is not sufficient for designing a biosensor highly specific to *L. pneumophila* SG1.

5.4.4 Selective detection of *L. pneumophila* SG1 and SG5 using AMP-Ab sandwich technique

The utilization of DIP GaAs/AlGaAs biosensors functionalized with Cys-WRK AMP peptides to capture *L. pneumophila* SG1 and SG5 and use of pAb to detect them is summarized in Figure 5.7 and Table 5.2. We show examples of the biosensing runs for *L. pneumophila* SG1 (red full circles) and SG5 (green full squares) bacterial suspensions at 100 CFU/mL. The reference runs in this figure were collected for GaAs/AlGaAs functionalized withCys-WRK

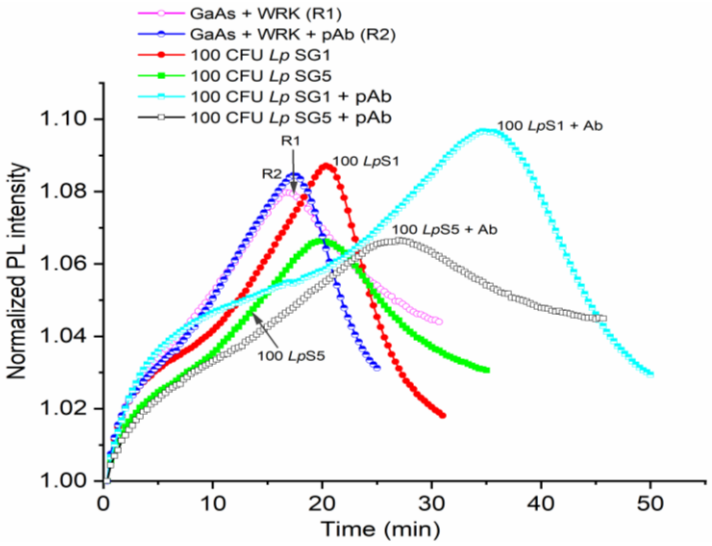

Figure 5.7 Normalized PL intensity of AMP functionalized GaAs/AlGaAs DIP biochips (wafer D3422) exposed to bacteria in 1x PBS. The open circles (R1) and semi-circles (R2) plots represent reference without exposing to bacteria. The red full circle and green square plots represent the exposure to 100 CFU/mL of *L. pneumophila* SG1 and SG5, respectively. The black open square and cyan semi-square plots represent the exposure to 100 CFU/mL of pAb decorated *L. pneumophila* SG1 and SG5, respectively.

(plot R1, purple open circles) and after the exposure of GaAs/AlGaAs functionalized with Cys-WRK to anti *L. pneumophila* SG1 pAb (plot R2, blue semi-circles). As discussed in (Aziziyan et al., 2016), the time-dependent positions of PL intensity maxima correspond to the front passing through the GaAs/AlGaAs interface and, thus, it is a measure of the rate of photocorrosion. The identical positions of PL maxima (~20 min) revealed for SG1 and SG5 illustrate the inability of a biosensor to distinguish the investigated strains. However, the capture of bacteria from 100 CFU/mL suspensions of *L. pneumophila* SG1 and SG5, followed by the incubation in pAb showed PL maxima occurring at 36 min (cyan semi-squares) and 25 min (black open squares), respectively. This significant delay of the PL maximum for pAb decorated *L. pneumophila* SG1 (~16 min) demonstrates that the sensitivity of DIP PL biosensors is enhanced after decorating bacteria with pAb. We attribute this to the interaction of pAb with AMP-captured *L. pneumophila* SG1 and transfer of additional charge from the negatively charged pAb (Yadav et al., 2011) to the biochip surface.

The influence of pAb on the photocorrosion rate of GaAs/AlGaAs chips was investigated in separate experiments concerning DIP runs (see Figure 5.8) collected for a biochip functionalized with MHDA self-assembled monolayer, and for a biochip

functionalized with pAb after the -COOH group of MHDA was activated with the EDC/NHS procedure. A significantly delayed the PL maximum was observed for the MHDA-pAb

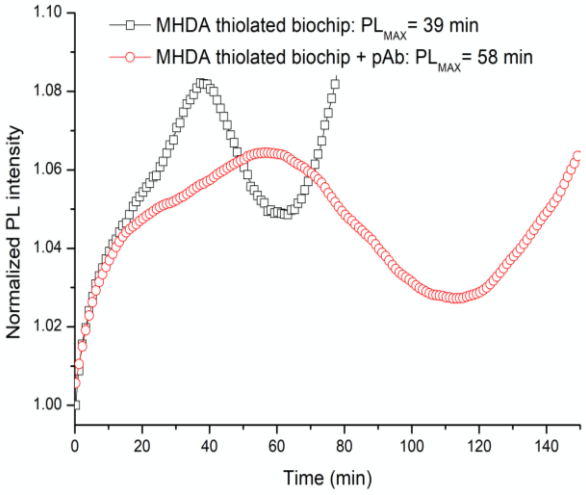

Figure 5.8 Examples of DIP runs for MHDA thiolated GaAs/AlGaAs biochip before (black square) and after (red circle) pAb attachment. The figure presents example of PL data for the GaAs/AlGaAs biochips following a 20-hours functionalization with 1mM mercaptohexadecanoic acid (MHDA) thiol (black square) and after Ab attachment (incubation in 100 µg/mL Ab solution for 1-hour, red circle). We note that this architecture (GaAs/MHDA/EDC-NHS/pAb) was designed to conduct control experiment; however, the other PL data were collected using different architecture as described in section 5.3.2.

architecture compared to the PL maximum observed for the MHDA only functionalized biochip. This behaviour is consistent with the flow of a negative charge to the biochip surface observed also for other GaAs/AlGaAs nanoheterostructures (Aithal and Dubowski, 2018; Aithal et al., 2017; Aziziyan et al., 2020; Aziziyan et al., 2019).

A greater delay of the PL maximum observed in Figure 5.7 for *L. pneumophila* SG1 compared to SG5 (~11 min) is consistent with the relatively greater selectivity of pAb towards *L. pneumophila* SG1 (see Figure 5.5). Furthermore, the exposure of a reference sample to pAb alone did not show a significant change in the delay of a PL intensity maximum (blue semi-circles), which is related to the weak pAb-AMP interaction (Olsson et al., 2012). We also observed similar response of the GaAs/AlGaAs biochips to 50 CFU/mL of *L. pneumophila* SG1 and SG5 decorated with pAb as shown in Table 5.2 and Figure 5.9. These results are consistent with the observation that decorating *L. pneumophila* SG1 with negatively charged

sodium dodecyl sulphate (SDS) molecules significantly enhanced the sensitivity of DIP biosensors as reported in (Aziziyan et al., 2020).

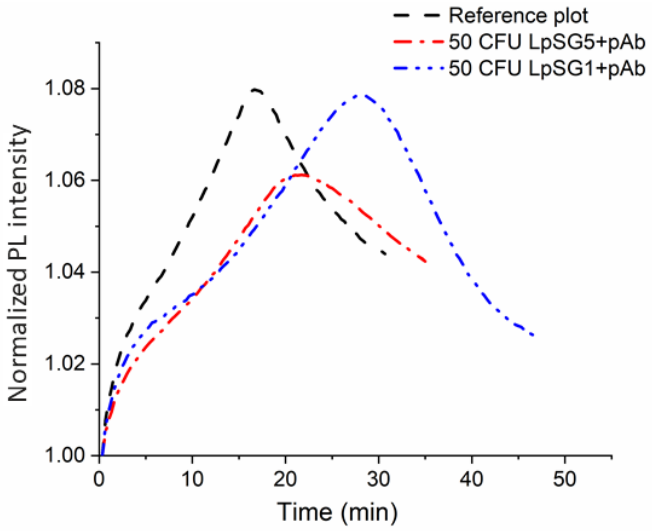

Figure 5.9 Normalized PL intensity of AMP functionalized GaAs/AlGaAs DIP biochips (wafer D3422) exposed *L. pneumophila* (SG1 and SG5) at 50 CFU/mL and decorated with pAb.

Examples of biosensing runs of DIP GaAs/AlGaAs biosensors responding to *L. pneumophila* captured from CTW suspensions with *L. pneumophila* SG1 and SG5 at 100 CFU/mL (see Section 5.3.5) are presented in Figure 5.10 and Table 5.2. It can be seen that PL maxima for *L. pneumophila* SG5 (red full circles) and SG1 (brown open squares) occur at 22

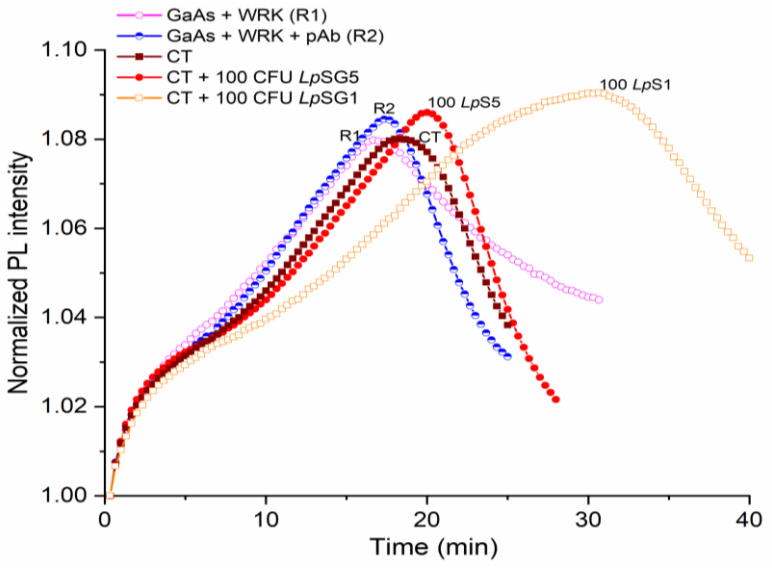

Figure 5.10 Normalized PL intensity of AMP functionalized GaAs/AlGaAs DIP biochips (wafer D3422) exposed to CTW spiked with *L. pneumophila* at 100 CFU/mL. The purple open circle (R1) and blue semi-circle (R2) plots represent reference without exposing to bacteria. The red full circle and brown square plots represent the biochip response to pAb decorated *L. pneumophila* SG5 and SG1, respectively.

min and 31 min, respectively. The significantly greater delayed PL maximum for *L. pneumophila* SG1 compared to *L. pneumophila* SG5 could be attributed to the selectivity generated through pAb conjugation. We note that the weaker delay of PL maxima observed

Table 5.2 PL maxima obtained for the reference (PBS) run and after the exposure of *L. pneumophila* (all experiments repeated for at least 3 times).

Bacteria and reference	**PL maxima (minutes)**	**Significantly Different vs. Control (p value)**
Pristine condition		
GaAs+Cys-WRK	16±1.12	Control
GaAs+Cys-WRK + Anti *Lp* pAb	17.50±1.18	No
GaAs+Cys-WRK + 100 CFU/mL of *Lp*SG1	21.05±1.5	No
GaAs+Cys-WRK + 100 CFU/mL of *Lp*SG5	19.23±1.2	No
GaAs+Cys-WRK + 50 CFU/mL of *Lp*SG1 + Anti *Lp*SG1 pAb decorated bacteria	27.83±2	Yes ($p<0.0001$)
GaAs+Cys-WRK + 50 CFU/mL of *Lp*SG5 + Anti *Lp*SG1 pAb decorated bacteria	21±1.14	No
GaAs+Cys-WRK+100 CFU/mL of *Lp*SG1 + Anti *Lp*SG1 pAb decorated bacteria	36.2±2.1	Yes ($p<0.0001$)
GaAs+Cys-WRK+100 CFU/mL of *Lp*SG5 + Anti *Lp*SG1 pAb decorated bacteria	25.75±1.16	Yes ($p<0.0019$)
Cooling tower condition		
Cooling tower water (3IT)	18.37±1.5	Control
GaAs+Cys-WRK+ water originated from cooling tower +100 CFU/mL of *Lp*SG5+Anti *Lp*SG1 pAb	22.20±2	No
GaAs+Cys-WRK+ water originated from cooling tower+100 CFU/mL of *Lp*SG1+Anti *Lp*SG1 pAb	31.5±2	Yes ($p<0.0043$)

for *L. pneumophila* SG1 and SG5 in CTW compared to pristine conditions (Figure 5.7) might be related to the presence of ionic species in CTW that affect the capture efficiency of bacteria by AMP functionalized GaAs/AlGaAs chips. Under these conditions, we were not able to

detect *L. pneumophila* SG1 at 50 CFU/mL and, thus, detection at 100 CFU/mL determines the current limit of detection (LOD). The DIP biosensor technology has been investigated for detection of a number of bacteria including *E. coli*, *Bacillus sp.,* and *L. pneumophila* (Islam et al., 2020; Nazemi et al., 2015), with typical LOD at 10^3 CFU/mL. Therefore, detection of *L. pneumophila* SG1 at 100 CFU/mL represents a significant step towards development of a field operating DIP biosensor that is expected to deliver enhanced biosensing based on the introduction of filtration and pre-concentration techniques of water samples originating from different sources.

The application of Cys-WRK AMP for functionalization of GaAs-based DIP biosensors allowed us to eliminate the 20-hour step required for a) formation of MHDA SAM, and b) EDC/NHS activation of the -COOH group for binding with pAb through their amine group. Consequently, the ~15 nm long bacteria binding architecture was replaced with a significantly shorter, ~2 nm long ligand fabricated within less than 3 hours. While the elimination of the extra EDC/NHS biofunctionalization step contributes to the more consistent data collection, the short chain ligands support more efficient charge transfer between pAb decorated bacteria and the surface of a biosensor. Thus, the short-chain AMP architectures supplemented with the sandwich biosensing step is highly attractive for rapid, sensitive, and specific detection of pathogenic bacteria at least with the charge sensing devices, such as DIP biosensors.

5.5 Conclusions

We have investigated an innovative concept of an AMP-pAb sandwich architecture for the construction of a DIP GaAs/AlGaAs biosensor and selective detection of *L. pneumophila* SG1 and SG5. The biosensor was first functionalized with Cys-AMPs and incubated with *L. pneumophila*. This was followed by decorating bacteria with anti-*L. pneumophila* pAb. Our results demonstrate the detection sensitivity as low as 50 CFU/mL for bacterial suspensions in pristine conditions, and 100 CFU/mL in samples originating from cooling tower water. The proposed method enhanced the sensitivity and specificity of biosensor and allowed selective detection of *L. pneumophila* SG1 in both pristine and industrial water conditions. These results are attractive for the development of quasi-continuous monitoring of the water environment for the presence of bacteria with DIP biosensors comprising stacks of GaAs/AlGaAs bilayers

designed to deliver a series of data with a single device. The results have potential to be applied to the development of other biosensing devices.

5.6 Acknowledgements

The fabrication of GaAs/AlGaAs wafers was subsidized by CMC Microsystems (Kingston, Canada). MAI acknowledges the B2X scholarship from the Fonds de Recherche sur la Nature et les Technologies du Québec (FRQNT). The authors are indebted to Prof. E.H. Frost and Dr. K. Moumanis for helpful discussions.

Chapter 6 Conclusion and future recommendations

In this study, we investigated an AMP based DIP biosensing technique to detect *L. pneumophila*. AMP attracted our attention due to their high affinity towards bacteria. We designed a prototype of the warnericin RK AMP GaAs/AlGaAs biosensors for detecting *L. pneumophila*. The performance of warnericin RK AMP biosensors was investigated, primarily, for their sensitivity and specificity versus selected bacteria. We verified biosensors functionalization efficiency using FTIR. The FTIR measurement confirmed the peptide immobilization on the biosensor surface. The *L. pneumophila* capture efficiency by the warnericin RK functionalized GaAs biochip was compared to anti-*L. pneumophila* polyclonal antibody. The specificity of the biosensor was tested by exposing it to several non-targeted bacteria. It was observed that *L. pneumophila* was captured with ~5-fold greater binding efficiency than other non-targeted bacteria (*E. coli* ATCC 25922, *Bacillus subtilis* ATCC 60514, and *Pseudomonas fluorescens* ATCC 13525). Thus, the warnericin RK conjugated GaAs/AlGaAs sensor demonstrated reasonable specificity against *L. pneumophila*. The 10^3 CFU/mL LOD achieved with this biosensor is comparable to what was previously reported for an Ab-based GaAs/AlGaAs DIP biosensor but in that case the negative charge carried by the *L. pneumophila* cells was increased by the use of low concentration of SDS. This detection limit is comparable or even one order of magnitude better than the direct detection of *L. pneumophila* previously reported antibody-based GaAs/AlGaAs DIP biosensor and other biosensors based on optical and electrochemical signals. The proposed AMP based bioarchitecture paves the way towards the replacement of mammalian antibody-based biosensors that suffer by the low sensitivity and reproducibility due to the issues concerning animal dependent production of antibodies related to batch-to-batch variations.

One of the inconveniences of the Ab-based or AMP-based DIP biosensors investigated thus far was the relatively long preparation time (more than 20 hours) required for completing the biofunctionalization steps. To address this problem, we designed a DIP biosensor employing cysteine modified warnericin RK AMP (Cys-WRK). The overall length of the bacteria immobilizing ligand in this case was ~2 nm, compared to the previous ~12 nm achieved with COOH-based architectures activated with the EDC/NHS process. The new biosensor could be functionalized within ~1h, and detection of *L. pneumophila* was

demonstrated with LOD at 2 x 10^2 CFU/mL. In addition to the more reliable biofunctionalization procedure involving reduced number of steps, this result seems related to the more efficient charge transfer between bacteria and the digitally photocorroded GaAs/AlGaAs biochip although this conclusion requires further study. The results suggest the short length ligand could potentially enhance charge transfer between biochip surface and bacteria leading to an increased performance of charge sensing based DIP biosensors. In addition, the application of Cys-WRK AMP for functionalization of GaAs-based DIP biosensors provide an alternative way to eliminate the 20-hour step required for the formation of MHDA SAM and subsequent EDC/NHS activation of the -COOH group for binding with pAb through the amine group. In addition, the ~15 nm bacteria binding bioarchitecture could be replaced with a significantly shorter, ~2 nm ligand with this technique and the biosensors fabrication process including detection of *L. pneumophila* can be completed within 3 hours. The elimination of extra EDC/NHS biofunctionalization step contributes to the more consistent reproducible data collection, while the short chain interface allows more efficient charge transfer between the bacteria and surface of biosensor. Thus, the short-chain AMP architecture offers rapid, sensitive, and specific detection of *L. pneumophila* with charge sensing DIP biosensors.

The third challenge of this project was to overcome possible specificity limitation of warnericin RK AMP ligands when used for *L. pneumophila* DIP detection. For that we decided to use the sandwich-type biosensor configuration consists of an AMP sandwiched with polyclonal antibodies for specific detection of *L. pneumophila* SG1 and SG5 antibodies. The biosensing protocol was based on the verified ~4-fold greater specificity of commercially available polyclonal antibody against *L. pneumophila* SG1 than SG5. The biochips were functionalized with Cys-WRK AMP for capturing bacteria decorated with anti-*L. pneumophila* polyclonal antibodies for enhanced specificity of biosensing. This configuration allowed rapid detection of *L. pneumophila* SG1 at 50 CFU/mL. The 2-fold improved LOD of *L. pneumophila* SG1 suggests that additional negative charge was transferred from bacteria decorated with antibodies to the surface of charge-sensitive DIP GaAs/AlGaAs biosensor response. The influence of the environment for detection of bacteria was investigated for water samples originating from a cooling tower spiked with *L. pneumophila*. The designed biosensor selectively detected 100 CFU/mL of *L. pneumophila* SG1 and SG5 in samples originating

from cooling tower water. The results suggest the AMP-Ab sandwich DIP biosensor is a potential approach to detect low concentrated *L. pneumophila* in CTW conditions. Moreover, the proposed sensor is promising to solve the problem concerning relatively broad specificity spectrum of AMP for detecting selective bacteria. In this sensing technique, additional negative charge from antibodies decorated with bacteria significantly enhanced sensitivity of DIP biosensors and this configuration could be implemented to the other charge-sensitive sensors. This method has the potential to offer highly specific and sensitive detection of *L. pneumophila* as well as other pathogenic bacteria and viruses.

The specificity of AMP is one of the significant concerns for selectively detecting targeted bacteria since most AMPs show broad-spectrum reactivity against bacteria. Although few reports have shown that an individual bacterium, even at the strain level, could be detected by AMP conjugated biosensors, it is still hard to determine the performance of such sensors for specific bacterium detection in the real samples with the interference of similar species. Now-a-days, the bioinformatics techniques are commonly used for screening bacteria specific peptides with low cost and time. The tertiary structures, thermo-dynamic characteristics, binding affinity and, target-relevant interactions of AMPs could be predicted using computational *in-silico* docking strategies. Some other techniques such as molecular docking, molecular dynamics simulations study, machine learning and artificial intelligence could also be applied for designing or screening bacteria specific AMPs. Few of pre-screening techniques such as rational design, and high-throughput screening are recommended to apply for identifying highly specific peptides against *L. pneumophila*.

The sensitivity of AMP conjugated biosensors is another challenge for developing practically applicable *L. pneumophila* biosensors. In general, the sensitivity of biosensors is associated with the bacteria capture efficiency of the biorecognition ligands and signal transmitting efficiency between target analytes and transducers. In both contexts, AMPs have been reported as potential biorecognition ligands since they can capture higher numbers of bacteria than other ligands and efficiently transmit signals by maintaining a lower distance between target analytes and transducers. The sensitivity of AMP functionalized DIP biosensors could be enhanced by integrating highly conductive nanomaterials (*i. e.* carbon

nano-tubes) through the enhancement of signal transduction between target analytes and transducers.

Specific recommendations are suggested for designing future experiments:

i) The role of short ligands for improving the LOD of GaAs/AlGaAs biosensors could be investigated in futures studies. For this purpose, the Cys-AMP could be replaced with short chain thiolated antibodies, and nucleic acids to evaluate the influence of short linker thiol in charge sensitive DIP biosensors.

ii) In this study, pAb are used for making a sandwich configuration. Future studies can be designed with monoclonal or recombinant Ab for decorating AMP captured *L. pneumophila* to investigate the influence of these antibodies on specificity and sensitivity of the biosensors.

iii) Future experiments are recommended to verify the influence of additional negatively charge molecules (*i.e.* Ab, aptamers, and nucleic acids) on the biochip. In this context, a series of DIP runs could be performed involving some negatively and positively charged molecules immobilized on the functionalized surface of biochip

Conclusions et recommandations futures

La présence de *L. pneumophila* dans les systèmes d'eaux anthropogéniques (SPA, piscine, tour d'eau, etc.), dans les lacs et rivières a été bien démontré dans la littérature. Vue le nombre grandissant d'éclosions de la maladie du Légionnaire, le contrôle de la présence de *L. pneumophila* est devenu un enjeu critique pour assurer la protection des populations. Divers appareils de biosensure ont été développé pour répondre à cette problématique. Parmi eux, on peut citer la technologie de la photocorrosion digitale de nanohéterostructures de GaAs/AlGaAs utilisée pour le développement de biocapteur de *L. pneumophila* à un bas coût. L'efficacité de cette technologie a été déjà démontré pour la détection de la Légionnelle dans les travaux de recherche antérieurs menés par les membres du QS-group. Mon projet de thèse consistait à investiguer les stratégies permettant d'améliorer les performances du biocapteur DIP pour la détection de *L. pneumophila* dans l'eau.

La première stratégie était de substituer l'architecture de reconnaissance à base d'anticorps par d'autres molécules. En effet, l'usage d'anticorps pourrait affecter la reproductibilité des résultats de notre biocapteur au simple fait que les anticorps polyclonaux utilisés peuvent varier d'un batch à un autre. Pour trouver notre substitut, nous avions le choix entre plusieurs molécules disponibles dans la littérature comme les acides nucléiques, les enzymes, les bactériophages et les peptides antimicrobiens (PAMs). Les PAMs présentait plusieurs avantages tels que; une certaine affinité pour des groupes de bactéries, disponibles naturellement, facilement manipulable pour améliorer leurs spécificités, flexibles, stables et pouvant être synthétisés à relativement bas coût sans risque de variabilité dans les batchs. Tous ces avantages font des PAMs un bon choix pour le développement d'un biocateur DIP pour la détection de la légionnelle dans l'eau.

Nous avons donc développé en premier lieu un biocapteur DIP en utilisant des puces de GaAs/AlGaAs fonctionnalisées par de la warnericine RK (un PAM reporté à être spécifique à la légionnelle). Cette architecture a tout d'abord été évaluée pour sa capacité d'interaction avec notre bactérie cible ainsi que pour l'efficacité de la fonctionnalisation de surface par des mesures FTIR. Par le biais de cette dernière, nous avons identifié des pics d'absorbance reliés à la présence du peptide sur la surface du GaAs/AlGaAs et par microscopie optique nous avons pu démontrer que la warnericine Rk permettait d'attacher 5 fois plus de *L. pneumophila* que d' *E. coli*, *Bacillus subtilis*, et *Pseudomonas fluorescens.* En utilisant notre technologie DIP nous avons pu démontrer une détection de *L. pneumophila* à une concentration de 10^3 UFC/mL, comparable à la meilleure performance obtenue avec des architectures à base d'anticorps dans le cas d'utilisation de bactéries dont leurs charges négative a été boosté par le greffage molécules de SDS.

En un second lieu nous avons décidé de baisser le temps de préparation des puces fonctionnalisées (environ 20 heures) en utilisant de la warnericin taguée avec de la cystéine (cys-warnericin) permettant ainsi sa directe immobilisation sur la surface du GaAs/AlGaAs. Dans ce cas la bactérie une fois attachée sera à seulement ~ 2 nm de la surface comparé à ~ 12 nm pour une architecture impliquant l'usage des thiols à terminaison COOH activé par l'EDC-NHS pour attacher la warnericin. En utilisant l'attachement direct de la cys-warnericin, le temps de préparation de la puce est d'environ 1h. Nous avons pu démontrer une détection à 2 x

10^2 UFC/mL. Nous pensons que cette configuration avec un fonctionnalisation en une seule étape permet un meilleur transfert de charge entre les bactéries et la biopuce de GaAs/AlGaAs en cours de photocorrosion digitale.

Le troisième point de mon projet est de palier la possible problématique de manque de spécificité de la warnericin, pour cela nous avons investigué l'utilisation d'une configuration de détection de la *Légionnelle* en sandwich (PAM-*Legionella*-Anticorps polyclonaux). Les anticoprs utilisés ont été produit en réponse à une souche de *Légionnelle* du sérogroupe (SG1) avec lesquels nous avons observé 4-fois plus d'interactions avec le SG1 comparé au SG5. Dans ce cas, la biopuce préalablement fonctionnalisée par la warnericin a été utilisé pour la capture des *Légionnelles* qui ont à la suite été décorées par les anticorps. Nous avons démontré une limite de détection (LDD) de 50 UFC/ml. L'amélioration de la LDD peut être associée au charges négatives que les anticorps ont ramené en s'attachant sur les bactéries et transmises à la surface du GaAs/AlGaAs et ralentissant encore plus la vitesse de sa photocorrosion. Nous avons observé que la configuration en sandwich permet une LDD de 100 CFU/ml de *Legionella pneumophila* SG1 et 5 collectées d'échantillons de tour d'eau.

Le premier est la spécificité du PAM qui va déterminer la sélectivité de détection, en effet, la majorité des PAMs ont un spectre de réactivité large incluant plusieurs bactéries. Bien que certains biocapteurs décrit en littérature aient démontré une sélectivité des PAMs utilisés envers certaines souches bactériennes et cela même entre sérogroupes, affirmer leurs efficacités en cas de tests sur des échantillons réels restent à vérifier vue la complexité des flores microbiennes pouvant coexister avec notre bactérie cible. De nos jours, les outils de la bio-informatiques ont permis de prédire les interactions possible entre bactéries et PAMs réduisant fortement le temps de validation et pouvant même venir améliorer la spécifié des PAMs en introduisant des substitutions positives

Certaines autres techniques telles que l'amarrage moléculaire, l'étude des simulations de dynamique moléculaire, l'apprentissage automatique et l'intelligence artificielle pourraient également être appliquées pour concevoir ou cribler des AMP spécifiques aux bactéries. Cependant, jusqu'à date peu de techniques de pré-criblage telles que la conception rationnelle et le criblage à haut débit sont recommandées pour identifier des peptides hautement spécifiques contre *L. pneumophila.*

Le second point est la sensibilité du biocapteur à base de PAM. D'une manière générale la sensibilité d'un biocapteur dépend de la capacité du ligand utilisé à capturer la bactérie cible en grand nombre et l'efficacité de transférer le signal amené par les bactéries au transducteur. Pour ces deux paramètres, les PAMs seront favorables puisqu'ils permettent un attachement de bactérie élevé ainsi un transfert facilité des charges vue leurs courtes longueurs. Intégrer des nanotubes de carbone dans la couche de PAM fonctionnalisant la surface du GaAs/AlGaAs permettrait aussi de promouvoir le transfert de charge.

En troisième point vient la régénération de la surface des biocapteurs qui sera indispensable pour assurer des opérations de détection à faible coût. Il est crucial de disposer de méthodes de régénération des surfaces GaAs/AlGaAs qui préservent la structure cristalline initiale et la morphologie de GaAs en plus de l'intégrité de la molécule de reconnaissance. Un des avantages des puces GaAs par rapport aux autres surfaces de biodétection est qu'elles comprennent plusieurs interfaces de GaAs/AlGaAs pouvant être utilisées pour plusieurs mesures en utilisant une seule puce. Les PAMs modifiés par la cystéine sont très avantageux pour régénérer chacune des interfaces de GaAs/AlGaAs puisque les peptides peuvent être attachés en une seule étape d'une durée de 1h. Ainsi, un biocapteur DIP régénératif à base de PAM comprenant un empilement d'interfaces de GaAs/AlGaAs peut être conçu/étudié pour faire fonctionner un biocapteur régénérable capable de faire plusieurs cycles de biodétection avec la même puce.

Comme recommandations pour les futures directions de recherche, nous proposons d'étudier :

i) Le rôle des ligands courts pour améliorer la limite de détection des biocapteurs GaAs/AlGaAs pourrait être étudié. À cette fin, le Cys-PAM pourrait être remplacé par des anticorps thiolés ou des apatmères.

ii) Des anticorps monoclonaux ou recombinants pour décorer la *L. pneumophila* capturée par le PAM et ainsi ramener une meilleure spécifié comparée aux anticorps polyclonaux.

iii) Des expériences futures sont recommandées pour vérifier l'influence d'autres molécules chargées négativement (Ab et acides nucléiques) sur la sensibilité du capteur DIP.

References

Abshar Hasan, D., Lee, K., Tewari, K., Pandey, L.M., Messersmith, P.B., Faulds, K., Maclean, M., Lau, K.H.A., (2020). Surface design for immobilization of an antimicrobial peptide mimic for efficient anti-biofouling. *Chemistry (Weinheim an der Bergstrasse, Germany)*, vol. 26(26), p. 5789.

Ahmad, M., Rehman, G., Ali, L., Shafiq, M., Iqbal, R., Ahmad, R., Khan, T., Jalali-Asadabadi, S., Maqbool, M., Ahmad, I., (2017). Structural, electronic and optical properties of CsPbX3 (X= Cl, Br, I) for energy storage and hybrid solar cell applications. *Journal of Alloys and Compounds*, vol. 705, p. 828-839.

Ahmed, A., Rushworth, J.V., Hirst, N.A., Millner, P.A., (2014). Biosensors for whole-cell bacterial detection. *Clinical microbiology reviews*, vol. 27(3), p. 631-646.

Aithal, S., Dubowski, J.J., (2018). Open circuit potential monitored digital photocorrosion of GaAs/AlGaAs quantum well microstructures. *Applied Physics Letters*, vol. 112(15), p. 153102.

Aithal, S., Liu, N., Dubowski, J.J., (2017). Photocorrosion metrology of photoluminescence emitting GaAs/AlGaAs heterostructures. *Journal of Physics D: Applied Physics*, vol. 50(3), p. 035106.

Akrami, M., Balalaie, S., Hosseinkhani, S., Alipour, M., Salehi, F., Bahador, A., Haririan, I., (2016). Tuning the anticancer activity of a novel pro-apoptotic peptide using gold nanoparticle platforms. *Scientific reports*, vol. 6, p. 31030.

Albalat, G.R., Broch, B.B., Bono, M.J., (2014). Method modification of the Legipid® Legionella fast detection test kit. *Journal of AOAC International*, vol. 97(5), p. 1403-1409.

Albanese, D., Garofalo, F., Pilloton, R., Capo, S., Malvano, F., (2019). Development of an Antimicrobial Peptide-based Biosensor for the Monitoring of Bacterial Contaminations. *Chemical Engineering Transactions*, vol. 75, p. 61-66.

Aliakbar Ahovan, Z., Hashemi, A., De Plano, L.M., Gholipourmalekabadi, M., Seifalian, A., (2020). Bacteriophage based biosensors: Trends, outcomes and challenges. *Nanomaterials*, vol. 10(3), p. 501.

Ami, D., Posteri, R., Mereghetti, P., Porro, D., Doglia, S.M., Branduardi, P., (2014). Fourier transform infrared spectroscopy as a method to study lipid accumulation in oleaginous yeasts. *Biotechnology for biofuels*, vol. 7(1), p. 12.

Andrade, C.A., Nascimento, J.M., Oliveira, I.S., de Oliveira, C.V., de Melo, C.P., Franco, O.L., Oliveira, M.D., (2015). Nanostructured sensor based on carbon nanotubes and clavanin A for bacterial detection. *Colloids and Surfaces B: Biointerfaces*, vol. 135, p. 833-839.

Arora, P., Sindhu, A., Dilbaghi, N., Chaudhury, A., (2011). Biosensors as innovative tools for the detection of food borne pathogens. *Biosensors and Bioelectronics*, vol. 28(1), p. 1-12.

Ashbolt, N.J., (2004). Microbial contamination of drinking water and disease outcomes in developing regions. *Toxicology*, vol. 198(1-3), p. 229-238.

Aziziyan, M.R., Hassen, W.M., Morris, D., Frost, E.H., Dubowski, J.J., (2016). Photonic biosensor based on photocorrosion of GaAs/AlGaAs quantum heterostructures for detection of Legionella pneumophila. *Biointerphases*, vol. 11(1), p. 019301.

Aziziyan, M.R., Hassen, W.M., Sharma, H., Shirzaei Sani, E., Annabi, N., Frost, E.H., Dubowski, J.J., (2020). Sodium dodecyl sulfate decorated Legionella pneumophila for enhanced detection with a GaAs/AlGaAs nanoheterostructure biosensor. *Sensors and Actuators B: Chemical*, vol. 304, p. 127007.

Aziziyan, M.R., Sharma, H., Dubowski, J.J., (2019). Photo-Atomic Layer Etching of GaAs/AlGaAs Nanoheterostructures. *ACS Applied Materials & Interfaces*, vol. 11(19), p. 17968-17978.

Azmi, S., Jiang, K., Stiles, M., Thundat, T., Kaur, K., (2015). Detection of Listeria monocytogenes with short peptide fragments from class IIa bacteriocins as recognition elements. *ACS combinatorial science*, vol. 17(3), p. 156-163.

Baer, D.R., Gaspar, D.J., Nachimuthu, P., Techane, S.D., Castner, D.G., (2010). Application of surface chemical analysis tools for characterization of nanoparticles. *Analytical and bioanalytical chemistry*, vol. 396(3), p. 983-1002.

Bagheri, M., Beyermann, M., Dathe, M., (2009). Immobilization reduces the activity of surface-bound cationic antimicrobial peptides with no influence upon the activity spectrum. *Antimicrobial agents and chemotherapy*, vol. 53(3), p. 1132-1141.

Bal, B., Nayak, S., Das, A., 2017. Recent advances in molecular techniques for the diagnosis of foodborne diseases, Nanotechnology Applications in Food. Elsevier, pp. 267-285.

Ballard, A., Fry, N., Chan, L., Surman, S., Lee, J., Harrison, T., Towner, K., (2000). Detection of Legionella pneumophila using a real-time PCR hybridization assay. *Journal of clinical microbiology*, vol. 38(11), p. 4215-4218.

Barbosa, M., Vale, N., Costa, F.M., Martins, M.C.L., Gomes, P., (2017). Tethering antimicrobial peptides onto chitosan: Optimization of azide-alkyne "click" reaction conditions. *Carbohydrate polymers*, vol. 165, p. 384-393.

Bazin, I., Tria, S.A., Hayat, A., Marty, J.-L., (2017). New biorecognition molecules in biosensors for the detection of toxins. *Biosensors and Bioelectronics*, vol. 87, p. 285-298.

Bedrina, B., Macian, S., Solis, I., Fernandez-Lafuente, R., Baldrich, E., Rodriguez, G., (2013). Fast immunosensing technique to detect Legionella pneumophila in different natural and anthropogenic environments: comparative and collaborative trials. *BMC microbiology*, vol. 13(1), p. 88.

Behets, J., Declerck, P., Delaedt, Y., Creemers, B., Ollevier, F., (2007). Development and evaluation of a Taqman duplex real-time PCR quantification method for reliable enumeration of Legionella pneumophila in water samples. *Journal of microbiological methods*, vol. 68(1), p. 137-144.

Berjeaud, J.-M., Chevalier, S., Schlusselhuber, M., Portier, E., Loiseau, C., Aucher, W., Lesouhaitier, O., Verdon, J., (2016). Legionella pneumophila: the paradox of a highly sensitive opportunistic waterborne pathogen able to persist in the environment. *Frontiers in microbiology*, vol. 7, p. 486.

Beveridge, T.J., Lawrence, J.R., Murray, R.G., (2007). Sampling and staining for light microscopy. *Methods for general and molecular microbiology*, p. 19-33.

Birteksoz-Tan, A.S., Zeybek, Z., Hacioglu, M., Savage, P.B., Bozkurt-Guzel, C., (2019). In vitro activities of antimicrobial peptides and ceragenins against Legionella pneumophila. *The Journal of Antibiotics*, vol. 72(5), p. 291-297.

Bookout, A.L., Mangelsdorf, D.J., (2003). Quantitative real-time PCR protocol for analysis of nuclear receptor signaling pathways. *Nuclear receptor signaling*, vol. 1(1), p. nrs. 01012.

Bouguelia, S., Roupioz, Y., Slimani, S., Mondani, L., Casabona, M.G., Durmort, C., Vernet, T., Calemczuk, R., Livache, T., (2013). On-chip microbial culture for the specific detection of very low levels of bacteria. *Lab on a Chip*, vol. 13(20), p. 4024-4032.

Brigati, J.R., Petrenko, V.A., (2005). Thermostability of landscape phage probes. *Analytical and bioanalytical chemistry*, vol. 382(6), p. 1346-1350.

Buchan, B.W., Ledeboer, N.A., (2014). Emerging technologies for the clinical microbiology laboratory. *Clinical microbiology reviews*, vol. 27(4), p. 783-822.

Burlage, R.S., Tillmann, J., (2017). Biosensors of bacterial cells. *Journal of microbiological methods*, vol. 138, p. 2-11.

Byrne, B., Stack, E., Gilmartin, N., O'Kennedy, R., (2009). Antibody-based sensors: principles, problems and potential for detection of pathogens and associated toxins. *Sensors (Basel, Switzerland)*, vol. 9(6), p. 4407-4445.

Cambray, G., Guimaraes, J.C., Arkin, A.P., (2018). Evaluation of 244,000 synthetic sequences reveals design principles to optimize translation in Escherichia coli. *Nature biotechnology*, vol. 36(10), p. 1005-1015.

Carpi, G., Cagnacci, F., Wittekindt, N.E., Zhao, F., Qi, J., Tomsho, L.P., Drautz, D.I., Rizzoli, A., Schuster, S.C., (2011). Metagenomic profile of the bacterial communities associated with Ixodes ricinus ticks. *PloS one*, vol. 6(10).

Castle, L.M., Schuh, D.A., Reynolds, E.E., Furst, A.L., (2021). Electrochemical sensors to detect bacterial foodborne pathogens. *ACS sensors*, vol. 6(5), p. 1717-1730.

Chambers, S.T., Slow, S., Scott-Thomas, A., Murdoch, D.R., (2021). Legionellosis Caused by Non-Legionella pneumophila Species, with a Focus on Legionella longbeachae. *Microorganisms*, vol. 9(2), p. 291.

Choi, K.J., Moon, J.K., Park, M., Kim, H., Lee, J.-L., (2002). Effects of photowashing treatment on gate leakage current of GaAs metal-semiconductor field-effect transistors. *Japanese journal of applied physics*, vol. 41(5R), p. 2894.

Choinière, S., Frost, E.H., Dubowski, J.J., (2019). Binding strategies for capturing and growing Escherichia coli on surfaces of biosensing devices. *Talanta*, vol. 192, p. 270-277.

Cieplak, M., Kutner, W., (2016). Artificial biosensors: how can molecular imprinting mimic biorecognition? *Trends in biotechnology*, vol. 34(11), p. 922-941.

Conover, G.M., Martinez-Morales, F., Heidtman, M.I., Luo, Z.Q., Tang, M., Chen, C., Geiger, O., Isberg, R.R., (2008). Phosphatidylcholine synthesis is required for optimal function of Legionella pneumophila virulence determinants. *Cellular microbiology*, vol. 10(2), p. 514-528.

Corrales-Ureña, Y.R., Souza-Schiaber, Z., Lisboa-Filho, P.N., Marquenet, F., Noeske, P.-L.M., Gätjen, L., Rischka, K., (2020). Functionalization of hydrophobic surfaces with antimicrobial peptides immobilized on a bio-interfactant layer. *RSC Advances*, vol. 10(1), p. 376-386.

Corre, M.-H., Delafont, V., Legrand, A., Berjeaud, J.-M., Verdon, J., (2018). Exploiting the richness of environmental waterborne bacterial species to find natural anti-Legionella active biomolecules. *Frontiers in microbiology*, vol. 9, p. 3360.

Costa, F., Gomes, P., Martins, M., 2018. Antimicrobial peptides (AMP) biomaterial coatings for tissue repair, Peptides and proteins as biomaterials for tissue regeneration and repair. Elsevier, pp. 329-345.

Cruz, J., Ortiz, C., Guzman, F., Fernandez-Lafuente, R., Torres, R., (2014). Antimicrobial peptides: promising compounds against pathogenic microorganisms. *Current medicinal chemistry*, vol. 21(20), p. 2299-2321.

D'Souza, G., Shitut, S., Preussger, D., Yousif, G., Waschina, S., Kost, C., (2018). Ecology and evolution of metabolic cross-feeding interactions in bacteria. *Natural Product Reports*, vol. 35(5), p. 455-488.

da Silva, E.T., Souto, D.E., Barragan, J.T., de F. Giarola, J., de Moraes, A.C., Kubota, L.T., (2017). Electrochemical biosensors in point-of-care devices: recent advances and future trends. *ChemElectroChem*, vol. 4(4), p. 778-794.

Date, T., Sawada, T., Serizawa, T., (2013). Self-assembled peptides on polymer surfaces: towards morphology-dependent surface functionalization. *Soft Matter*, vol. 9(13), p. 3469-3472.

De Bruyne, K., Slabbinck, B., Waegeman, W., Vauterin, P., De Baets, B., Vandamme, P., (2011). Bacterial species identification from MALDI-TOF mass spectra through data analysis and machine learning. *Systematic and applied microbiology*, vol. 34(1), p. 20-29.

de Campos Vidal, B., Mello, M.L.S., (2016). FT-IR microspectroscopy of rat ear cartilage. *PloS one*, vol. 11(3).

de Miranda, J.L., Oliveira, M.D., Oliveira, I.S., Frias, I.A., Franco, O.L., Andrade, C.A., (2017). A simple nanostructured biosensor based on clavanin A antimicrobial peptide for gram-negative bacteria detection. *Biochemical engineering journal*, vol. 124, p. 108-114.

Dennison, S.R., Morton, L.H., Harris, F., Phoenix, D.A., (2007). Antimicrobial properties of a lipid interactive α-helical peptide VP1 against Staphylococcus aureus bacteria. *Biophysical chemistry*, vol. 129(2-3), p. 279-283.

Deshmukh, R.A., Joshi, K., Bhand, S., Roy, U., (2016). Recent developments in detection and enumeration of waterborne bacteria: a retrospective minireview. *MicrobiologyOpen*, vol. 5(6), p. 901-922.

Dinc, M., Esen, C., Mizaikoff, B., (2019). Recent advances on core–shell magnetic molecularly imprinted polymers for biomacromolecules. *TrAC Trends in Analytical Chemistry*.

Dinesh, B., Squillaci, M.A., Ménard-Moyon, C., Samorì, P., Bianco, A., (2015). Self-assembly of diphenylalanine backbone homologues and their combination with functionalized carbon nanotubes. *Nanoscale*, vol. 7(38), p. 15873-15879.

Dingle, T.C., Butler-Wu, S.M., (2013). MALDI-TOF mass spectrometry for microorganism identification. *Clinics in laboratory medicine*, vol. 33(3), p. 589-609.

Doiron, K., Beaulieu, L., St-Louis, R., Lemarchand, K., (2018). Reduction of bacterial biofilm formation using marine natural antimicrobial peptides. *Colloids and Surfaces B: Biointerfaces*, vol. 167, p. 524-530.

Dong, Z.-M., Zhao, G.-C., (2015). Label-free detection of pathogenic bacteria via immobilized antimicrobial peptides. *Talanta*, vol. 137, p. 55-61.

Duan, N., Chang, B., Zhang, H., Wang, Z., Wu, S., (2016). Salmonella typhimurium detection using a surface-enhanced Raman scattering-based aptasensor. *International journal of food microbiology*, vol. 218, p. 38-43.

Dufrêne, Y.F., (2002). Atomic force microscopy, a powerful tool in microbiology. *Journal of bacteriology*, vol. 184(19), p. 5205-5213.

Dusserre, E., Ginevra, C., Hallier-Soulier, S., Vandenesch, F., Festoc, G., Etienne, J., Jarraud, S., Molmeret, M., (2008). A PCR-based method for monitoring Legionella pneumophila in

water samples detects viable but noncultivable legionellae that can recover their cultivability. *Applied and Environmental Microbiology*, vol. 74(15), p. 4817-4824.

Dwivedi, H.P., Jaykus, L.-A., (2011). Detection of pathogens in foods: the current state-of-the-art and future directions. *Critical reviews in microbiology*, vol. 37(1), p. 40-63.

Eddy, N.O., Ebenso, E.E., Ibok, U.J., (2010). Adsorption, synergistic inhibitive effect and quantum chemical studies of ampicillin (AMP) and halides for the corrosion of mild steel in H2SO4. *Journal of Applied Electrochemistry*, vol. 40(2), p. 445-456.

Elakkiya, E., Matheswaran, M., (2013). Comparison of anodic metabolisms in bioelectricity production during treatment of dairy wastewater in Microbial Fuel Cell. *Bioresource technology*, vol. 136, p. 407-412.

Ertürk, G., Lood, R., (2018). Bacteriophages as biorecognition elements in capacitive biosensors: Phage and host bacteria detection. *Sensors and Actuators B: Chemical*, vol. 258, p. 535-543.

Eslami, B., Caputo, D., (2021). Effect of Eigenmode Frequency on Loss Tangent Atomic Force Microscopy Measurements. *Applied Sciences*, vol. 11(15), p. 6813.

Estevez, M.-C., Otte, M.A., Sepulveda, B., Lechuga, L.M., (2014). Trends and challenges of refractometric nanoplasmonic biosensors: A review. *Analytica chimica acta*, vol. 806, p. 55-73.

Etayash, H., Jiang, K., Thundat, T., Kaur, K., (2014a). Impedimetric detection of pathogenic gram-positive bacteria using an antimicrobial peptide from class IIa bacteriocins. *Analytical chemistry*, vol. 86(3), p. 1693-1700.

Etayash, H., Norman, L., Thundat, T., Kaur, K., (2013). Peptide-bacteria interactions using engineered surface-immobilized peptides from class IIa bacteriocins. *Langmuir*, vol. 29(12), p. 4048-4056.

Etayash, H., Norman, L., Thundat, T., Stiles, M., Kaur, K., (2014b). Surface-conjugated antimicrobial peptide leucocin a displays high binding to pathogenic gram-positive bacteria. *ACS applied materials & interfaces*, vol. 6(2), p. 1131-1138.

Fears, K.P., Petrovykh, D.Y., Clark, T.D., (2013). Evaluating protocols and analytical methods for peptide adsorption experiments. *Biointerphases*, vol. 8(1), p. 20.

Foddai, A.C., Grant, I.R., (2020). Methods for detection of viable foodborne pathogens: Current state-of-art and future prospects. *Applied Microbiology and Biotechnology*, vol. 104(10), p. 4281-4288.

Forsting, T., Gottschalk, H.C., Hartwig, B., Mons, M., Suhm, M.A., (2017). Correcting the record: the dimers and trimers of trans-N-methylacetamide. *Physical Chemistry Chemical Physics*, vol. 19(17), p. 10727-10737.

Fricke, C., Xu, J., Jiang, F.L., Liu, Y., Harms, H., Maskow, T., (2020). Rapid culture-based detection of Legionella pneumophila using isothermal microcalorimetry with an improved evaluation method. *Microbial biotechnology*.

Friedrich, C., Scott, M.G., Karunaratne, N., Yan, H., Hancock, R.E., (1999). Salt-resistant alpha-helical cationic antimicrobial peptides. *Antimicrobial agents and chemotherapy*, vol. 43(7), p. 1542-1548.

Garbeva, P., Van Veen, J., Van Elsas, J., (2003). Predominant Bacillus spp. in agricultural soil under different management regimes detected via PCR-DGGE. *Microbial Ecology*, vol. 45(3), p. 302-316.

Garcia, R., (2020). Nanomechanical mapping of soft materials with the atomic force microscope: methods, theory and applications. *Chemical Society Reviews*, vol. 49(16), p. 5850-5884.

Geitani, R., Ayoub Moubareck, C., Touqui, L., Karam Sarkis, D., (2019). Cationic antimicrobial peptides: alternatives and/or adjuvants to antibiotics active against methicillin-resistant Staphylococcus aureus and multidrug-resistant Pseudomonas aeruginosa. *BMC microbiology*, vol. 19(1), p. 1-12.

Geitani, R., Moubareck, C.A., Xu, Z., Karam Sarkis, D., Touqui, L., (2020). Expression and Roles of Antimicrobial Peptides in Innate Defense of Airway Mucosa: Potential Implication in Cystic Fibrosis. *Frontiers in Immunology*, vol. 11, p. 1198.

Gervais, L., Gel, M., Allain, B., Tolba, M., Brovko, L., Zourob, M., Mandeville, R., Griffiths, M., Evoy, S., (2007). Immobilization of biotinylated bacteriophages on biosensor surfaces. *Sensors and Actuators B: Chemical*, vol. 125(2), p. 615-621.

Gilbride, K.A., Lee, D.-Y., Beaudette, L., (2006). Molecular techniques in wastewater: understanding microbial communities, detecting pathogens, and real-time process control. *Journal of microbiological methods*, vol. 66(1), p. 1-20.

Giuliani, A., Pirri, G., Nicoletto, S., (2007). Antimicrobial peptides: an overview of a promising class of therapeutics. *Open Life Sciences*, vol. 2(1), p. 1-33.

Gleason, J.A., Cohn, P.D., (2022). A review of legionnaires' disease and public water systems–Scientific considerations, uncertainties and recommendations. *International Journal of Hygiene and Environmental Health*, vol. 240, p. 113906.

Gocalinska, A., Gradkowski, K., Dimastrodonato, V., Mereni, L., Juska, G., Huyet, G., Pelucchi, E., (2011). Wettability and "petal effect" of GaAs native oxides. *Journal of Applied Physics*, vol. 110(3), p. 034319.

Gomez, D., Sunyer, J.O., Salinas, I., (2013). The mucosal immune system of fish: the evolution of tolerating commensals while fighting pathogens. *Fish & shellfish immunology*, vol. 35(6), p. 1729-1739.

Gopinath, S.C., Tang, T.-H., Chen, Y., Citartan, M., Lakshmipriya, T., (2014). Bacterial detection: From microscope to smartphone. *Biosensors and Bioelectronics*, vol. 60, p. 332-342.

Grishagin, I.V., (2015). Automatic cell counting with ImageJ. *Analytical biochemistry*, vol. 473, p. 63-65.

Guan, Z.P., Jiang, Y., Gao, F., Zhang, L., Zhou, G.H., Guan, Z.J., (2013). Rapid and simultaneous analysis of five foodborne pathogenic bacteria using multiplex PCR. *European Food Research and Technology*, vol. 237(4), p. 627-637.

Guler, Z., Sarac, A., (2016). Electrochemical impedance and spectroscopy study of the EDC/NHS activation of the carboxyl groups on poly (ε-caprolactone)/poly (m-anthranilic acid) nanofibers. *Express Polymer Letters*, vol. 10(2).

Guo, X., Kulkarni, A., Doepke, A., Halsall, H.B., Iyer, S., Heineman, W.R., (2012). Carbohydrate-based label-free detection of Escherichia coli ORN 178 using electrochemical impedance spectroscopy. *Analytical chemistry*, vol. 84(1), p. 241-246.

Gupta, S., Kakkar, V., (2020). Development of environmental biosensors for detection, monitoring, and assessment. *Nanomat. Environ. Biotechnol. Springer*, p. 107-125.

Guralp, S.A., Gubbuk, I.H., Kucukkolbasi, S., Gulari, E., (2015). Universal cell capture by immobilized antimicrobial peptide plantaricin. *Biochemical Engineering Journal*, vol. 101, p. 18-22.

Guyard, C., Low, D.E., (2011). Legionella infections and travel associated legionellosis. *Travel Medicine and Infectious Disease*, vol. 9(4), p. 176-186.

Haas, J., Mizaikoff, B., (2016). Advances in mid-infrared spectroscopy for chemical analysis. *Annual Review of Analytical Chemistry*, vol. 9, p. 45-68.

Habimana, J.d.D., Ji, J., Sun, X., (2018). Minireview: trends in optical-based biosensors for point-of-care bacterial pathogen detection for food safety and clinical diagnostics. *Analytical Letters*, vol. 51(18), p. 2933-2966.

Hameed, S., Xie, L., Ying, Y., (2018). Conventional and emerging detection techniques for pathogenic bacteria in food science: A review. *Trends in Food Science & Technology*, vol. 81, p. 61-73.

Han, F., Wang, F., Ge, B., (2011). Detecting potentially virulent Vibrio vulnificus strains in raw oysters by quantitative loop-mediated isothermal amplification. *Appl. Environ. Microbiol.*, vol. 77(8), p. 2589-2595.

Han, H.M., Ko, S., Cheong, M.-J., Bang, J.K., Seo, C.H., Luchian, T., Park, Y., (2017). Myxinidin2 and myxinidin3 suppress inflammatory responses through STAT3 and MAPKs to promote wound healing. *Oncotarget*, vol. 8(50), p. 87582.

Hancock, R.E., Sahl, H.-G., (2006). Antimicrobial and host-defense peptides as new anti-infective therapeutic strategies. *Nature biotechnology*, vol. 24(12), p. 1551-1557.

Hao, R., Wang, D., Zuo, G., Wei, H., Yang, R., Zhang, Z., Cheng, Z., Guo, Y., Cui, Z., Zhou, Y., (2009). Rapid detection of Bacillus anthracis using monoclonal antibody functionalized QCM sensor. *Biosensors and Bioelectronics*, vol. 24(5), p. 1330-1335.

Harada, L.K., Silva, E.C., Campos, W.F., Del Fiol, F.S., Vila, M., Dąbrowska, K., Krylov, V.N., Balcão, V.M., (2018). Biotechnological applications of bacteriophages: State of the art. *Microbiological research*, vol. 212, p. 38-58.

Hassen, W.M., Sanyal, H., Hammood, M., Moumanis, K., Frost, E.H., Dubowski, J.J., (2016). Chemotaxis for enhanced immobilization of Escherichia coli and Legionella pneumophila on biofunctionalized surfaces of GaAs. *Biointerphases*, vol. 11(2), p. 021004.

Hebert, B.L., (2016). Molecularly Imprinted Polymers for Enantiomer Separations and Biomolecular Sensors.

Hiep, H.M., Saito, M., Nakamura, Y., Tamiya, E., (2010). RNA aptamer-based optical nanostructured sensor for highly sensitive and label-free detection of antigen-antibody reactions. *Analytical and Bioanalytical Chemistry*, vol. 396, p. 2575-2581.

Hilpert, K., Elliott, M., Jenssen, H., Kindrachuk, J., Fjell, C.D., Körner, J., Winkler, D.F., Weaver, L.L., Henklein, P., Ulrich, A.S., (2009). Screening and characterization of surface-tethered cationic peptides for antimicrobial activity. *Chemistry & biology*, vol. 16(1), p. 58-69.

Hindahl, M.S., Iglewski, B.H., (1984). Isolation and characterization of the Legionella pneumophila outer membrane. *Journal of bacteriology*, vol. 159(1), p. 107-113.

Hong, K.L., Sooter, L.J., (2015). Single-stranded DNA aptamers against pathogens and toxins: identification and biosensing applications. *BioMed research international*, vol. 2015.

Hossein-Nejad-Ariani, H., Kim, T., Kaur, K., (2018). Peptide-based biosensor utilizing fluorescent gold nanoclusters for detection of Listeria monocytogenes. *ACS Applied Nano Materials*.

Hoyos-Nogués, M., Brosel-Oliu, S., Abramova, N., Muñoz, F.-X., Bratov, A., Mas-Moruno, C., Gil, F.-J., (2016). Impedimetric antimicrobial peptide-based sensor for the early detection of periodontopathogenic bacteria. *Biosensors and Bioelectronics*, vol. 86, p. 377-385.

Hoyos-Nogués, M., Gil, F., Mas-Moruno, C., (2018). Antimicrobial peptides: powerful biorecognition elements to detect bacteria in biosensing technologies. *Molecules*, vol. 23(7), p. 1683.

Huang, H.W., (2000). Action of antimicrobial peptides: two-state model. *Biochemistry*, vol. 39(29), p. 8347-8352.

Huang, X.H., Liu, N., Moumanis, K., Dubowski, J.J., (2013). Water-Mediated Self-Assembly of 16-Mercaptohexadecanoic Acid on GaAs (001). *Journal of Physical Chemistry C*, vol. 117(29), p. 15090-15097.

Huang, Y.H., Ho, H.P., Kong, S.K., Kabashin, A.V., (2012). Phase-sensitive surface plasmon resonance biosensors: methodology, instrumentation and applications. *Annalen der Physik*, vol. 524(11), p. 637-662.

Humblot, V., Yala, J.-F., Thebault, P., Boukerma, K., Héquet, A., Berjeaud, J.-M., Pradier, C.-M., (2009). The antibacterial activity of Magainin I immobilized onto mixed thiols Self-Assembled Monolayers. *Biomaterials*, vol. 30(21), p. 3503-3512.

Hussain, W., Ullah, M.W., Farooq, U., Aziz, A., Wang, S., (2021). Bacteriophage-based advanced bacterial detection: Concept, mechanisms, and applications. *Biosensors and Bioelectronics*, vol. 177, p. 112973.

Hwang, K., Hosseinzadeh, P., Lu, Y., (2016). Biochemical and biophysical understanding of metal ion selectivity of DNAzymes. *Inorganica chimica acta*, vol. 452, p. 12-24.

Iqbal, S.S., Mayo, M.W., Bruno, J.G., Bronk, B.V., Batt, C.A., Chambers, J.P., (2000). A review of molecular recognition technologies for detection of biological threat agents. *Biosensors and Bioelectronics*, vol. 15(11-12), p. 549-578.

Islam, M.A., Hassen, W.M., Tayabali, A.F., Dubowski, J.J., (2020). Antimicrobial warnericin RK peptide functionalized GaAs/AlGaAs biosensor for highly sensitive and selective detection of Legionella pneumophila. *Biochemical Engineering Journal*, vol. 154, p. 107435.

Islam, M.A., Hassen, W.M., Tayabali, A.F., Dubowski, J.J., (2021). Short Ligand, Cysteine-Modified Warnericin RK Antimicrobial Peptides Favor Highly Sensitive Detection of Legionella pneumophila. *ACS Omega*, vol. 6(2), p. 1299-1308.

Islam, M.A., Karim, A., Woon, C.W., Ethiraj, B., Cheng, C.K., Yousuf, A., Khan, M.M.R., (2017). Augmentation of air cathode microbial fuel cell performance using wild type Klebsiella variicola. *RSC Advances*, vol. 7(8), p. 4798-4805.

Jafari, S., Dehghani, M., Nasirizadeh, N., Baghersad, M.H., Azimzadeh, M., (2019). Label-free electrochemical detection of Cloxacillin antibiotic in milk samples based on molecularly imprinted polymer and graphene oxide-gold nanocomposite. *Measurement*, vol. 145, p. 22-29.

Jayan, H., Pu, H., Sun, D.-W., (2019). Recent development in rapid detection techniques for microorganism activities in food matrices using bio-recognition: A review. *Trends in Food Science & Technology*.

Jeevithan, E., Bao, B., Bu, Y., Zhou, Y., Zhao, Q., Wu, W., (2014). Type II collagen and gelatin from silvertip shark (Carcharhinus albimarginatus) cartilage: Isolation, purification, physicochemical and antioxidant properties. *Marine drugs*, vol. 12(7), p. 3852-3873.

Jeverica, S., Nagy, E., Mueller-Premru, M., Papst, L., (2018). Sample preparation method influences direct identification of anaerobic bacteria from positive blood culture bottles using MALDI-TOF MS. *Anaerobe*, vol. 54, p. 231-235.

Jiang, K., Etayash, H., Azmi, S., Naicker, S., Hassanpourfard, M., Shaibani, P.M., Thakur, G., Kaur, K., Thundat, T., (2015). Rapid label-free detection of E. coli using antimicrobial peptide assisted impedance spectroscopy. *Analytical Methods*, vol. 7(23), p. 9744-9748.

Justino, C.I., Freitas, A.C., Pereira, R., Duarte, A.C., Santos, T.A.R., (2015). Recent developments in recognition elements for chemical sensors and biosensors. *TrAC Trends in Analytical Chemistry*, vol. 68, p. 2-17.

Kanayeva, D.A., Wang, R., Rhoads, D., Erf, G.F., Slavik, M.F., Tung, S., Li, Y., (2012). Efficient separation and sensitive detection of Listeria monocytogenes using an impedance immunosensor based on magnetic nanoparticles, a microfluidic chip, and an interdigitated microelectrode. *Journal of food protection*, vol. 75(11), p. 1951-1959.

Karcz, J., Bernas, T., Nowak, A., Talik, E., Woznica, A., (2012). Application of lyophilization to prepare the nitrifying bacterial biofilm for imaging with scanning electron microscopy. *Scanning*, vol. 34(1), p. 26-36.

Karimzadeh, A., Hasanzadeh, M., Shadjou, N., de la Guardia, M., (2018). Peptide based biosensors. *TrAC Trends in Analytical Chemistry*, vol. 107, p. 1-20.

Kaur, H., Bruno, J.G., Kumar, A., Sharma, T.K., (2018). Aptamers in the therapeutics and diagnostics pipelines. *Theranostics*, vol. 8(15), p. 4016.

Keserue, H.A., Baumgartner, A., Felleisen, R., Egli, T., (2012). Rapid detection of total and viable L egionella pneumophila in tap water by immunomagnetic separation, double fluorescent staining and flow cytometry. *Microbial biotechnology*, vol. 5(6), p. 753-763.

Khan, S.A., Khan, S.B., Khan, L.U., Farooq, A., Akhtar, K., Asiri, A.M., 2018. Fourier transform infrared spectroscopy: fundamentals and application in functional groups and nanomaterials characterization, Handbook of materials characterization. Springer, pp. 317-344.

Kim, H.-J., Choi, S.-J., (2020). Rapid single-cell detection of pathogenic bacteria for in situ determination of food safety. *Analytical Methods*, vol. 12(46), p. 5621-5627.

Kim, J., Campbell, A.S., de Ávila, B.E.-F., Wang, J., (2019). Wearable biosensors for healthcare monitoring. *Nature biotechnology*, vol. 37(4), p. 389-406.

Kulagina, N.V., Lassman, M.E., Ligler, F.S., Taitt, C.R., (2005). Antimicrobial peptides for detection of bacteria in biosensor assays. *Analytical chemistry*, vol. 77(19), p. 6504-6508.

Kulagina, N.V., Shaffer, K.M., Anderson, G.P., Ligler, F.S., Taitt, C.R., (2006). Antimicrobial peptide-based array for Escherichia coli and Salmonella screening. *Analytica chimica acta*, vol. 575(1), p. 9-15.

Kulagina, N.V., Shaffer, K.M., Ligler, F.S., Taitt, C.R., (2007). Antimicrobial peptides as new recognition molecules for screening challenging species. *Sensors and Actuators B: Chemical*, vol. 121(1), p. 150-157.

Kumar, M., Ghosh, S., Nayak, S., Das, A., (2016). Recent advances in biosensor based diagnosis of urinary tract infection. *Biosensors and Bioelectronics*, vol. 80, p. 497-510.

Kumar, S., Balakrishna, K., Batra, H., (2008). Enrichment-ELISA for detection of Salmonella typhi from food and water samples. *Biomedical and environmental sciences*, vol. 21(2), p. 137-143.

Lacour, V., Elie-Caille, C., Leblois, T., Dubowski, J.J., (2016). Regeneration of a thiolated and antibody functionalized GaAs (001) surface using wet chemical processes. *Biointerphases*, vol. 11(1), p. 019302.

Lai, Z., Tan, P., Zhu, Y., Shao, C., Shan, A., Li, L., (2019). Highly stabilized α-helical coiled coils kill gram-negative bacteria by multicomplementary mechanisms under acidic condition. *ACS applied materials & interfaces*, vol. 11(25), p. 22113-22128.

Lambert, B., Sermage, B., Deveaud, B., Clerot, F., Chomette, A., Regreny, A., (1990). Radiative and non-radiative recombination in GaAs□ AlGaAs superlattices. *Surface science*, vol. 228(1-3), p. 210-212.

Laribi, A., Allegra, S., Souiri, M., Mzoughi, R., Othmane, A., Girardot, F., (2020). Legionella pneumophila sg1-sensing signal enhancement using a novel electrochemical immunosensor in dynamic detection mode. *Talanta*, vol. 215, p. 120904.

Law, J.W.-F., Ab Mutalib, N.-S., Chan, K.-G., Lee, L.-H., (2015). Rapid methods for the detection of foodborne bacterial pathogens: principles, applications, advantages and limitations. *Frontiers in microbiology*, vol. 5, p. 770.

Lazcka, O., Del Campo, F.J., Munoz, F.X., (2007). Pathogen detection: A perspective of traditional methods and biosensors. *Biosensors and bioelectronics*, vol. 22(7), p. 1205-1217.

Lei, K.F., Leung, P.H., (2012). Microelectrode array biosensor for the detection of Legionellapneumophila. *Microelectronic engineering*, vol. 91, p. 174-177.

Leonard, P., Hearty, S., Brennan, J., Dunne, L., Quinn, J., Chakraborty, T., O'Kennedy, R., (2003). Advances in biosensors for detection of pathogens in food and water. *Enzyme and Microbial Technology*, vol. 32(1), p. 3-13.

Leoni, E., Catalani, F., Marini, S., Dallolio, L., (2018). Legionellosis associated with recreational waters: a systematic review of cases and outbreaks in swimming pools, spa pools, and similar environments. *International journal of environmental research and public health*, vol. 15(8), p. 1612.

Li, J., Koh, J.-J., Liu, S., Lakshminarayanan, R., Verma, C.S., Beuerman, R.W., (2017). Membrane active antimicrobial peptides: translating mechanistic insights to design. *Frontiers in neuroscience*, vol. 11, p. 73.

Li, N., Brahmendra, A., Veloso, A.J., Prashar, A., Cheng, X.R., Hung, V.W., Guyard, C., Terebiznik, M., Kerman, K., (2012). Disposable immunochips for the detection of Legionella pneumophila using electrochemical impedance spectroscopy. *Analytical chemistry*, vol. 84(8), p. 3485-3488.

Li, X., Chen, S., Zhang, W.-D., Hu, H.-G., (2020). Stapled helical peptides bearing different anchoring residues. *Chemical Reviews*, vol. 120(18), p. 10079-10144.

Li, Y., Afrasiabi, R., Fathi, F., Wang, N., Xiang, C., Love, R., She, Z., Kraatz, H.-B., (2014). Impedance based detection of pathogenic E. coli O157: H7 using a ferrocene-antimicrobial peptide modified biosensor. *Biosensors and Bioelectronics*, vol. 58, p. 193-199.

Li, Y., Xie, G., Qiu, J., Zhou, D., Gou, D., Tao, Y., Li, Y., Chen, H., (2018). A new biosensor based on the recognition of phages and the signal amplification of organic-inorganic hybrid nanoflowers for discriminating and quantitating live pathogenic bacteria in urine. *Sensors and Actuators B: Chemical*, vol. 258, p. 803-812.

Li, Z., Yang, H., Sun, L., Qi, H., Gao, Q., Zhang, C., (2015). Electrogenerated chemiluminescence biosensors for the detection of pathogenic bacteria using antimicrobial peptides as capture/signal probes. *Sensors and Actuators B: Chemical*, vol. 210, p. 468-474.

Lillehoj, P.B., Kaplan, C.W., He, J., Shi, W., Ho, C.-M., (2014). Rapid, electrical impedance detection of bacterial pathogens using immobilized antimicrobial peptides. *Journal of laboratory automation*, vol. 19(1), p. 42-49.

Lin, H.-Y., Tsao, Y.-C., Tsai, W.-H., Yang, Y.-W., Yan, T.-R., Sheu, B.-C., (2007). Development and application of side-polished fiber immunosensor based on surface plasmon

resonance for the detection of Legionella pneumophila with halogens light and 850 nm-LED. *Sensors and actuators A: Physical*, vol. 138(2), p. 299-305.

Liu, W., Song, H., Chen, Q., Yu, J., Xian, M., Nian, R., Feng, D., (2018). Recent advances in the selection and identification of antigen-specific nanobodies. *Molecular immunology*, vol. 96, p. 37-47.

Lucarelli, F., Tombelli, S., Minunni, M., Marrazza, G., Mascini, M., (2008). Electrochemical and piezoelectric DNA biosensors for hybridisation detection. *analytica chimica acta*, vol. 609(2), p. 139-159.

Lui, C., Cady, N., Batt, C., (2009). Nucleic acid-based detection of bacterial pathogens using integrated microfluidic platform systems. *Sensors*, vol. 9(5), p. 3713-3744.

Lv, E., Ding, J., Qin, W., (2018). Potentiometric detection of Listeria monocytogenes via a short antimicrobial peptide pair-based sandwich assay. *Analytical chemistry*, vol. 90(22), p. 13600-13606.

Ma, K., Deng, Y., Bai, Y., Xu, D., Chen, E., Wu, H., Li, B., Gao, L., (2014). Rapid and simultaneous detection of Salmonella, Shigella, and Staphylococcus aureus in fresh pork using a multiplex real-time PCR assay based on immunomagnetic separation. *Food Control*, vol. 42, p. 87-93.

Maffert, P., Reverchon, S., Nasser, W., Rozand, C., Abaibou, H., (2017). New nucleic acid testing devices to diagnose infectious diseases in resource-limited settings. *European Journal of Clinical Microbiology & Infectious Diseases*, vol. 36(10), p. 1717-1731.

Magonov, S., Elings, V., Whangbo, M.-H., (1997). Phase imaging and stiffness in tapping-mode atomic force microscopy. *Surface science*, vol. 375(2-3), p. L385-L391.

Mahlapuu, M., Björn, C., Ekblom, J., (2020). Antimicrobial peptides as therapeutic agents: Opportunities and challenges. *Critical reviews in biotechnology*, vol. 40(7), p. 978-992.

Mahlapuu, M., Håkansson, J., Ringstad, L., Björn, C., (2016). Antimicrobial peptides: an emerging category of therapeutic agents. *Frontiers in cellular and infection microbiology*, vol. 6, p. 194.

Majdinasab, M., Hayat, A., Marty, J.L., (2018). Aptamer-based assays and aptasensors for detection of pathogenic bacteria in food samples. *TrAC Trends in Analytical Chemistry*, vol. 107, p. 60-77.

Malanovic, N., Lohner, K., (2016). Antimicrobial peptides targeting gram-positive bacteria. *Pharmaceuticals*, vol. 9(3), p. 59.

Malic, S., Hill, K.E., Hayes, A., Percival, S.L., Thomas, D.W., Williams, D.W., (2009). Detection and identification of specific bacteria in wound biofilms using peptide nucleic acid fluorescent in situ hybridization (PNA FISH). *Microbiology*, vol. 155(8), p. 2603-2611.

Manera, M.G., Montagna, G., Cimaglia, F., Chiesa, M., Poltronieri, P., Santino, A., Rella, R., (2013). SPR based immunosensor for detection of Legionella pneumophila in water samples. *Optics Communications*, vol. 294, p. 420-426.

Mannoor, M.S., Zhang, S., Link, A.J., McAlpine, M.C., (2010). Electrical detection of pathogenic bacteria via immobilized antimicrobial peptides. *Proceedings of the National Academy of Sciences*, vol. 107(45), p. 19207-19212.

Manzo, G., Scorciapino, M.A., Wadhwani, P., Bürck, J., Montaldo, N.P., Pintus, M., Sanna, R., Casu, M., Giuliani, A., Pirri, G., (2015). Enhanced amphiphilic profile of a short β-stranded peptide improves its antimicrobial activity. *PloS one*, vol. 10(1), p. e0116379.

Marchand, A., Augenstreich, J., Loiseau, C., Verdon, J., Lecomte, S., Berjeaud, J.-M., (2015). Effect of amino acid substitution in the staphylococcal peptides warnericin RK and PSMα on their anti-Legionella and hemolytic activities. *Molecular and Cellular Biochemistry*, vol. 405(1-2), p. 159-167.

Marchand, A., Verdon, J., Lacombe, C., Crapart, S., Hechard, Y., Berjeaud, J., (2011). Anti-Legionella activity of staphylococcal hemolytic peptides. *Peptides*, vol. 32(5), p. 845-851.

Marshall, G.M., (2011). Electro-optic investigation of the n-alkanethiol GaAs (001) interface: surface phenomena and applications to photoluminescence-based biosensing. *Ph. D. Thesis*.

Marshall, S.H., Arenas, G., (2003). Antimicrobial peptides: A natural alternative to chemical antibiotics and a potential for applied biotechnology. *Electronic Journal of Biotechnology*, vol. 6(3), p. 271-284.

Martín, M., Salazar, P., Jiménez, C., Lecuona, M., Ramos, M.J., Ode, J., Alcoba, J., Roche, R., Villalonga, R., Campuzano, S., (2015). Rapid Legionella pneumophila determination based on a disposable core–shell Fe3O4@ poly (dopamine) magnetic nanoparticles immunoplatform. *Analytica chimica acta*, vol. 887, p. 51-58.

Mascini, M., Palchetti, I., Tombelli, S., (2012). Nucleic acid and peptide aptamers: fundamentals and bioanalytical aspects. *Angewandte Chemie International Edition*, vol. 51(6), p. 1316-1332.

Mazzotta, M., Salaris, S., Pascale, M.R., Girolamini, L., Cristino, S., (2021). Occurrence of Legionella spp. in man-made water sources: isolates distribution and phylogenetic characterization in the Emilia-Romagna region. *Pathogens*, vol. 10(5), p. 552.

Meneghello, A., Sonato, A., Ruffato, G., Zacco, G., Romanato, F., (2017). A novel high sensitive surface plasmon resonance Legionella pneumophila sensing platform. *Sensors and Actuators B: Chemical*, vol. 250, p. 351-355.

Miranda-Castro, R., de-Los-Santos-Alvarez, P., Lobo-Castañón, M.J., Miranda-Ordieres, A.J., Tuñón-Blanco, P., (2007). Hairpin-DNA probe for enzyme-amplified electrochemical detection of Legionella pneumophila. *Analytical chemistry*, vol. 79(11), p. 4050-4055.

Mo, L., Drancourt, M., (2004). Monoclonal antibodies for specific detection of Encephalitozoon cuniculi. *Clinical and Vaccine Immunology*, vol. 11(6), p. 1060-1063.

Mobed, A., Hasanzadeh, M., Agazadeh, M., Mokhtarzadeh, A., Rezaee, M.A., Sadeghi, J., (2019). Bioassays: The best alternative for conventional methods in detection of Legionella pneumophila. *International journal of biological macromolecules*, vol. 121, p. 1295-1307.

Moghaddam, M.M., Aghamollaei, H., Kooshki, H., Barjini, K.A., Mirnejad, R., Choopani, A., (2015). The development of antimicrobial peptides as an approach to prevention of antibiotic resistance. *Reviews in Medical Microbiology*, vol. 26(3), p. 98-110.

Mollasalehi, H., Yazdanparast, R., (2013). Development and evaluation of a novel nucleic acid sequence-based amplification method using one specific primer and one degenerate primer for simultaneous detection of Salmonella Enteritidis and Salmonella Typhimurium. *Analytica chimica acta*, vol. 770, p. 169-174.

Mondani, L., Delannoy, S., Mathey, R., Piat, F., Mercey, T., Slimani, S., Fach, P., Livache, T., Roupioz, Y., (2016). Fast detection of both O157 and non-O157 shiga-toxin producing Escherichia coli by real-time optical immunoassay. *Letters in applied microbiology*, vol. 62(1), p. 39-46.

Mothershed, E.A., Whitney, A.M., (2006). Nucleic acid-based methods for the detection of bacterial pathogens: present and future considerations for the clinical laboratory. *Clinica Chimica Acta*, vol. 363(1-2), p. 206-220.

Munje, R.D., Muthukumar, S., Jagannath, B., Prasad, S., (2017). A new paradigm in sweat based wearable diagnostics biosensors using Room Temperature Ionic Liquids (RTILs). *Scientific reports*, vol. 7(1), p. 1950.

Najafi, R., Mukherjee, S., Hudson Jr, J., Sharma, A., Banerjee, P., (2014). Development of a rapid capture-cum-detection method for Escherichia coli O157 from apple juice comprising nano-immunomagnetic separation in tandem with surface enhanced Raman scattering. *International journal of food microbiology*, vol. 189, p. 89-97.

Nayak, M., Singh, D., Singh, H., Kant, R., Gupta, A., Pandey, S.S., Mandal, S., Ramanathan, G., Bhattacharya, S., (2013). Integrated sorting, concentration and real time PCR based detection system for sensitive detection of microorganisms. *Scientific reports*, vol. 3(1), p. 1-7.

Nazemi, E., Aithal, S., Hassen, W.M., Frost, E.H., Dubowski, J.J., (2015). GaAs/AlGaAs heterostructure based photonic biosensor for rapid detection of Escherichia coli in phosphate buffered saline solution. *Sensors and Actuators B: Chemical*, vol. 207, p. 556-562.

Nazemi, E., Hassen, W.M., Frost, E.H., Dubowski, J.J., (2017). Monitoring growth and antibiotic susceptibility of Escherichia coli with photoluminescence of GaAs/AlGaAs quantum well microstructures. *Biosensors and Bioelectronics*, vol. 93, p. 234-240.

Nazemi, E., Hassen, W.M., Frost, E.H., Dubowski, J.J., (2018). Growth of Escherichia coli on the GaAs (001) surface. *Talanta*, vol. 178, p. 69-77.

Nguyen-Tri, P., Ghassemi, P., Carriere, P., Nanda, S., Assadi, A.A., Nguyen, D.D., (2020). Recent applications of advanced atomic force microscopy in polymer science: A review. *Polymers*, vol. 12(5), p. 1142.

Nocker, A., Schulte-Illingheim, L., Frösler, J., Welp, L., Sperber, O., Hugo, A., (2020). Microbiological examination of water and aerosols from four industrial evaporative cooling systems in regard to risk of Legionella emissions and methodological suggestions for surveillance. *International Journal of Hygiene and Environmental Health*, vol. 229, p. 113591.

Nuthong, B., Wilailuckana, C., Tavichakorntrakool, R., Boonsiri, P., Daduang, S., Bunyaraksyotin, G., Suphan, O., Daduang, J., (2018). One step for Legionella pneumophila detection in environmental samples by DNA-gold nanoparticle probe. *Journal of applied microbiology*, vol. 125(5), p. 1534-1540.

Oblath, E.A., Henley, W.H., Alarie, J.P., Ramsey, J.M., (2013). A microfluidic chip integrating DNA extraction and real-time PCR for the detection of bacteria in saliva. *Lab on a Chip*, vol. 13(7), p. 1325-1332.

Oger, P.-C., Piesse, C., Ladram, A., Humblot, V., (2019). Engineering of antimicrobial surfaces by using temporin analogs to tune the biocidal/antiadhesive effect. *Molecules*, vol. 24(4), p. 814.

Oh, B.-K., Kim, Y.-K., Lee, W., Bae, Y.M., Lee, W.H., Choi, J.-W., (2003). Immunosensor for detection of Legionella pneumophila using surface plasmon resonance. *Biosensors and Bioelectronics*, vol. 18(5-6), p. 605-611.

Olsson, N., Wallin, S., James, P., Borrebaeck, C.A., Wingren, C., (2012). Epitope-specificity of recombinant antibodies reveals promiscuous peptide-binding properties. *Protein Science*, vol. 21(12), p. 1897-1910.

Ongey, E.L., Pflugmacher, S., Neubauer, P., (2018). Bioinspired designs, molecular premise and tools for evaluating the ecological importance of antimicrobial peptides. *Pharmaceuticals*, vol. 11(3), p. 68.

Paniel, N., Baudart, J., Hayat, A., Barthelmebs, L., (2013). Aptasensor and genosensor methods for detection of microbes in real world samples. *Methods*, vol. 64(3), p. 229-240.

Pardoux, É., Boturyn, D., Roupioz, Y., (2020). Antimicrobial peptides as probes in biosensors detecting whole bacteria: A review. *Molecules*, vol. 25(8), p. 1998.

Park, E.J., Lee, J.-Y., Kim, J.H., Lee, C.J., Kim, H.S., Min, N.K., (2010). Investigation of plasma-functionalized multiwalled carbon nanotube film and its application of DNA sensor for Legionella pneumophila detection. *Talanta*, vol. 82(3), p. 904-911.

Pashazadeh, P., Mokhtarzadeh, A., Hasanzadeh, M., Hejazi, M., Hashemi, M., de la Guardia, M., (2017). Nano-materials for use in sensing of salmonella infections: Recent advances. *Biosensors and Bioelectronics*, vol. 87, p. 1050-1064.

Passlack, M., Hong, M., Schubert, E., Kwo, J., Mannaerts, J., Chu, S., Moriya, N., Thiel, F., (1995). In situ fabricated Ga2O3–GaAs structures with low interface recombination velocity. *Applied physics letters*, vol. 66(5), p. 625-627.

Pathak, N., Ghosh, P.S., Gupta, S.K., Kadam, R.M., Arya, A., (2016). Defects induced changes in the electronic structures of MgO and their correlation with the optical properties: a

special case of electron–hole recombination from the conduction band. *RSC advances*, vol. 6(98), p. 96398-96415.

Pavan, S., Berti, F., (2012). Short peptides as biosensor transducers. *Analytical and bioanalytical chemistry*, vol. 402(10), p. 3055-3070.

Pérez-López, B., Merkoçi, A., (2011). Nanomaterials based biosensors for food analysis applications. *Trends in Food Science & Technology*, vol. 22(11), p. 625-639.

Pienaar, J.A., Singh, A., Barnard, T.G., (2016). The viable but non-culturable state in pathogenic Escherichia coli: a general review. *African journal of laboratory medicine*, vol. 5(1), p. 1-9.

Pinel, I., Hankinson, P., Moed, D., Wyseure, L., Vrouwenvelder, J.S., van Loosdrecht, M.C., (2021). Efficient cooling tower operation at alkaline pH for the control of Legionella pneumophila and other pathogenic genera. *Water Research*, p. 117047.

Poortinga, A., Bos, R., Busscher, H., (1999). Measurement of charge transfer during bacterial adhesion to an indium tin oxide surface in a parallel plate flow chamber. *Journal of microbiological methods*, vol. 38(3), p. 183-189.

Puiu, M., Bala, C., (2018). Peptide-based biosensors: From self-assembled interfaces to molecular probes in electrochemical assays. *Bioelectrochemistry*, vol. 120, p. 66-75.

Qiao, Z., Fu, Y., Lei, C., Li, Y., (2020a). Advances in antimicrobial peptides-based biosensing methods for detection of foodborne pathogens: A review. *Food Control*, p. 107116.

Qiao, Z., Fu, Y., Lei, C., Li, Y., (2020b). Advances in antimicrobial peptides-based biosensing methods for detection of foodborne pathogens: A review. *Food Control*, vol. 112, p. 107116.

Qiao, Z., Lei, C., Fu, Y., Li, Y., (2017a). An antimicrobial peptide-based colorimetric bioassay for rapid and sensitive detection of E. coli O157: H7. *RSC advances*, vol. 7(26), p. 15769-15775.

Qiao, Z., Lei, C., Fu, Y., Li, Y., (2017b). Rapid and sensitive detection of E. coli O157: H7 based on antimicrobial peptide functionalized magnetic nanoparticles and urease-catalyzed signal amplification. *Analytical Methods*, vol. 9(35), p. 5204-5210.

Quirino, A., Pulcrano, G., Rametti, L., Puccio, R., Marascio, N., Catania, M.R., Matera, G., Liberto, M.C., Focà, A., (2014). Typing of Ochrobactrum anthropi clinical isolates using automated repetitive extragenic palindromic-polymerase chain reaction DNA fingerprinting

and matrix-assisted laser desorption/ionization–time-of-flight mass spectrometry. *BMC microbiology*, vol. 14(1), p. 1-8.

Rai, A., Pinto, S., Evangelista, M.B., Gil, H., Kallip, S., Ferreira, M.G., Ferreira, L., (2016). High-density antimicrobial peptide coating with broad activity and low cytotoxicity against human cells. *Acta biomaterialia*, vol. 33, p. 64-77.

Rajapaksha, P., Elbourne, A., Gangadoo, S., Brown, R., Cozzolino, D., Chapman, J., (2019). A review of methods for the detection of pathogenic microorganisms. *Analyst*, vol. 144(2), p. 396-411.

Ramanavičius, A., Ramanavičienė, A., Malinauskas, A., (2006). Electrochemical sensors based on conducting polymer—polypyrrole. *Electrochimica acta*, vol. 51(27), p. 6025-6037.

Rana, M., Pota, H.R., Petersen, I.R., (2016). Improvement in the imaging performance of atomic force microscopy: A survey. *IEEE Transactions on Automation Science and Engineering*, vol. 14(2), p. 1265-1285.

Reuter, C., Slesiona, N., Hentschel, S., Aehlig, O., Breitenstein, A., Csáki, A., Henkel, T., Fritzsche, W., (2020). Loop-mediated amplification as promising on-site detection approach for Legionella pneumophila and Legionella spp. *Applied microbiology and biotechnology*, vol. 104(1), p. 405-415.

Richter, Ł., Janczuk-Richter, M., Niedziółka-Jönsson, J., Paczesny, J., Hołyst, R., (2018). Recent advances in bacteriophage-based methods for bacteria detection. *Drug discovery today*, vol. 23(2), p. 448-455.

Riedel, M., Lisdat, F., 2017. Biosensorial Application of Impedance Spectroscopy with Focus on DNA Detection, Label-Free Biosensing. Springer, pp. 133-178.

Roda, A., Mirasoli, M., Roda, B., Bonvicini, F., Colliva, C., Reschiglian, P., (2012). Recent developments in rapid multiplexed bioanalytical methods for foodborne pathogenic bacteria detection. *Microchimica Acta*, vol. 178(1-2), p. 7-28.

Rodrigues Ribeiro Teles, F.S., Pires de Tavora Tavira, L.A., Pina da Fonseca, L.J., (2010). Biosensors as rapid diagnostic tests for tropical diseases. *Critical reviews in clinical laboratory sciences*, vol. 47(3), p. 139-169.

Rose, J.B., Epstein, P.R., Lipp, E.K., Sherman, B.H., Bernard, S.M., Patz, J.A., (2001). Climate variability and change in the United States: potential impacts on water-and foodborne

diseases caused by microbiologic agents. *Environmental health perspectives*, vol. 109(suppl 2), p. 211-221.

Ruberto, M.N., Zhang, X., Scarmozzino, R., Willner, A.E., Podlesnik, D.V., Osgood, R.M., (1991). The Laser-Controlled Micrometer-Scale Photoelectrochemical Etching of III–V Semiconductors. *Journal of The Electrochemical Society*, vol. 138(4), p. 1174-1185.

Rydlo, T., Rotem, S., Mor, A., (2006). Antibacterial properties of dermaseptin S4 derivatives under extreme incubation conditions. *Antimicrobial agents and chemotherapy*, vol. 50(2), p. 490-497.

Sadsri, V., Trakulsujaritchok, T., Tangwattanachuleeporn, M., Hoven, V.P., Na Nongkhai, P., (2020). Simple Colorimetric Assay for Vibrio parahaemolyticus Detection Using Aptamer-Functionalized Nanoparticles. *ACS omega*, vol. 5(34), p. 21437-21442.

Saha, K., Agasti, S.S., Kim, C., Li, X., Rotello, V.M., (2012). Gold nanoparticles in chemical and biological sensing. *Chemical reviews*, vol. 112(5), p. 2739-2779.

Sanchez-Gomez, S., Martinez-de-Tejada, G., (2017). Antimicrobial peptides as anti-biofilm agents in medical implants. *Current topics in medicinal chemistry*, vol. 17(5), p. 590-603.

Schiller, J.L., (2019). Selective Tuning of Biogels and Antibodies to Enhance Trapping of Pathogens.

Schmelcher, M., Loessner, M.J., (2016). Bacteriophage endolysins: applications for food safety. *Current opinion in biotechnology*, vol. 37, p. 76-87.

Sharma, H., Moumanis, K., Dubowski, J.J., (2016). pH-Dependent Photocorrosion of GaAs/AlGaAs Quantum Well Microstructures. *The Journal of Physical Chemistry C*, vol. 120(45), p. 26129-26137.

Sharma, S., Vyas, S., Periasamy, C., Chakrabarti, P., (2014). Structural and optical characterization of ZnO thin films for optoelectronic device applications by RF sputtering technique. *Superlattices and Microstructures*, vol. 75, p. 378-389.

Shen, M., Rusling, J.F., Dixit, C.K., (2017). Site-selective orientated immobilization of antibodies and conjugates for immunodiagnostics development. *Methods*, vol. 116, p. 95-111.

Shen, Z., Hou, N., Jin, M., Qiu, Z., Wang, J., Zhang, B., Wang, X., Wang, J., Zhou, D., Li, J., (2014). A novel enzyme-linked immunosorbent assay for detection of Escherichia coli O157: H7 using immunomagnetic and beacon gold nanoparticles. *Gut pathogens*, vol. 6(1), p. 1-8.

Shi, X.-M., Long, F., Suo, B., (2010). Molecular methods for the detection and characterization of foodborne pathogens. *Pure and Applied Chemistry*, vol. 82(1), p. 69-79.

Shi, X., Zhang, X., Yao, Q., He, F., (2017). A novel method for the rapid detection of microbes in blood using pleurocidin antimicrobial peptide functionalized piezoelectric sensor. *Journal of microbiological methods*, vol. 133, p. 69-75.

Shockley, W., Read Jr, W., (1952). Statistics of the recombinations of holes and electrons. *Physical review*, vol. 87(5), p. 835.

Shukla, S., Leem, H., Lee, J.-S., Kim, M., (2014). Immunochromatographic strip assay for the rapid and sensitive detection of Salmonella Typhimurium in artificially contaminated tomato samples. *Canadian journal of microbiology*, vol. 60(6), p. 399-406.

Silva, N.F., Neves, M.M., Magalhães, J.M., Freire, C., Delerue-Matos, C., (2020). Emerging electrochemical biosensing approaches for detection of Listeria monocytogenes in food samples: An overview. *Trends in Food Science & Technology*, vol. 99, p. 621-633.

Simmel, F.C., Yurke, B., Singh, H.R., (2019). Principles and applications of nucleic acid strand displacement reactions. *Chemical reviews*, vol. 119(10), p. 6326-6369.

Singh, A., Arutyunov, D., Szymanski, C.M., Evoy, S., (2012). Bacteriophage based probes for pathogen detection. *Analyst*, vol. 137(15), p. 3405-3421.

Singhal, N., Kumar, M., Kanaujia, P.K., Virdi, J.S., (2015). MALDI-TOF mass spectrometry: an emerging technology for microbial identification and diagnosis. *Frontiers in microbiology*, vol. 6, p. 791.

Šípová, H., Zhang, S., Dudley, A.M., Galas, D., Wang, K., Homola, J.i., (2010). Surface plasmon resonance biosensor for rapid label-free detection of microribonucleic acid at subfemtomole level. *Analytical chemistry*, vol. 82(24), p. 10110-10115.

Skottrup, P.D., Nicolaisen, M., Justesen, A.F., (2008). Towards on-site pathogen detection using antibody-based sensors. *Biosensors and Bioelectronics*, vol. 24(3), p. 339-348.

Soares, J., Morin, K., Mello, C., 2004. Antimicrobial peptides for use in biosensing applications. Army Natick Research Development and Engineering Center MA.

Sousa, P.S., Silva, I.N., Moreira, L.M., Veríssimo, A., Costa, J., (2018). Differences in Virulence Between *Legionella pneumophila* Isolates From Human and Non-human Sources Determined in Galleria mellonella Infection Model. *Frontiers in Cellular and Infection Microbiology*, vol. 8(97).

Soylemez, S., Demir, B., Eyrilmez, G.O., Kesici, S., Saylam, A., Demirkol, D.O., Özçubukçu, S., Timur, S., Toppare, L., (2016). Comparative cell adhesion properties of cysteine extended peptide architectures. *RSC advances*, vol. 6(4), p. 2695-2702.

Stassen, I., Burtch, N., Talin, A., Falcaro, P., Allendorf, M., Ameloot, R., (2017). An updated roadmap for the integration of metal–organic frameworks with electronic devices and chemical sensors. *Chemical Society Reviews*, vol. 46(11), p. 3185-3241.

Templier, V., Roux, A., Roupioz, Y., Livache, T., (2016). Ligands for label-free detection of whole bacteria on biosensors: A review. *TrAC Trends in Analytical Chemistry*, vol. 79, p. 71-79.

Tran, N.K., Howard, T., Walsh, R., Pepper, J., Loegering, J., Phinney, B., Salemi, M.R., Rashidi, H.H., (2021). Novel application of automated machine learning with MALDI-TOF-MS for rapid high-throughput screening of COVID-19: A proof of concept. *Scientific reports*, vol. 11(1), p. 1-10.

Trevino, M., Navarro, D., Barbeito, G., Garcia-Riestra, C., Crespo, C., Regueiro, B.J., (2011). Molecular and epidemiological analysis of nosocomial carbapenem-resistant Klebsiella spp. using repetitive extragenic palindromic-polymerase chain reaction and matrix-assisted laser desorption/ionization-time of flight. *Microbial Drug Resistance*, vol. 17(3), p. 433-442.

Tsen, H., Lin, C., Chi, W., (1998). Development and use of 16S rRNA gene targeted PCR primers for the identification of *Escherichia coli* cells in water. *Journal of applied microbiology*, vol. 85(3), p. 554-560.

Valones, M.A.A., Guimarães, R.L., Brandão, L.A.C., Souza, P.R.E.d., Carvalho, A.d.A.T., Crovela, S., (2009). Principles and applications of polymerase chain reaction in medical diagnostic fields: a review. *Brazilian Journal of Microbiology*, vol. 40(1), p. 1-11.

Váradi, L., Luo, J.L., Hibbs, D.E., Perry, J.D., Anderson, R.J., Orenga, S., Groundwater, P.W., (2017). Methods for the detection and identification of pathogenic bacteria: past, present, and future. *Chemical Society Reviews*, vol. 46(16), p. 4818-4832.

Vasilescu, A., Nunes, G., Hayat, A., Latif, U., Marty, J.-L., (2016). Electrochemical affinity biosensors based on disposable screen-printed electrodes for detection of food allergens. *Sensors*, vol. 16(11), p. 1863.

Velusamy, V., Arshak, K., Korostynska, O., Oliwa, K., Adley, C., (2010). An overview of foodborne pathogen detection: In the perspective of biosensors. *Biotechnology advances*, vol. 28(2), p. 232-254.

Verdon, J., Berjeaud, J.-M., Lacombe, C., Héchard, Y., (2008). Characterization of anti-*Legionella* activity of warnericin RK and delta-lysin I from Staphylococcus warneri. *Peptides*, vol. 29(6), p. 978-984.

Verdon, J., Falge, M., Maier, E., Bruhn, H., Steinert, M., Faber, C., Benz, R., Hechard, Y., (2009). Detergent-like activity and alpha-helical structure of warnericin RK, an anti-Legionella peptide. *Biophys J*, vol. 97(7), p. 1933-1940.

Verdon, J., Labanowski, J., Sahr, T., Ferreira, T., Lacombe, C., Buchrieser, C., Berjeaud, J.-M., Héchard, Y., (2011). Fatty acid composition modulates sensitivity of *Legionella pneumophila* to warnericin RK, an antimicrobial peptide. *Biochimica et Biophysica Acta (BBA)-Biomembranes*, vol. 1808(4), p. 1146-1153.

Vogiazi, V., de la Cruz, A., Mishra, S., Shanov, V., Heineman, W.R., Dionysiou, D.D., (2019). A comprehensive review: Development of electrochemical biosensors for detection of cyanotoxins in freshwater. *ACS sensors*, vol. 4(5), p. 1151-1173.

Voskuil, J.L.A., (2014). Commercial antibodies and their validation. *F1000Research*, vol. 3, p. 232-232.

Voznyy, O., Dubowski, J.J., (2009). c (4× 2) structures of alkanethiol monolayers on Au (111) compatible with the constraint of dense packing. *Langmuir*, vol. 25(13), p. 7353-7358.

Wackerlig, J., Schirhagl, R., (2016). Applications of molecularly imprinted polymer nanoparticles and their advances toward industrial use: a review. *Analytical chemistry*, vol. 88(1), p. 250-261.

Wang, J., Tao, K., Yang, Y., Zhang, L., Wang, D., Cao, M., Sun, Y., Xia, D., (2016). Short peptide mediated self-assembly of platinum nanocrystals with selective spreading property. *RSC advances*, vol. 6(63), p. 58099-58105.

Wang, L., Shi, L., Su, J., Ye, Y., Zhong, Q., (2013). Detection of Vibrio parahaemolyticus in food samples using in situ loop-mediated isothermal amplification method. *Gene*, vol. 515(2), p. 421-425.

Wilson, D., Materón, E.M., Ibáñez-Redín, G., Faria, R.C., Correa, D.S., Oliveira Jr, O.N., (2019). Electrical detection of pathogenic bacteria in food samples using information

visualization methods with a sensor based on magnetic nanoparticles functionalized with antimicrobial peptides. *Talanta*, vol. 194, p. 611-618.

Wisuthiphaet, N., Yang, X., Young, G.M., Nitin, N., (2019). Rapid detection of Escherichia coli in beverages using genetically engineered bacteriophage T7. *AMB Express*, vol. 9(1), p. 55.

Wu, W., Li, J., Pan, D., Li, J., Song, S., Rong, M., Li, Z., Gao, J., Lu, J., (2014). Gold nanoparticle-based enzyme-linked antibody-aptamer sandwich assay for detection of Salmonella Typhimurium. *ACS applied materials & interfaces*, vol. 6(19), p. 16974-16981.

Wunderlich, A., Torggler, C., Elsässer, D., Lück, C., Niessner, R., Seidel, M., (2016). Rapid quantification method for Legionella pneumophila in surface water. *Analytical and bioanalytical chemistry*, vol. 408(9), p. 2203-2213.

Xia, Y., Liu, Z., Yan, S., Yin, F., Feng, X., Liu, B.-F., (2016). Identifying multiple bacterial pathogens by loop-mediated isothermal amplification on a rotate & react slipchip. *Sensors and Actuators B: Chemical*, vol. 228, p. 491-499.

Yacobi, B.G., 2003. Semiconductor materials: an introduction to basic principles. Springer Science & Business Media.

Yadav, S., Sreedhara, A., Kanai, S., Liu, J., Lien, S., Lowman, H., Kalonia, D.S., Shire, S.J., (2011). Establishing a link between amino acid sequences and self-associating and viscoelastic behavior of two closely related monoclonal antibodies. *Pharmaceutical research*, vol. 28(7), p. 1750-1764.

Yamaguchi, N., Tokunaga, Y., Goto, S., Fujii, Y., Banno, F., Edagawa, A., (2017). Rapid on-site monitoring of Legionella pneumophila in cooling tower water using a portable microfluidic system. *Scientific reports*, vol. 7(1), p. 1-8.

Yang, C.-W., Hwang, S., Chen, Y.F., Chang, C.S., Tsai, D.P., (2007). Imaging of soft matter with tapping-mode atomic force microscopy and non-contact-mode atomic force microscopy. *Nanotechnology*, vol. 18(8), p. 084009.

Yeaman, M.R., Yount, N.Y., (2003). Mechanisms of antimicrobial peptide action and resistance. *Pharmacological reviews*, vol. 55(1), p. 27-55.

Yi-Xian, W., Zun-Zhong, Y., Cheng-Yan, S., Yi-Bin, Y., (2012). Application of aptamer based biosensors for detection of pathogenic microorganisms. *Chinese Journal of Analytical Chemistry*, vol. 40(4), p. 634-642.

Yoo, S.M., Lee, S.Y., (2016). Optical biosensors for the detection of pathogenic microorganisms. *Trends in biotechnology*, vol. 34(1), p. 7-25.

Zasloff, M., (2002). Antimicrobial peptides of multicellular organisms. *nature*, vol. 415(6870), p. 389-395.

Zelada-Guillén, G.A., Sebastián-Avila, J.L., Blondeau, P., Riu, J., Rius, F.X., (2012). Label-free detection of Staphylococcus aureus in skin using real-time potentiometric biosensors based on carbon nanotubes and aptamers. *Biosensors and bioelectronics*, vol. 31(1), p. 226-232.

Zhang, C., Yang, M., Ericsson, A.C., (2019). Antimicrobial peptides: potential application in liver cancer. *Frontiers in microbiology*, vol. 10, p. 1257.

Zhou, C., Zou, H., Li, M., Sun, C., Ren, D., Li, Y., (2018). Fiber optic surface plasmon resonance sensor for detection of *E. coli* O157: H7 based on antimicrobial peptides and AgNPs-rGO. *Biosensors and Bioelectronics*, vol. 117, p. 347-353.

Zoppe, J.O., Ataman, N.C., Mocny, P., Wang, J., Moraes, J., Klok, H.-A., (2017). Surface-initiated controlled radical polymerization: state-of-the-art, opportunities, and challenges in surface and interface engineering with polymer brushes. *Chemical reviews*, vol. 117(3), p. 1105-1318.

Appendix

List of article submission and obtained awards/scholarships

- ***Publications***

M. Amirul Islam, Walid M Hassen, Azam Tayebali, Jan Dubowski, Antimicrobial warnericin RK peptide functionalized GaAs/AlGaAs biosensor for highly sensitive and selective detection of *Legionella pneumophila*, 2020, 154, 1-5, **Biochemical Engineering Journal**, (ISI-index-Q2, **impact factor: 3.97**)

M. Amirul Islam, Walid M Hassen, Azam Tayebali, Jan Dubowski,Short ligand, cysteine modified warnericin RK antimicrobial peptides favor highly-sensitive detection of *Legionella pneumophila*, 2021, 6, 1299-1308, **ACS Omega**, (ISI-index-Q2, **impact factor: 3.51**)

M. Amirul Islam, Walid M Hassen, Ishika Ishika, Azam Tayebali, Jan Dubowski, Selective Detection of *Legionella pneumophila* Serogroup 1 and 5 with a Digital Photocorrosion Biosensor Using Antimicrobial Peptide-Antibody Sandwich Strategy, 2022, 12, 1-14, **Biosensors** (ISI-index-Q2, **impact factor: 5.31**)

- ***Conference proceedings***

M. Amirul Islam, Walid M Hassen, Azam Tayebali, Jan Dubowski, "Antimicrobial peptide biosensing of *Legionella pneumophila* with digital photocorrosion biosensor" Photonics West (*Nanoscale and Quantum Materials: From Synthesis and Laser Processing to Applications*, *Proceedings volume: PC11990*), San Francisco, USA, 06 – 11 March 2022

- ***Awards***

Best poster award (2nd Place) along with 300 CA$, "Antimicrobial peptide based digital photocorrosion biosensors for detecting *Legionella pneumophila*" DecBio workshop, June 17 – 18 2019, Universite de Sherbrooke, Sherbrooke, Quebec, Canada

- ***Scholarships***

FRQNT B2X Scholarship, Quebec govt. scholarship, 63000 CA$, June 2020, Quebec, Canada

Eureka Scholarship, Faculty level dean award, 7000 CA$, November 2018, Universite de Sherbrooke, Sherbrooke, Quebec, Canada